CANADIAN THESES

THÈSES CANADIENNES

NOTICE

The quality of this microfiche is heavily dependent upon the quality of the original thesis submitted for microfilming. Every effort has been made to ensure the highest quality of reproduction possible.

If pages are missing, contact the university which granted the degree.

Some pages may have indistinct print especially if the original pages were typed with a poor typewriter ribbon or if the university sent us an inferior photocopy.

Previously copyrighted materials (journal articles, published tests, etc.) are not filmed.

Reproduction in full or in part of this film is governed by the Canadian Copyright Act, R.S.C. 1970, c. C-30.

AVIS

La qualité de cette microfiche dépend grandement de la qualité de la thèse soumise au microfilmage. Nous avons tout fait pour assurer une qualité supérieure de reproduction.

S'il manque des pages, veuillez communiquer avec l'université qui a conféré le grade.

La qualité d'impression de certaines pages peut laisser à désirer, surtout si les pages originales ont été dactylographiées à l'aide d'un ruban usé ou si l'université nous a fait parvenir une photocopie de qualité inférieure.

Les documents qui font déjà l'objet d'un droit d'auteur (articles de revue, examens publiés, etc.) ne sont pas microfilmés.

La reproduction, même partielle, de ce microfilm est soumise à la Loi canadienne sur le droit d'auteur, SRC 1970, c. C-30.

THIS DISSERTATION HAS BEEN MICROFILMED EXACTLY AS RECEIVED

LA THÈSE A ÉTÉ MICROFILMÉE TELLE QUE NOUS L'AVONS REÇUE

Approximate Seismic Analysis of Single and Coupled Shear Walls on Flexible Bases

Pranab Nandimajumdar

A Thesis
in
The Department
of
Civil Engineering

Presented in Partial Fulfillment of the
Requirements for the Degree of Master of Engineering
at Concordia University
Montréal, Québec, Canada

December 1985

ISBN 0-315-30597-5

ABSTRACT

Approximate Seismic Analysis of Single and Coupled Shear Walls on Flexible Bases

Pranab Nandimajumdar

A simple and approximate seismic analysis of single and coupled shear walls on rotationally flexible support has been carried out to determine the importance of soil-structure interaction, assuming elastic behaviour in both the structure and the supporting soil. To avoid the complexity of using exact mode shapes, the mode shapes of flexibly mounted cantilever beams are assumed. Analyses are performed in a parametric manner employing structures of different heights.

For the single shear walls 5, 10 15 and 20 storeys are considered, with rotational base flexibility parameter R varied from rigid to very flexible condition. Data for various responses are presented, namely base shear, base moment and top deflection.

For coupled shear walls situated on rotationally flexible foundations similar response data are generated. Results are examined in terms of base flexibility as well as structural parameters αH and μ, which define the ratio of the stiffnesses of connecting beams to the walls and the measure of axial deformation of the walls, respectively. In addition, two prototype structures with flexible bases, 26 and 10 storeys in height are compared with rigid base condition.

ACKNOWLEDGEMENTS

The author wishes to express his sincere gratitude to his supervisor Dr. O.A. Pekau. His guidance, suggestions and criticism were indispensible for the progress of this research.

The financial support for this research was provided by the Natural Sciences and Engineering Research Council of Canada under Grant No. A8258. The use of the facilities of Concordia University's Computer Centre are greatfully acknowledged.

Acknowledgement is also due to Dr. P.K. Syamal and to the authors sister, Mitra, for their patience, encouragement and major financial support for the author's education in Canada. Thanks are also extended to Mrs. Marie Berryman for her typing of this thesis.

Finally, the author extends his very special and heartful thanks to his parents and all his brothers for their never ending encouragement, financial and moral support, all of which contributed to the author's education.

In memory of my mother, Shefali Nandimajumdar

TABLE OF CONTENTS

LIST OF TABLES

LIST OF FIGURES

NOMENCLATURE

A_1, A_2 = cross-sectional area of walls 1 and 2, respectively

A_b^* = effective shear area of lintel beam

a = distance between centroids of walls

c = connecting beam span

E = Young's modulus

E_s = Young's modulus of supporting soil

G = shear modulus

g = acceleration due to gravity

H = overall height

h = storey height

I = moment of inertia of single wall; for coupled shear wall $I = I_1 + I_2$

I_1, I_2 = moment of inertia of walls 1 and 2, respectively

I_b = moment of inertia of connecting beam

K_θ = rotational stiffness of foundation

$K_{\theta 1}$, $K_{\theta 2}$ = rotational stiffness of the foundations for walls 1 and 2, respectively

M = bending moment or overturning moment

M_w = wall moment

m = mass per unit height

P_r = modal participation factor in mode r

q_a = allowable bearing stress in soil

R = nondimensional flexibility parameter = $\frac{K_\theta H}{EI}$

RSS = root-sum-squares

S_a = spectral acceleration

t = time

$\ddot{U}_g$ = ground acceleration

V = share force.

W = weight per unit height of building

w = distributed horizontal force

x = spatial coordinate

y = horizontal deflection

α^2 = $ka^2\mu/EI$

β_r = coefficient of ϕ_r

γ_r = coefficient of ϕ_r

λ_r = frequency parameter in mode r

μ = $1 + [I(A_1+A_2)/A_1A_2a^2]$

ϕ_r = rth mode shape of cantilever beam with flexible support

ω_r = natural frequency in mode r

CHAPTER I

INTRODUCTION

1.1 DESCRIPTION OF THE PROBLEM

During the last few decades special attention has focussed on determining the behaviour of shear walls, coupled shear walls and related structures as lateral load-resistant systems.

In multistorey buildings shear walls are provided in conjunction with moment frames because the latter, alone, are frequently not adequate. The provision of windows, doors and service ducts produce single or multiple vertical rows of openings throughout the height, separated by either connecting beams which form part of the walls or by floor slabs, or a combination of both. Such walls are usually termed coupled shear walls, shear walls with openings or pierced shear walls.

It is not always reasonable to assume that such structures are situated on a rigid foundation medium, since the foundation flexibility plays an important role. Since these structures invariably rest on elastic soil, they experience vertical lateral and, or rotational settlements at the base. The assumption of a rigid foundation for analysis may, therefore, yield inaccurate estimates of response.

1.2 REVIEW OF EXISTING WORK

1.2.1. Static and Dynamic Analysis for Fixed-Base Structures

In the existing literature the continuum approach suggested by Beck [4] is a very useful technique to analyse shear wall structures.

As a result, most investigators [5-19] have used this technique for the static and dynamic analysis of coupled shear walls and wall-frame structures on fixed and flexible bases.

Beck [4] investigated the static analysis of coupled shear walls of identical properties considering fixed-base conditions and presented mathematical expressions for the design unknowns, such as lateral and longitudinal deformation, wall shear and bending moment and shear force and moment in the connecting beams, all expressed as function of height. Rosman [5] used the same technique and investigated coupled shear wall structures with double rows of openings.

The stresses and maximum deflection of coupled shear walls with fixed bases and subjected to static lateral loadings have been reported by Coull and Choudhury [6,7] as design curves.

Heidebrecht and Stafford-Smith [8] proposed a simplified method for the static and dynamic analysis of uniform structures consisting of frames and shear walls, assuming a combination of flexural and shear cantilever beams, and presented design curves for response under uniformly distributed loadings, as well as the first few natural frequencies. However, they did not provide information concerning the mode shapes or axial deformation in the walls. Basu et al [14] included shear deformation in the walls and obtained accurate natural frequencies by an iterative solution of the nonlinear frequency equation.

Many investigators [9,10,11,12,13] have reported the natural frequencies of coupled shear walls on fixed bases. Tso and Chan [9] carried out dynamic analysis of fixed-base coupled shear walls subjected to time-dependent loading and obtained the fundamental frequencies of equal and unequal piers to provide essential information for use of the

response spectrum technique in seismic design. Tso and Biswas [10] proposed an approximate technique to evaluate the natural frequencies of fixed-base coupled shear walls using Rayleigh's principle, considering the vibrating cantilever modes as the approximate mode shapes for the coupled shear walls. They also performed seismic analysis using the response spectrum technique. On the other hand, Coull and Mukherjee [11, 12] used the Galerkin method to obtain the fundamental frequency and mode shape for coupled shear walls. Rutenberg [13] proposed an approximate formula for the calculation of natural frequencies of coupled shear walls assuming the deflected shape of the structure as the sum of the deflections due to pure flexure cantilever action and shear-flexure cantilever action using the Dunkerley formula.

Tso and Rutenberg [15] performed a seismic spectral response analysis of coupled shear walls on rigid foundations. They used the cantilever mode shapes as the approximate shapes of the shear wall structure, thus avoiding the complexity of using the exact mode shapes. They used the response spectrum technique suggested by NBCC (1980) and presented curves and charts for various dynamic response parameters. Actually, their investigation is an extension of that by Tso and Biswas [10].

1.2.2 Analysis of Structures Considering Base Flexibility

There is little literature [16-20] available which concerns the base flexibility of coupled shear walls. Since the footings rest on soil and the soil has elastic properties, the flexibility of the foundation affects response. There are three types of flexibility associated with two-dimensional isolated footings; there are vertical, horizontal and

rotational flexibilities. Usually, in single walls and beams, the rotational and horizontal flexibilities are considered, whereas in coupled shear walls the vertical and rotational flexibilities are important.

Coull [16] studied the effect of foundation flexibility on coupled shear walls considering two walls of different cross-sections and moments of inertia, basing the solution on the continuim technique. He considered the vertical and rotational settlements independently and gave closed form solution for lateral static loadings. It was also suggested that the proposed theory may be used for nonlinear foundation behaviour. Tso and Chan [17] used the same method to study the combined effect of vertical and rotational flexibilities on uniform coupled shear walls. Coull and Chantaksinopas [18] provided design curves for rapid evaluation of the stresses and maximum deflection of coupled shear walls supported by elastic foundation, portal frames or columns assuming a static lateral loading system.

More recently, free vibration analysis of flexibly mounted coupled shear walls have been reported by a number of researchers [19,20]. Mukherjee and Coull [19] obtained the natural frequencies of coupled shear walls on elastic foundations using the Ritz-Galerkin technique. They also provided the first two mode shapes. In addition, they compared the natural frequencies obtained by using their proposed analysis with matrix progression and showed that the results are reasonable.

Cheung and Swaddiwudhipong [20] studied the free vibration of coupled frame-shear wall structures on flexible foundations. They observed the effect of foundation flexibility on natural frequencies utilizing the finite strip method and compared the results with other existing methods such as the finite element method and the method proposed

by Mukherjee and Coull [19].

1.3 SCOPE AND OBJECTIVE OF PRESENT STUDY

The objective of the present study is to investigate the dynamic response of both single (isolated) shear walls and coupled shear walls supported on rotationally flexible foundations.

The analysis is approximate and is based on the response spectrum technique. For this approximate analysis the first three mode shapes of a vibrating cantilever beam with rotationally flexible support are used to calculate various dynamic responses.

1.4 ORGANIZATION OF THE THESIS

The investigation reported herein is organized in the following manner.

The basic formulation for the free vibration of cantilever beams with rotationally flexible support represented by a spring (i.e., frequency equation, mode shapes and participation factor) are derived in Chapter II.

The approximate seismic analysis of isolated (single) shear walls on flexible foundations is carried out in Chapter III, where the mode shapes derived in Chapter II are utilized to calculate the modal loading, base shear, base moment and top deflection.

Chapter IV is devoted to investigating the seismic analysis of coupled shear walls on flexible foundations. Using the mode shapes of a vibrating cantilever beam with rotational spring support, the base shear, base moment and top deflection of coupled shear walls are presented as

functions of structural parameters and base flexibility. Also, numerical examples are presented to show the importance of base flexibility for two prototype shear wall buildings.

Finally, the general conclusions are presented in Chapter V.

CHAPTER II

DYNAMIC PROPERTIES OF CANTILEVER BEAM WITH ROTATIONAL SUPPORT FLEXIBILITY

2.1 INTRODUCTION

In this Chapter the vibration properties of a cantilever beam with rotational spring support are presented. These will later be applied to the problems of single walls and coupled shear walls on flexible foundations. The governing differential equation, the frequency equation, as well as the mode shapes and frequency parameters, will be reviewed here, although they are available in the literature [1,2].

Gorman [1] presented the frequency equations and expressions for the mode shapes of single-span beams with various non-classical boundary conditions, including cantilever beams with rotational spring support.

Macbain and Genin [2] on the other hand, studied the effect of support flexibility on only the fundamental frequency of vibrating beams. They showed the effect of rotational and translational support flexibility on the fundamental frequency of beams supported at both ends and flexibly supported cantilever beams. They showed that in each case the effect of rotational flexibility is more important for decreasing values of the length-to-depth ratio. They also provided an expression for the fundamental frequency as a function of support flexibility, length-to-depth ratio, and frequency of rigid support conditions.

2.2 FLEXURAL VIBRATION OF UNIFORM CANTILEVER BEAM WITH FLEXIBLE SUPPORT

The lateral vibration of a beam in the x-y plane is shown in Fig. 2.1(a). The free-body diagram of a short segment of length dx is shown in Fig. 2.1(b).

Defining E, I and m as modulus of elasticity, sectional inertia and mass per unit length respectively; shear force as V; bending moment as M; inertia force as $(m\,dx)\partial^2 y/\partial t^2$, and $f = f(x,t)$ as the load per unit length, dynamic equilibrium of forces in the y-direction for transverse vibration of the beam is given by

$$V - \left(V + \frac{\partial V}{\partial x}\,dx\right) - m\,dx\,\frac{\partial^2 y}{\partial t^2} + f(x,t)\,dx = 0 \qquad (2.1)$$

which reduces to

$$\frac{\partial V}{\partial x} + m\,\frac{\partial^2 y}{\partial t^2} = f(x,t) \qquad (2.2)$$

Elementary flexural theory gives the relationship for moment-curvature

$$M = EI\,\frac{\partial^2 y}{\partial x^2} \qquad (2.3)$$

and shear force

$$V = \frac{\partial M}{\partial x} \qquad (2.4)$$

Substituting Eq. (2.3) into Eq. (2.4) yields

$$V = EI \frac{\partial^3 y}{\partial x^3} \tag{2.5}$$

After substitution of Eqs. (2.3) and (2.4), Eq. (2.2) becomes

$$EI \frac{\partial^4 y}{\partial x^4} + m \frac{\partial^2 y}{\partial t^2} = f(x,t) \tag{2.6}$$

or

$$\frac{\partial^4 y}{\partial x^4} + \frac{m}{EI} \frac{\partial^2 y}{\partial t^2} = \frac{f}{EI}(x,t) \tag{2.7}$$

Eq. (2.7) is an approximate equation because it is derived considering only flexural deflection, neglecting deflection due to shear and rotary inertia of the cross-section. The equation also excludes flexural effects due to the presence of axial force.

If only free vibration of the beam is considered, $f(x,t) = 0$ and Eq. (2.7) reduces to the homogeneous differential equation

$$\frac{\partial^4 y}{\partial x^4} + \frac{m}{EI} \frac{\partial^2 y}{\partial t^2} = 0 \tag{2.8}$$

This equation may also be written as

$$\frac{\partial^4 y}{\partial x^4} + \frac{1}{b^2} \frac{\partial^2 y}{\partial x^2} = 0 \tag{2.9}$$

where

$$b = \sqrt{\frac{EI}{m}} \tag{2.10}$$

For harmonic motion, direct substitution leads to the general solution

$$y(x) = B_1 \sin \beta x + B_2 \cos \beta x + B_3 \sinh \beta x + B_4 \cosh \beta x \qquad (2.11)$$

where parameter β is related to natural frequency ω by $\beta^4 = \omega^2 m/EI$ and B_1, B_2, B_3 and B_4 are arbitrary constants.

The boundary conditions for the cantilever beam with rotationally flexible support are:

a) at base where $x = 0$,

$$y(o) = 0 \qquad (2.12)$$

$$K_\theta y'(o) = EI\, y''(o) \qquad (2.13)$$

b) at top where $x = H$,

$$y''(H) = 0 \qquad (2.14)$$

$$y'''(H) = 0 \qquad (2.15)$$

Here, K_θ represents the support rotational spring stiffness.

2.3 FREQUENCY EQUATION

From Eqs. (2.11) and (2.12)

$$y(o) = 0, \quad B_2 = -B_4 \qquad (2.16)$$

$$y'(0) = \beta (B_1 + B_3) \tag{2.17}$$

$$y''(o) = \beta^2 (-B_2 + B_4) \tag{2.18}$$

From Eqs. (2.16) and (2.18)

$$y''(o) = 2B_4\beta^2 \tag{2.19}$$

Substituting $y'(o)$ and $y''(o)$ from Eqs. (2.17) and (2.19) into Eq. (2.13) gives

$$B_4 = \frac{K_\theta}{2\beta EI} (B_1 + B_3) \tag{2.20}$$

From Eq. (2.14)

$$y''(H) = \beta^2 (-B_1 \sin \beta H - B_2 \cos \beta H + B_3 \sinh \beta H + B_4 \cosh \beta H) = 0 \tag{2.21}$$

After substitution of Eqs. (2.16) and (2.20)

$$B_1 (\cos \beta H + \cosh \beta H - \frac{2\beta EI}{K_\theta} \sin \beta H) +$$

$$B_3 (\cos \beta H + \cosh \beta H + \frac{2\beta EI}{K_\theta} \sinh \beta H) = 0 \tag{2.22}$$

Similarly, from Eq. (2.15), the following expression is obtained

$$B_1 (\sin \beta H - \sinh \beta H + \frac{2\beta EI}{K_\theta} \cos \beta H) +$$

$$B_3 \left(\sin \beta H - \sinh \beta H - \frac{2\beta EI}{K_\theta} \sinh \beta H\right) = 0 \qquad (2.23)$$

Equations (2.22) and (2.23) can be written in matrix form as

$$\begin{bmatrix} \cos \beta H + \cosh \beta H - \frac{2\beta EI}{K_\theta} \sin \beta H & \cos \beta H + \cosh \beta H + \frac{2\beta EI}{K_\theta} \sinh \beta H \\ \sin \beta H - \sinh \beta H + \frac{2\beta EI}{K_\theta} \cos \beta H & \sin \beta H - \sinh \beta H - \frac{2\beta EI}{K_\theta} \cosh \beta H \end{bmatrix} \times \begin{Bmatrix} B_1 \\ B_3 \end{Bmatrix} = \begin{Bmatrix} 0 \\ 0 \end{Bmatrix} \qquad (2.24)$$

For coefficients B_1 and B_3 to be non-zero, this equation requires that the determinent of the square matrix vanish. Setting this determinant to zero provides the following frequency equation:

$$\left(\cos \beta H + \cosh \beta H - \frac{2\beta EI}{K_\theta} \sin \beta H\right)\left(\sin \beta H - \sinh \beta H - \frac{2\beta EI}{K_\theta} \cosh \beta H\right) -$$

$$\left(\cos \beta H + \cosh \beta H + \frac{2\beta EI}{K_\theta} \sinh \beta H\right) \times$$

$$\left(\sin \beta H - \sinh \beta H + \frac{2\beta EI}{K_\theta} \cos \beta H\right) = 0 \qquad (2.25)$$

After simplification Eq. (2.25) becomes

$$R = \frac{\beta H(\sin \beta H \cosh \beta H - \cos \beta H \sinh \beta H)}{1 + \cos \beta H \cosh \beta H} \qquad (2.26)$$

where the non-dimensional parameter R represents the degree of rotational end fixity given by

$$R = K_\theta H/EI \tag{2.27}$$

Thus, Eq. (2.26) becomes the required frequency equation of the cantilever beam with rotationally flexible support.

The solution of transcendental Eq. (2.26) defines the values of βH which provides the frequencies of vibration as functions of end-fixity parameter R. In the present investigation, the values of βH for different modes of vibration are obtained employing the computer subroutine ZSCNT† from the IMSL* library. Once the magnitude of βH is known, the frequency parameter λ, defined as

$$\lambda = (\beta H)^2 \tag{2.28}$$

yields the natural frequencies of vibration

$$\omega = \lambda\sqrt{\frac{EI}{mH^4}} \tag{2.29}$$

2.4 MODE SHAPES

To determine the mode shapes, either of the two equations in matrix expression (2.24) may be used to express the coefficient B_3 in terms of B_1; using the first gives

---

† This is the subroutine in the IMSL library and it solves a system of nonlinear equations by an iterative process.

* International Mathematical and Statistical Library Inc. provides sets of computational Computer subroutines.

$$B_3 = B_1 = \left(\frac{\cos \beta H + \cosh \beta H - \frac{2\beta H}{R} \sin \beta H}{\cos \beta H + \cosh \beta H + \frac{2\beta H}{R} \sinh \beta H}\right) \tag{2.30}$$

This equation, together with Eqs. (2.16) and (2.20), expresses Eq. (2.11) in terms of only coefficient B_1 as

$$y(x) = B_1 \left[(\sin \beta x - \sinh \beta x) - \gamma(\cos \beta x - \cosh \beta x - \frac{2\beta H}{R} \sinh \beta x)\right] \tag{2.31}$$

where

$$\gamma = \frac{\sin \beta H + \sinh \beta H}{\cos \beta H + \cosh \beta H + \frac{2\beta H}{R} \sinh \beta H} \tag{2.32}$$

If it is assumed that $B_1 = 1$, Eq. (2.31) expresses mode shape $\phi(x)$ as

$$\phi(x) = \sin \beta x - \sinh \beta x - \gamma (\cos \beta x - \cosh \beta x - \frac{2\beta H}{R} \sinh \beta x) \tag{2.33}$$

This is the required mode shape of the cantilever beam with rotationally flexible support. After the modal values of βH are obtained from Eq. (2.26), the mode shapes may be obtained from Eq. (2.33) as functions of flexibility parameter R.

2.5 RESULTS AND DISCUSSION

Results are plotted in Figs. 2.2 to 2.5 for the first three modes. Fig. 2.2 shows the variation of frequency parameter λ with end fixity parameter R as given by Eq. (2.26), whereas Figs. 2.3 to 2.5 show the

mode shapes for R varied to assume the selected values ∞, 50, 10 and 1.0.

In the curves of Fig. 2.2 the effect of support flexibility on frequency parameter λ is seen to be prominent in the first mode. As base flexibility increases (i.e., R decreases), the magnitude of λ decreases as is to be expected. Over the entire range of R, the maximum reduction in λ is 98.0%, 29.5% and 20.5% for the first, second and third modes of vibration respectively. Thus, the fundamental mode frequency can be expected to be relatively sensitive to the rotational support flexibility, particularly for variation of R within the range 0.1 to 10, which represents the range in magnitude of R encountered in practice for shear walls. From the frequency parameter curves in Fig. 2.2 and the shapes of the first three modes of vibration, presented in Figs. 2.3 to 2.5, it is noted that the effect of base flexibility is not much significant when $R \geq 50$. Such foundations may therefore be treated as if rigid, because the error involved in considering the frequencies of such R values lies within 2% for all three modes of vibration. On the other hand, for R values between 1 and 10, rotational flexibility has considerable effect on the mode shapes. This implies that the dynamic response of wall structures for which the R values fall below 10 (or so) may be expected to show a strong dependence on the foundation flexibility.

2.6 CONCLUSION

This chapter has reviewed the dynamic properties of cantilever beams with rotational flexibility support. The mode shapes for selective values of flexibility parameter R and the effect of the variation of this parameter on the frequency parameter λ are presented in terms of curves.

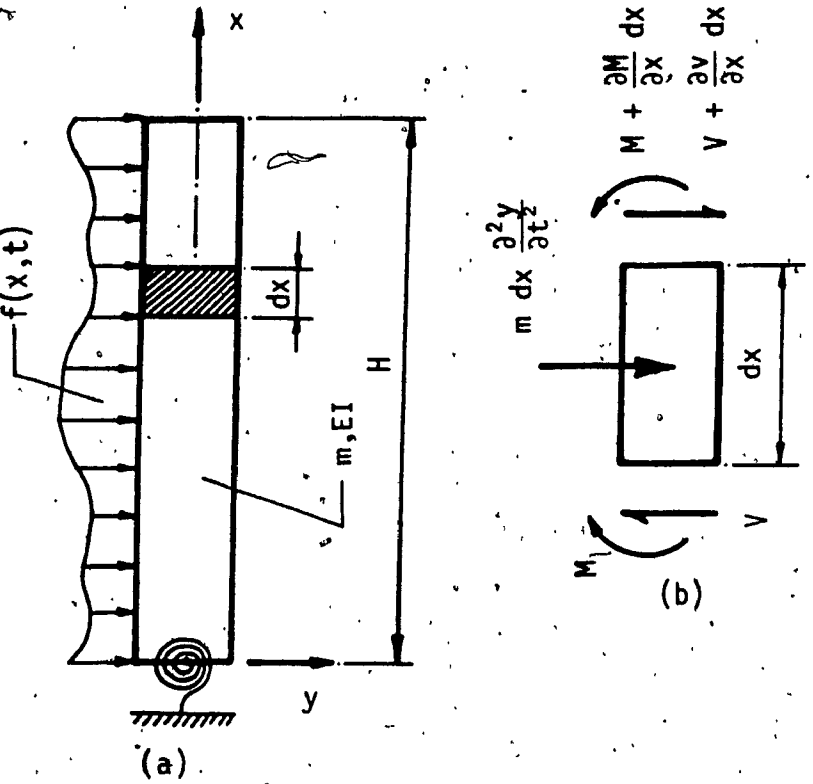

FIG. 2.1 Flexibly Supported Cantilever Beam with Distributed Mass and Loading.

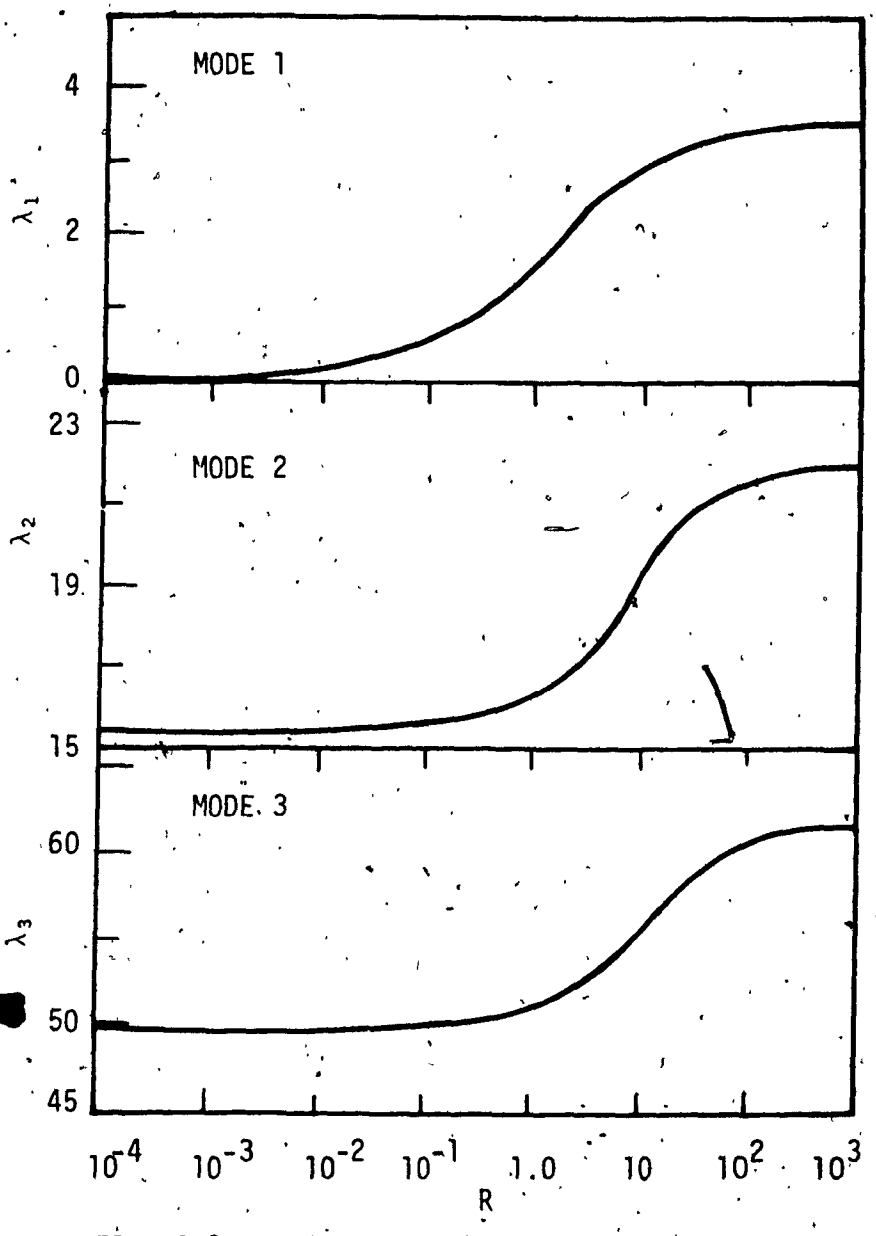

FIG. 2.2 Variation of Frequency Parameter λ with Foundation Flexibility Parameter R - Modes 1, 2 and 3.

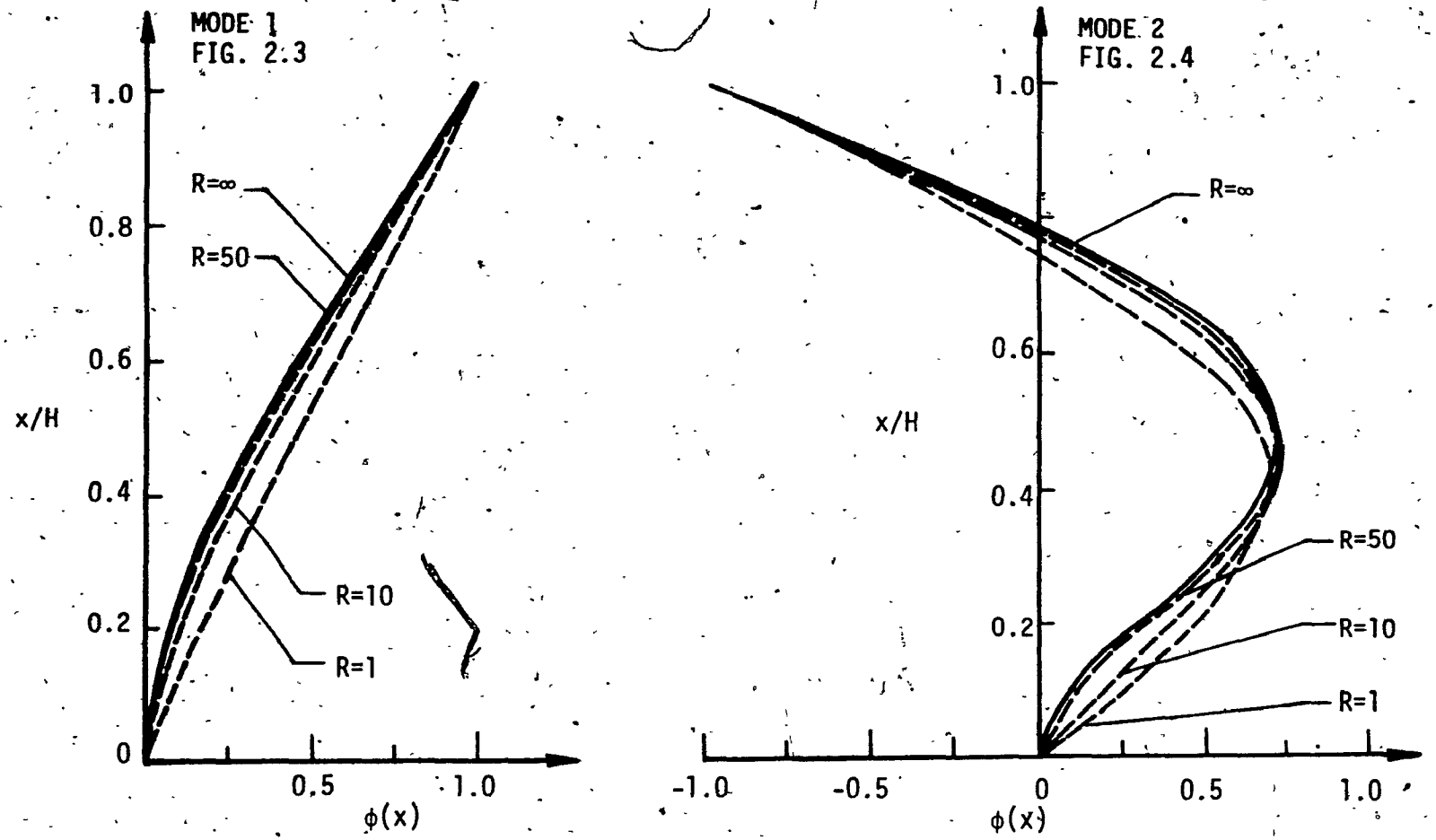

FIGS. 2.3 and 2.4 Mode Shape for Different Values of Foundation Flexibility Parameter R - Modes 1 and 2.

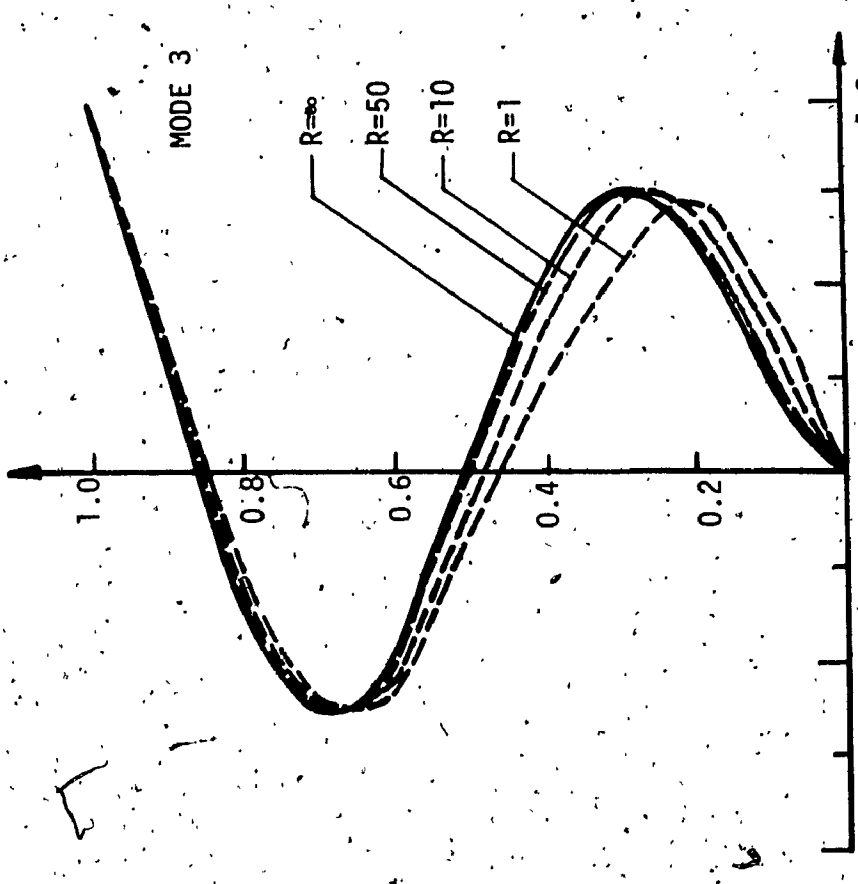

FIG. 2.5 Mode Shape for Different Values of Foundation Flexibility Parameter R - Mode 3.

CHAPTER III

SEISMIC RESPONSE OF SINGLE SHEAR WALLS WITH FLEXIBLE SUPPORT

3.1 INTRODUCTION

Employing the mode shapes and frequency parameters for cantilever beams with rotationally flexible support derived in Chapter II, this Chapter examines the importance of base flexibility on the seismic response of single shear walls. Studied are the response coefficients for base shear, base moment and top deflection as functions of foundation rotational flexibility parameter R. Also presented are the corresponding modal response curves for shear walls varying from 5,10 and 20-storeys in height subjected to the 1980 NBCC seismic design spectrum. The foundation flexibilities associated with these structures are represented by parameter R = 1, 3, 10 and ∞. Finally, to examine prototype cases 5, 10 and 20-storey walls are assumed to rest on dense sand and gravel, prototype foundation sizes are selected and the importance of rotational base flexibility is examined.

3.2 PROCEDURE FOR SEISMIC ANALYSIS

3.2.1 Governing Equations

The seismic response of a single shear wall on flexible foundations can be analized as a flexibly supported cantilever beam. The governing differential equation for the flexural vibration of such walls can be represented as (Eq. (2.8)):

$$EI \frac{d^4y}{dx^4} = w(t) \tag{3.1}$$

For seismic analysis, the loading term in the above equation takes the form

$$w(t) = -m\ \ddot{y}(t) - m\ \ddot{U}g(t) \tag{3.2}$$

in which m and $\ddot{U}g$ represent, respectively, mass per unit height and ground acceleration.

The general solution and boundary conditions for Eq. (3.1) have been given in Chapter II (see Eqs. (2.11 - 2.15)).

3.2.1a Participation Factor

Based on the mode shape of Eq. (2.33) of Chapter II, the modal participation factor for the rth mode becomes

$$P_r = \frac{\int_0^H \phi_r(x)\ dx}{\int_0^H [\phi_r(x)]^2\ dx} \tag{3.3}$$

which, after performing some mathematical steps, gives

$$P_r = \left[\frac{F_1}{F_2+F_3-F_4}\right] \tag{3.4}$$

where

$$F_1 = 4[2 - \cos \beta_r H - \cosh \beta_r H - \gamma_r (\sin \beta_r H - \sinh \beta_r H$$

$$- \frac{2\beta_r H}{R} \cosh \beta_r H + \frac{2\beta_r H}{R})] \quad (3.5)$$

$$F_2 = [\sinh 2\beta_r H - \sin 2\beta_r H - 4(\sin \beta_r H \cosh \beta_r H + \cos \beta_r H \sinh \beta_r H)] \quad (3.6)$$

$$F_3 = \gamma_r^2 [\sin 2\beta_r H + \sinh 2\beta_r H + 4(\beta_r H - \cos \beta_r H \sinh \beta_r H - \sin \beta_r H \cosh \beta_r H + \frac{\beta_r^2 H^2}{R^2} \sinh 2\beta_r H) - \frac{8\beta_r H}{R^2} (\beta_r^2 H^2 - R \cos \beta_r H \cosh \beta_r H - R \sin \beta_r H \sinh \beta_r H + \frac{R}{2} + \frac{R}{2} \cos 2\beta_r H)] \quad (3.7)$$

$$F_4 = 2\gamma_r [\cosh 2\beta_r H - \cos 2\beta_r H - 4 \sin \beta_r H \sinh \beta_r H - \frac{4\beta_r H}{R} \sin \beta_r H \cosh \beta_r H + \frac{4\beta_r H}{R} \cos \beta_r H \sinh \beta_r H + \frac{2\beta_r H}{R} \sinh 2\beta_r H - \frac{4\beta_r^2 H}{R}] \quad (3.8)$$

The effect of base flexibilities on the participation factors are presented in Fig. E1 (Appendix E).

3.2.1b Modal Loading

Associated with mode shape $\phi_r(x)$, the loading is

$$w_r(x) = m P_r S_{ar} \phi_r(x) \quad (3.9)$$

where S_{ar} = spectral acceleration for the rth mode.

3.2.2 Modal Response Expressions

3.2.2a Modal Base Shear and Base Moment

Once the modal loading is known the modal base shear is obtained

from

$$V_r(o) = \int_0^H w_r(x)\, dx \qquad (3.10)$$

which results in the expression

$$V_r(o) = \frac{N_r m H P_r S_{ar}}{\beta_r H} \qquad (3.11)$$

where

$$N_r = 2\left[1 - \frac{\beta_r H \gamma_r}{R}\right] \qquad (3.12)$$

and R is the nondimensional foundation flexibility parameter $= \frac{K_\theta H}{EI}$ (see Eq. (2.27) of Chapter II).

The modal base moment can be expressed as

$$M_r(o) = \int_0^H x\, w(x)\, dx \qquad (3.13)$$

which yields

$$M_r(o) = \left[\frac{2mH^2 P_r S_{ar} \gamma_r}{(\beta_r H)^2}\right] \qquad (3.14)$$

in terms of modal participation factor, spectral acceleration and mass per unit height. Expressed in terms of base shear $V_r(o)$ this becomes

$$M_r(o) = \frac{2V_r(o) H \gamma_r}{N_r \beta_r H} \qquad (3.15)$$

3.2.2b Top Deflection

The top deflection of the shear wall on a flexible foundation can be represented in terms of base shear, total height of the wall and the mode shape by

$$y_r(H) = \frac{V_r(o)H^3\phi_r(H)}{N_r\, EI(\beta_r H)^3} \tag{3.16}$$

3.2.3 Response Coefficients as Function of R

3.2.3a Governing Expressions

The modal dynamic responses can be represented by coefficients such as shear coefficient $C_{s,r}$, moment coefficient $C_{m,r}$ and top deflection coefficient $C_{d,r}$. The expression for these response coefficients are given below.

(a) Shear Coefficient:

$$C_{s,r} = \frac{V_r(o)}{mHS_{ar}} = \frac{N_r P_r}{\beta_r H} \tag{3.17}$$

(b) Moment Coefficient:

$$C_{m,r} = \frac{M_r(o)}{V_r(o)H} = \frac{2\gamma_r}{N_r\beta_r H} \tag{3.18}$$

(c) Top Deflection Coefficient:

$$C_{d,r} = \frac{y_r(H)EI}{V_r(o)H^3} = \frac{\phi_r(H)}{N_r(\beta_r H)^3} \tag{3.19}$$

3.2.3b Response Coefficient Curves

Since $\phi_r(H)$, N_r etc. are functions of the nondimensional foundation flexibility parameter, the response coefficients of Eqs. (3.17 - 3.19) may be plotted as curves for varying R. Figs. 3.1 to 3.3 represent such curves for values of R ranging from 0.1 to 1×10^4. It should be noted that the lower values of R represent foundations that are flexible, whereas high values ($R = 10^4$) define rigid foundations.

3.2.3c Results and Discussion

(A) Shear Coefficient Curves

Fig. 3.1 shows the variation of shear coefficient with variation of nondimensional foundation flexibility parameter R.

It is observed in Fig. 3.1 that if the value of parameter $R > 100$, the effect of base flexibility becomes insignificant and one may consider the base as fixed with $R = \infty$ ($C_{s,r} = 0.613$). However, if the value of R decreases from 100 to 0.1, then the effect of base flexibility becomes significant. It is noticed that, for the first mode, the magnitude of the shear coefficient increases to a maximum value of 0.743 for $R = 0.25$, which is 21.2 percent greater than the rigid foundation condition.

For modes 2 and 3 the effect of base flexibility on the shear coefficient is more significant than for mode 1, with the effect most prominent for mode 3. It is important to note that the shear coefficient increases for the first mode as R decreases, whereas in the higher modes $C_{s,r}$ decreases. The maximum decrease from rigid foundations ($R = \infty$) to very flexible foundations ($R = 0.1$) for the second and third modes is 25 percent and 38.5 percent, respectively.

(B) Moment Coefficient Curves

The moment coefficient curves presented in Fig. 3.2 show that $C_{m,r}$ generally decreases as the foundation becomes progressively more flexible. It is observed that the higher modes of vibration are more sensitive to the magnitude of R than is the fundamental mode. Values of moment coefficients for the most flexible foundation (R = 0.1) are 0.006 for mode 2 and 0.002 for mode 3. These are, respectively, 97.0 and 98.4 percent less than obtained for the rigid base.

(C) Top Deflection Coefficient Curves

The effect of the variation of the base flexibility on top deflection coefficient $C_{d,r}$ is shown in Figs. 3.3. It can be understood from this figure that the contribution to the top deflection, with decreasing R, is most important in the fundamental mode as compared to the two higher modes of vibration. The effect of the base flexibility for the very flexible condition (R = 0.1) results in magnitudes of $C_{d,r}$ that are 97, 59 and 50 percent higher than for the corresponding top deflection coefficient for a fixed base.

3.2.4 Seismic Response of Example Structures as Function of R

3.2.4a Prototype Structures

The prototype structures which are considered in this investigation consist of four walls of different heights. These walls are assumed to rest on elastic soil represented by differing magnitude of nondimensional flexibility parameter R (Fig. 3.4). To obtain numerical values of the seismic responses, it is assumed that each wall is associated with four separate R values, namely, R = ∞, 10, 3 and 1.

The properties of the walls considered are as follows: (1) 20-storey wall (H = 54.90m); (2) 15-storey wall (H = 41.18m); (3) 10-storey wall (H = 27.45m); (4) 5-storey wall (H = 13.73m); all are 7.32m wide and 0.305m thick, with A = 13.4m^2 and I = 10.0m^4.

3.2.4b Calculation of Seismic Responses

To evaluate the seismic responses, namely, base shear, base moment and the top deflection for the prototype structure the following steps are involved.

1. Determine frequency ω_r (from Eq. (2.29) of Chapter II). To calculate ω_r, λ_r is determined by using the curves presented in Fig. 2.2; modulus of elasticity E and mass per unit height m are 25×10^6 kN/m^2 and 32.5 kN-sec^2/m, respectively.

2. Calculate the period of vibration, $T_r = \frac{2\pi}{\omega_r}$, sec.

3. Determine spectral acceleration S_{ar} (NBCC 1980;5% damping and zone 3 seismicity) (see Subsection 3.25f and Fig. 3.16).

4. Calculate modal seismic responses $V_r(o)$, $M_r(o)$ and $y_r(H)$ from Eqs. (3.17 - 3.19).

3.2.4c Seismic Response Curves

The various responses which are calculated following the steps of Subsection 3.2.4b are examined in the form of curves as functions of base flexibility parameter R and height of structure H.

To determine spectral acceleration S_{ar} using the NBCC 1980 response spectrum, steps 1 and 2 in Subsection 3.2.4b are very important. Table 3.1 provides the necessary data along with the code spectral accelerations for the prototype structures. Once the spectral accelerations

and the response coefficients are known, the responses can easily be calculated and presented as curves (see Figs. 3.5 - 3.12). The related data for the generation of the seismic response curves presented in these figures are presented in Tables 3.2 to 3.7.

3.2.4d Results and Discussion

(A) Base Shear Curves

In Figs. 3.5 and 3.6 the effect of foundation flexibility on the base shear for the first three modes of vibration are examined for wall heights of 5, 10, 15 and 20-storeys. It is noticed that, in the first mode, the effect of foundation flexibility on base shear is not significant for 5-storey walls. The effect is, however, significant for higher walls. A 10-storey wall with flexibility parameter $R = 1$ exhibits a magnitude of base shear which is approximately 48 percent less than obtained for a rigid base ($R = \infty$). Similarly, for a 20-storey wall with $R = 3$, the corresponding decrease compared to a fixed base is 28.0 per cent. For the higher modes (Fig. 3.6(a,b)) the effect of base flexibility on base shear is less pronounced.

(B) Base Moment Curves

Figs. 3.7 and 3.8 show the variation of base moment with variation of storey height for different values of R.

It is observed that the effect of base flexibility on base moment increases for the higher modes. For example, for a 20-storey wall and $R = 3$, the base moment decreases by 32 percent, 54 percent and 66 percent for the first, second and third modes, respectively, compared to

magnitudes associated with a rigid foundation. Similarly, for a 10-storey wall and $R = 1$, the corresponding decreases are 50, 68 and 97 percent, respectively.

(C) Top Deflection Curves

Base flexibility results in large increases in top deflection as shown in Figs. 3.9 and 3.10 for the first, second and third modes.

The effect is most significant in the first mode. It is important to note that the top deflection is very small (almost zero) in mode 3 when the number of storeys ≤ 10 for all values of R. It is also noticed that in mode 3 the top deflections obtained for $R = 10$, 3 and 1 are very close and plot as a single curve.

In terms of typical effect of base flexibility, a 20-storey wall with $R = 3$ experiences increases in deflection of 32.4, 38.2 and 20.0 percent for modes 1, 2 and 3 compared to the rigid foundation assumption. Similarly, a 10-storey wall with $R = 1$ shows corresponding increases of 54.2, 40.0 and 0 percent.

(D) Response Curves Considering the RSS of Three Modes

Figs. 3.11 and 3.12 summarize the total response for base shear, base moment and top deflection expressed by the root-sum-of-squares of the modal contributions.

For any given value of base flexibility parameter R, the reduction in base moment and base shear from the fixed-base condition is approximately independent of the wall height when the height ≥ 10 storeys. For the 5-storey structure, on the other hand, the effect of base flexibility is relatively insignificant.

Fig. 3.12 shows that the effect of base flexibility on top deflection is important for any wall height. The percent increase in deflection can be expected to be as large for the 5-storey wall as for walls of greater height. Comparing magnitudes for $R = 1$ with those for $R = \infty$ indicates a relatively constant percent decrease in deflection for any height of the wall.

3.2.5 Effect of Base Flexibility for Typical Example Structures

In Section 3.2.4 the effect of base flexibility or seismic response was studied as a function of foundation flexibility R, where theoretical values for R were chosen as 1, 3, 10 and ∞. In real structures, however, values of R should be computed based on actual foundation size and properties of the supporting soil. The latter are discussed in the following subsections. A comparison is also made between the seismic responses for the actual foundation and those for the fixed base.

3.2.5a Prototype Structures

Three shear walls of heights H = 54.90m, 27.45m and 13.73m representing, respectively, 20, 10 and 5-storey structures are studied. The respective foundation sizes are 8.99m x 5.74m, 8.99m x 2.59m and 8.99m x 1.14m. It should be noted that all three walls are 7.32m x 0.305m in cross-section. Figs. 3.13 and 3.15 show the geometrical properties of the walls and foundations. The procedure for selecting the foundation sizes is described below.

3.2.5b Typical Elastic Properties of Soils

The modulus of elasticity E_s for soils and Poisson's ratio ν are principal properties of interest in soil-structure interaction problems. In the present investigation only homogeneous elastic soil is considered. Tables 3.8 and 3.9 provide the values of E_s, ν for different types of soils [21].

3.2.5c Calculation of K_θ

Once the modulus of elasticity and Poisson's ratio of the soil are known, the rotational stiffness K_θ [22] can be calculated from the expression given in the Table 3.10 for rectangular footings (the same expression is repeated below as Eq. (3.20)). Based on the elastic half-space theory for homogeneous soil, the rotational stiffness is given by

$$K_\theta = \frac{G\beta_\phi BL^2}{1-\nu} \qquad (3.20)$$

where

G = shear modulus of the soil

β_ϕ = coefficient from Fig. 3.15

L = length of foundation

B = width of foundation

3.2.5d Calculation of Foundation Sizes

The foundation sizes mentioned in Subsection 3.2.5a are calculated on the assumption that the example shear walls rest on dense sand and

gravel having bearing capacity q_a = 766 kPa [21]. Modulus of elasticity $E_s = 1.4 \times 10^5 kN/m^2$ and Poisson's ratio $\nu = 0.3$.

It should also be remembered that, to calculate the foundation sizes, one has to know the base shear. The static base shear used in this investigation is obtained according to NBCC 1980 [23]:

$$V = ASKIFW \tag{3.21}$$

where

A = design ground acceleration at the size (0.08g)

S = seismic factor = $0.05/\sqrt{T}$

K = structural factor (1.3)

T = fundamental period of vibration

I = importance factor (1.0)

F = foundation factor (1.0)

W = weight of the structure = $w_h H$

w_h = weight per unit height (321 kN/m)

h_n = height of wall = H

With the base shear known the overturning moment can be computed. This allows the size of the foundation to be determined based on combining stresses:

$$q_a = \frac{P}{A} + \frac{M}{S} \tag{3.22}$$

where

P = total load (DL + LL) on wall (18,703 kN, 14,030 kN, 9,353 kN, 4,676 kN for 20, 15, 10 and 5-storey structures)

DL = dead load of the structure (17,622 kN, 13,216 kN, 8,811 kN, 4,405 kN for 20, 15, 10 and 5-storey structures)

LL = live load of structure (1,081 kN, 814 kN, 542 kN, 271 kN for 20, 15, 10 and 5-storey structures)

S = section modulus = $\frac{BL^2}{6}$

For the sizes of the foundation shown in Fig. 3.14, Eq. (3.20) gives rotational spring stiffnesses K_θ = 2×10^7 kN.m/rad, 1.2×10^7 kN.m/rad, and 8.1×10^6 kN.m/rad, for 20, 10 and 5-storey walls, respectively.

3.2.5e Calculation of R

The expression $R = K_\theta H/EI$ (see Eq. (2.27)) gives the values of R for 20, 10 and 5-storey walls as 4.50, 1.36 and 0.50, respectively. The modulus of elasticity and moment of inertia of the walls are taken as 25×10^6 kN/m^2 and 10.0 m^4, respectively.

3.2.5f Design Ground Motion (Response Spectrum)

For the generation of the modal responses, the 5% damped NBCC 1980 [23] elastic design spectrum is used. The response spectrum is shown in Fig. 3.16, normalized to 1.0g ground acceleration. It is assumed that the shear walls are located at a seismic zone 3 site, for which the peak ground acceleration A = 0.08g.

3.2.5g Comparison of Fixed and Flexible-Base Response

The comparison between the rigid and flexible foundation behaviour

is presented in terms of response coefficients and magnitudes of modal responses. Table 3.11 lists the values of the parameters λ_r, T_r, S_{ar}, $C_{s,r}$, $C_{m,r}$ and $C_{d,r}$ for 5, 10 and 20-storey walls resting on fixed and and flexible foundations. Tables 3.12 through 3.14 present corresponding shear, base moment and top deflection for rigid and flexible foundation conditions. The tables also show the RSS of three modes for the different seismic responses.

Table 3.12 shows that for a 5-storey wall, the RSS values for base shear, base moment and top deflection of the flexible foundation are, respectively, 1.22, 1.13 and 8.99 times the values obtained for the rigid foundation. Similarly, for the 10-storey wall (R = 1.36, Table 3.13) the responses are 0.61, 0.54 and 1.46 times the responses for the rigid foundation. The RSS of base shear, base moment and top deflection for a 20-storey wall (R = 4.5) are 0.93, 0.71 and 1.24 times the responses obtained for the rigid foundation.

Therefore, from Tables 3.12 to 3.14, it can be concluded that the single consistent trend concerning the effect of base flexibility is that the flexibility of actual foundations increases the top deflection. The increase is most apparent for low-rise walls, with particularly dramatic increase observed for the 5-storey structure.

3.3 CONCLUSION

The seismic analysis of single shear walls on flexible foundations is investigated in this Chapter. A simple approximate method of analysis of such structures is presented based on the mode shape of a cantilever beam with rotationally flexible support. The response coefficients and the modal responses for varying magnitude of the foundation flexibility

parameter R are presented as curves and in tables for different wall heights. In addition, the seismic responses of three example structures with prototype foundations assumed resting on dense sand and gravel are compared with magnitudes of response associated with perfectly rigid bases.

TABLE 3.1

Frequency, Period and Spectral Acceleration
for Different Wall Heights and Parameter R

R	H (m)	ω(rad/sec) MODE			T (sec) MODE			Sa MODE		
		1	2	3	1	2	3	1	2	3
∞	54.90	3.227	20.224	56.631	1.947	0.31	0.111	0.053g	0.24g	0.24g
	41.18	5.737	35.953	100.677	1.095	0.175	0.062	0.094g	0.24g	0.164g
	27.45	12.908	80.894	226.524	0.487	0.078	0.028	0.211g	0.24g	0.08g
	13.73	51.633	323.575	906.096	0.122	0.019	0.007	0.24g	0.08g	0.08g
10	54.90	2.73	17.77	50.96	2.30	0.35	0.12	0.045g	0.24g	0.24g
	41.18	4.845	31.590	90.587	1.297	0.199	0.069	0.079g	0.24g	0.163g
	27.45	10.90	71.077	203.821	0.576	0.088	0.031	0.178g	0.24g	0.08g
	13.73	43.6	284.307	815.282	0.144	0.022	0.01	0.24g	0.08g	0.08g
3	54.90	2.101	15.990	48.097	2.991	0.393	0.131	0.034g	0.24g	0.24g
	41.18	3.735	28.427	85.506	1.682	0.221	0.074	0.061g	0.24g	0.174g
	27.45	8.404	63.962	192.388	0.748	0.098	0.033	0.137g	0.24g	0.078g
	13.73	33.615	255.847	762.552	0.187	0.025	0.008	0.24g	0.08g	0.08g
1	54.90	1.430	14.914	46.725	4.394	0.421	0.135	0.023g	0.24g	0.24g
	41.18	2.542	26.513	83.066	2.472	0.237	0.076	0.042g	0.24h	0.183g
	27.45	5.720	56.655	186.900	1.098	0.111	0.034	0.093g	0.24g	0.08g
	13.73	22.880	238.621	747.598	0.275	0.026	0.008	0.24g	0.08g	0.08g

TABLE 3.2

Base Shear for Different Wall Heights and Parameter R

R	H (m)	Base Shear V(o), kN		
		MODE		
		1	2	3
∞	54.90	572.6	795.2	274.9
	41.18	761.7	596.4	140.9
	27.45	1139.7	397.6	45.8
	13.73	648.4	66.3	22.9
10	54.90	520.2	795.2	249.5
	41.18	685.1	596.4	127.1
	27.45	1028.9	397.6	41.6
	13.73	693.9	66.3	20.8
3	54.90	412.2	719.0	219.9
	41.18	554.8	539.3	119.6
	27.45	830.5	359.5	35.7
	13.73	727.7	59.9	18.3
1	54.90	294.7	647.1	186.1
	41.18	403.6	485.4	106.4
	27.45	595.8	323.6	31.0
	13.73	769.0	54.0	15.5

TABLE 3.3

Base Moment for Different Wall Heights and Parameter R

R	H (m)	Base Moment M(o), kN.m		
		MODE		
		1	2	3
∞	54.90	22851.8	9123.6	1916.8
	41.18	22803.5	5133.3	737.0
	27.45	22744.0	2280.9	159.7
	13.73	6472.2	190.2	40.0
10	54.90	20192.3	6722.6	1054.9
	41.18	19944.7	3782.4	403.1
	27.45	19967.9	1680.7	87.9
	13.73	6735.7	140.2	22.0
3	54.90	15683.8	4184.2	652.0
	41.18	15831.8	2354.2	266.0
	27.45	15799.1	1046.1	63.8
	13.73	6924.4	87.2	13.6
1	54.90	10936.0	1705.3	183.9
	41.18	11235.9	959.5	78.9
	27.45	11054.9	426.3	15.3
	13.73	7137.4	35.6	3.8

TABLE 3.4

Top Deflection for Different Wall Heights and Parameter R

R	H (m)	Top Deflection Y(H), mm		
		MODE		
		1	2	3
∞	54.90	78.0	4.7	0.4
	41.18	44.0	1.5	0.1
	27.45	19.5	0.3	0.0
	13.73	1.4	0.0	0.0
10	54.90	93.0	6.3	0.5
	41.18	51.7	2.0	0.1
	27.45	23.0	0.4	0.0
	13.73	2.0	0.0	0.0
3	54.90	115.4	7.6	0.5
	41.18	65.6	2.4	0.1
	27.45	29.1	0.5	0.0
	13.73	3.2	0.0	0.0
1	54.9	168.5	8.1	0.5
	41.18	97.4	2.6	0.1
	27.45	42.6	0.5	0.0
	13.73	6.9	0.0	0.0

TABLE 3.5

RSS of Base Shear (kN)

R	No. of Storeys			
	20	15	10	5
∞	1017.7	977.6	1207.9	652.2
10	982.4	917.2	1103.8	697.4
3	857.5	782.9	905.7	730.4
1	735.0	640.2	678.7	771.0

TABLE 3.6

RSS of Base Moment (kN.m)

R	No. of Storeys			
	20	15	10	5
∞	24680.3	23385.7	22858.7	6475.1
10	21308.1	20304.2	20038.7	6737.2
3	16245.4	16008.1	15833.8	6924.9
1	11069.7	11277.1	11063.1	7137.5

TABLE 3.7

RSS of Top Deflection (mm)

R	No. of Storeys			
	20	15	10	5
∞	78.1	44.0	19.5	1.4
10	93.2	51.7	23.0	2.0
3	115.7	65.6	29.1	3.2
1	168.7	97.4	42.6	6.9

TABLE 3.8

Modulus of Elasticity for Different Types of Soil [21]

TYPE OF SOIL	E_s (kN/m²)
CLAY	
Very soft	3.5×10^2 - 2.8×10^3
Soft	1.4×10^3 - 4.1×10^3
Medium	4.1×10^3 - 8.3×10^3
Hard	7×10^3 - 2.1×10^4
Sandy	2.8×10^4 - 4.1×10^4
Glacial fill	1×10^4 - 1.5×10^5
Loose	1.4×10^4 - 5.5×10^4
SAND	
Silty	7×10^3 - 2.1×10^4
Loose	1×10^4 - 2.4×10^4
Dense	4.8×10^4 - 8.3×10^4
SAND AND GRAVEL	
Dense	9.7×10^4 - 2×10^5
Loose	4.8×10^4 - 1.4×10^5
Shale	1.4×10^5 - 1.4×10^7
Silt	2.1×10^3 - 2.1×10^7

TABLE 3.9

Poisson's Ratio for Different Soils [21]

TYPE OF SOIL	POISSON'S RATIO υ
Clay, saturated	0.4 - 0.5
Clay, unsaturated	0.1 - 0.3
Sandy, Clay	0.2 - 0.3
Silt	0.3 - 0.35
Sand (dense)	0.2 - 0.4
Course (void ratio = 0.4 - 0.7)	0.15
Fine - Granide (void ratio = 0.4 - 0.7)	0.25
Rock	0.1 - 0.4
Loose	0.1 - 0.3
Ice	0.36
Concrete	0.15

TABLE 3.10

Spring Stiffness K for Rigid Base Resting on Elastic Half-Space [22]

Motion	Circular Footings	Rectangular Footings
Vertical (k_v)	$\frac{4GR}{1-\upsilon}$	$\frac{G}{(1-\upsilon)}\beta_z\sqrt{(BL)}$
Horizontal (k_H)	$\frac{32(1-\upsilon)GR}{7-8\upsilon}$	$2G(1+\upsilon)\beta_x\sqrt{(BL)}$
Rocking (k_ϕ)	$\frac{8GR^3}{3(1-\upsilon)}$	$\frac{G\beta_\phi BL^2}{1-\upsilon}$
Torsion (k_θ)	$\frac{16GR^3}{3}$	

G is the shear modulus for the soil where $G=E/\{2(1+\upsilon)\}$, υ is Poisson's ratio for the soil, R is the radius of the footing, B, L, are the plan dimensions of rectangular pads and β_x, β_z, β_ϕ are coefficients given in Fig. 3.15 (taken from Reference 22)

TABLE 3.11

Computed Values of λ_r, T_r, S_{ar}, $C_{s,r}$ $C_{m,r}$, $C_{d,r}$ for Rigid and Flexible Foundations

H (m)	MODES	λ_r	T_r (sec)	S_{ar}	C_{sr}	C_{mr}	C_{dr}
		Rigid Foundation (R=∞)					
13.73	1	3.516	.122	.24g	.613	.727	.207
	2	22.034	.019	.08g	.188	.209	.009
	3	61.701	.01	.08g	.065	.127	.002
		Flexible Foundation (R=0.5)					
	1	1.5	.285	0.24g	.75	.670	1.5320
	2	16.0	.027	0.08g	.142	.026	.0205
	3	51.0	.010	0.08g	.041	.002	.0038
		Rigid Foundation (R=∞)					
27.45	1	3.516	.487	.211g	.613	.727	.207
	2	22.034	.078	.24g	.188	.209	.009
	3	61.701	.028	.08g	.065	.127	.002
		Flexible Foundation (R=1.36)					
	1	1.75	.978	0.105g	.713	.680	.520
	2	16.6	.103	0.24g	.160	.065	.0180
	3	51.3	.033	0.08g	.046	.015	.0035
		Rigid Foundation (R=∞)					
54.90	1	3.516	1.947	.053g	.613	.727	.207
	2	22.034	.310	.24g	.188	.209	.009
	3	61.701	.111	.24g	.065	.127	.002
		Flexible Foundation (R=4.5)					
	1	2.4	2.852	.036g	.675	.700	.3400
	2	18.0	.380	.24g	.192	.125	.0145
	3	53.5	.128	.24g	.054	.054	.0031

TABLE 3.12

Comparison of Seismic Response for Rigid and Flexible Prototype Foundations: 5-Storey Wall (H=13.73m)

Mode	Rigid Foundation (R=∞)			Flexible Foundation (R=0.5)		
	Base Shear V(o) (kN)	Base Moment M(o) (kN.m)	Top Deflection y(H) (mm)	Base Shear V(o) (kN)	Base Moment M(o) (kN.m)	Top Deflection y(H) (mm)
1	648.4	6472.2	1.4	793.3	7297.8	12.6
2	66.3	190.2	0.0	50.1	17.9	0.0
3	22.9	40.0	0.0	14.5	0.4	0.0
RSS	652.2	6475.1	1.4	795.0	7297.8	12.6

TABLE 3.13

Comparison of Seismic Response for Rigid and Flexible Prototype Foundations: 10-Storey Wall (H=27.45m)

MODES	Rigid Foundation (R=∞)			Flexible Foundation (R=1.36)		
	Base Shear V(o) (kN)	Base Moment M(o) (kN.m)	Top Deflection y(H) (mm)	Base Shear V(o) (kN)	Base Moment M(o) (kN.m)	Top Deflection y(H) (mm)
1	1139.7	22744.0	19.5	659.7	12313.4	28.4
2	397.6	2280.9	0.3	338.4	603.7	0.5
3	45.8	159.7	0.0	32.4	13.4	0.0
RSS	1207.9	22858.7	19.5	742.1	12328.2	28.4

TABLE 3.14

Comparison of Seismic Response for Rigid and Flexible Prototype Foundations: 20-storey Wall (H=54.90m)

	Rigid Foundation (R=∞)			Flexible Foundation (R=4.5)		
MODES	Base Shear V(o) (kN)	Base Moment M(o) (kN.m)	Top Deflection y(H) (mm)	Base Shear V(o) (kN)	Base Moment M(o) (kN.m)	Top Deflection y(H) (mm)
1	572.6	22851.8	78.0	428.2	16457.2	96.4
2	795.2	9123.6	4.7	812.1	5572.8	7.8
3	274.9	1916.8	0.4	228.4	677.1	0.5
RSS	1017.7	24680.3	78.1	946.0	17388.3	96.7

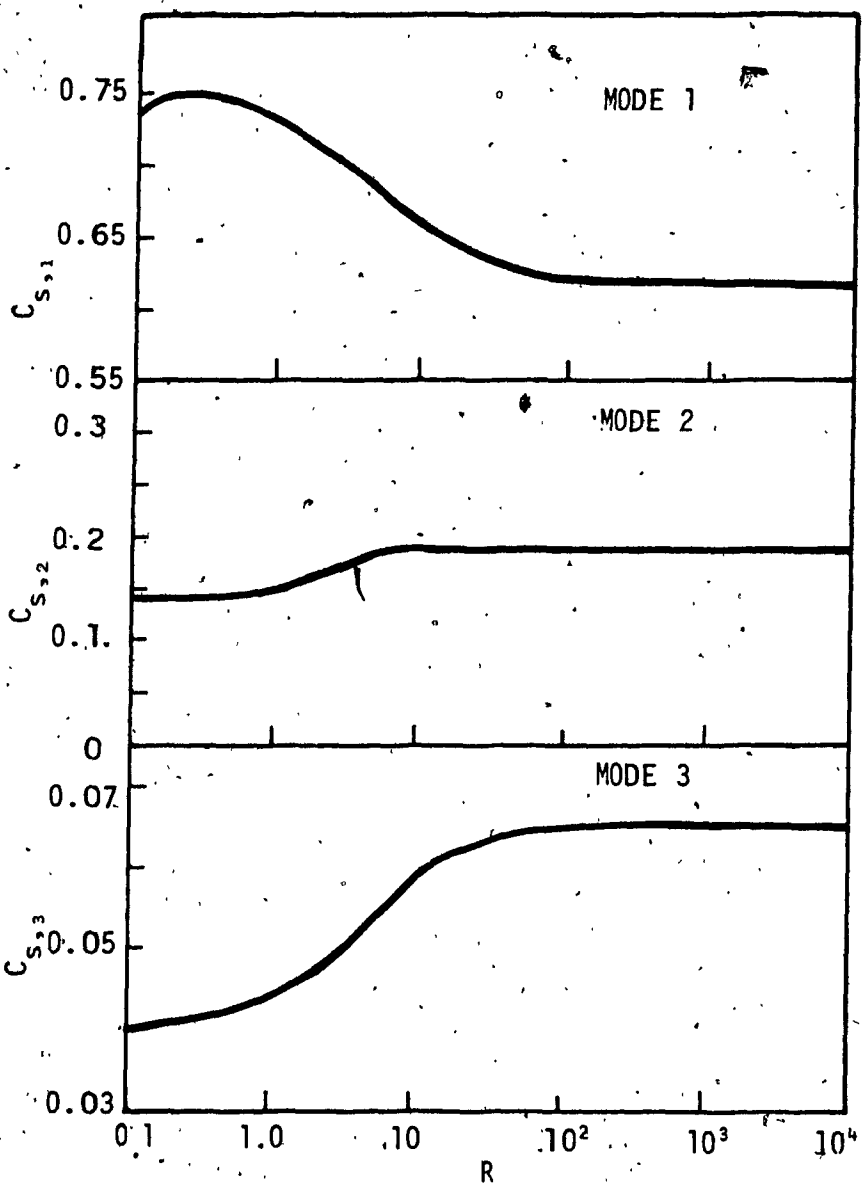

FIG. 3.1 Variation of Shear Coefficient with Foundation Flexibility Parameter R. - Modes 1, 2 and 3.

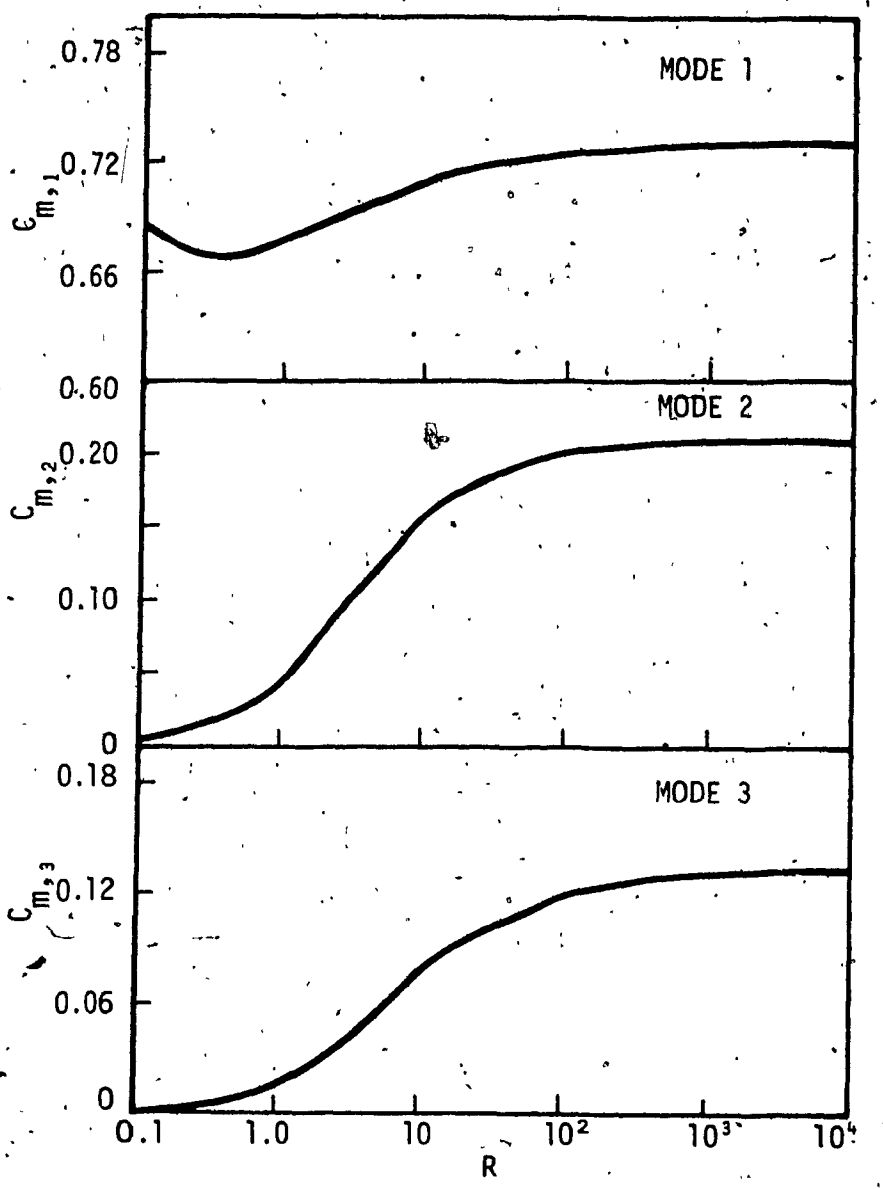

FIG. 3.2 Variation of Moment Coefficient with Foundation Flexibility Parameter R - Modes 1, 2 and 3.

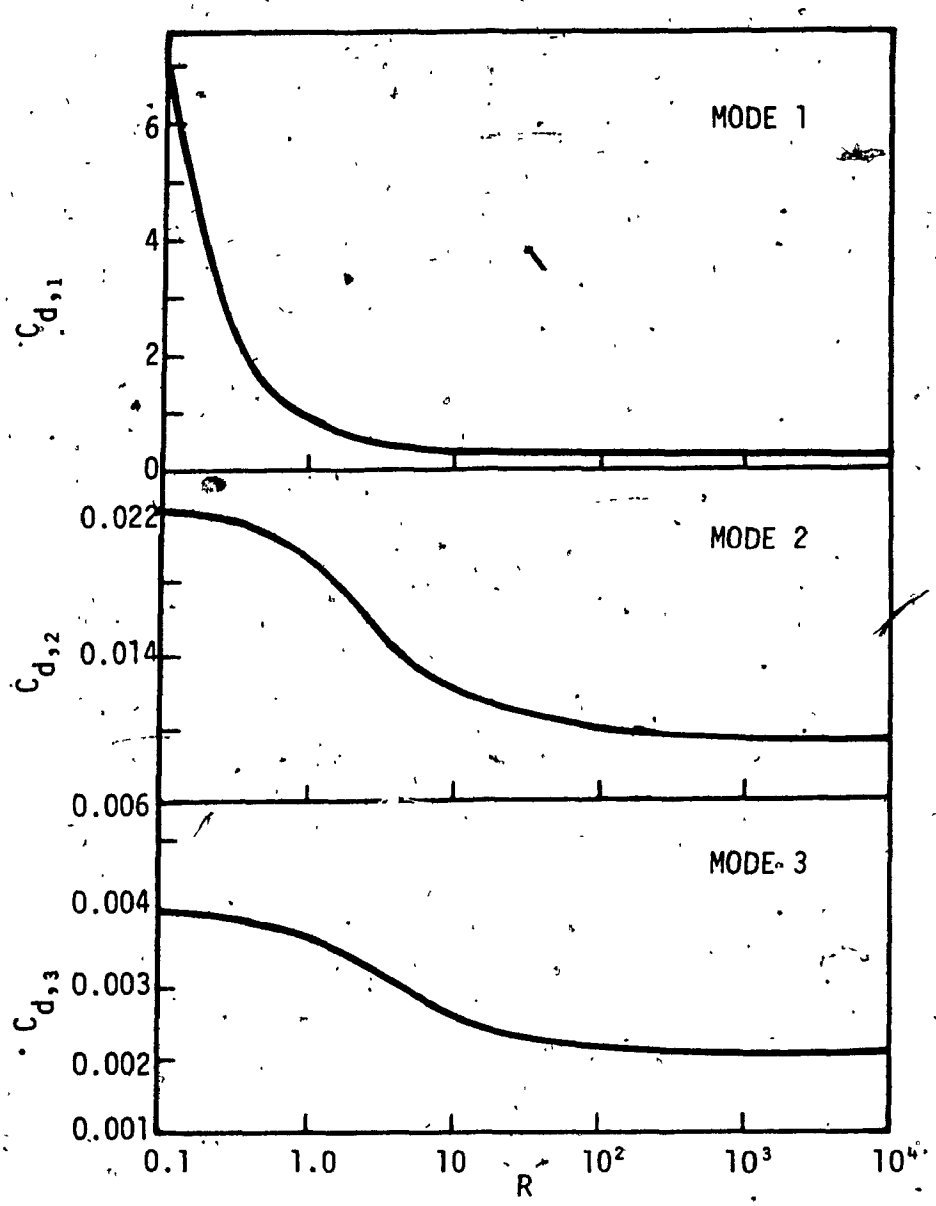

FIG. 3.3 Variation of Top Deflection Coefficient with Foundation Flexibility Parameter R - Modes 1, 2 and 3.

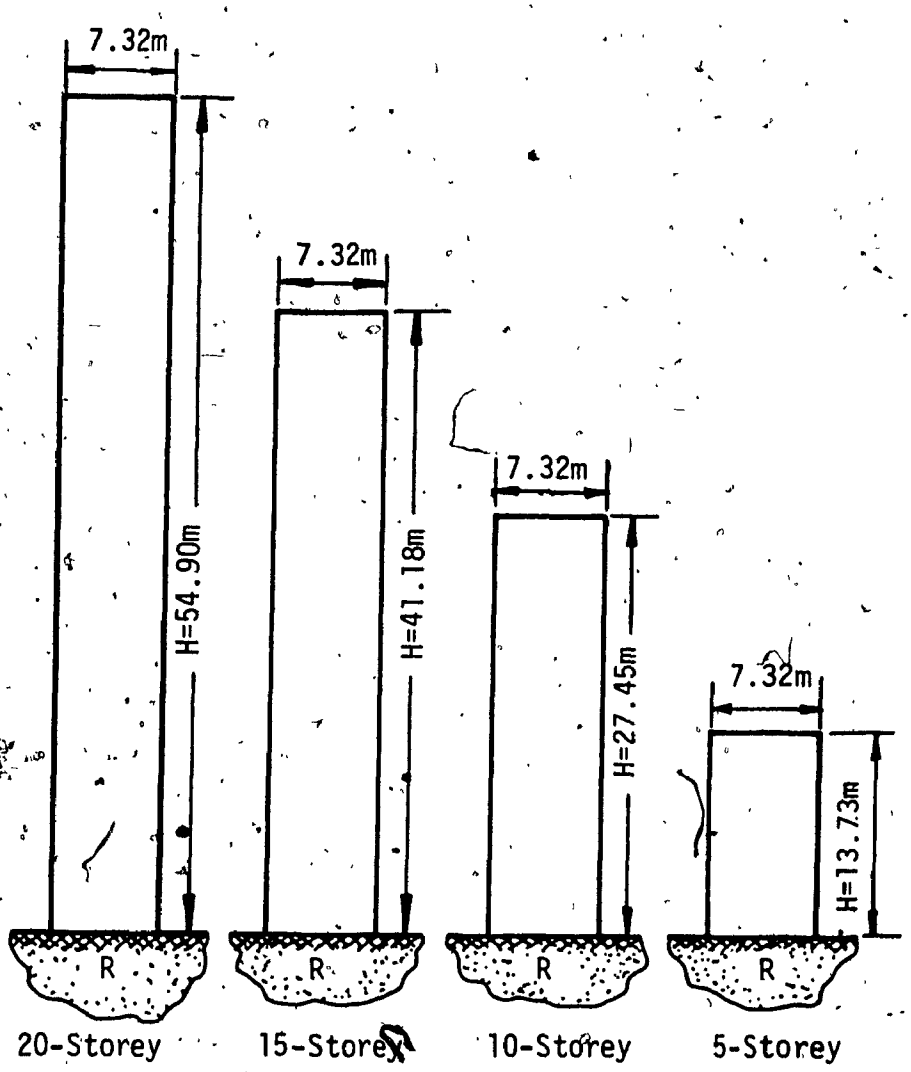

FIG. 3.4 Four Shear Walls with Soil Support Denoted by Foundation Flexibility Parameter R.

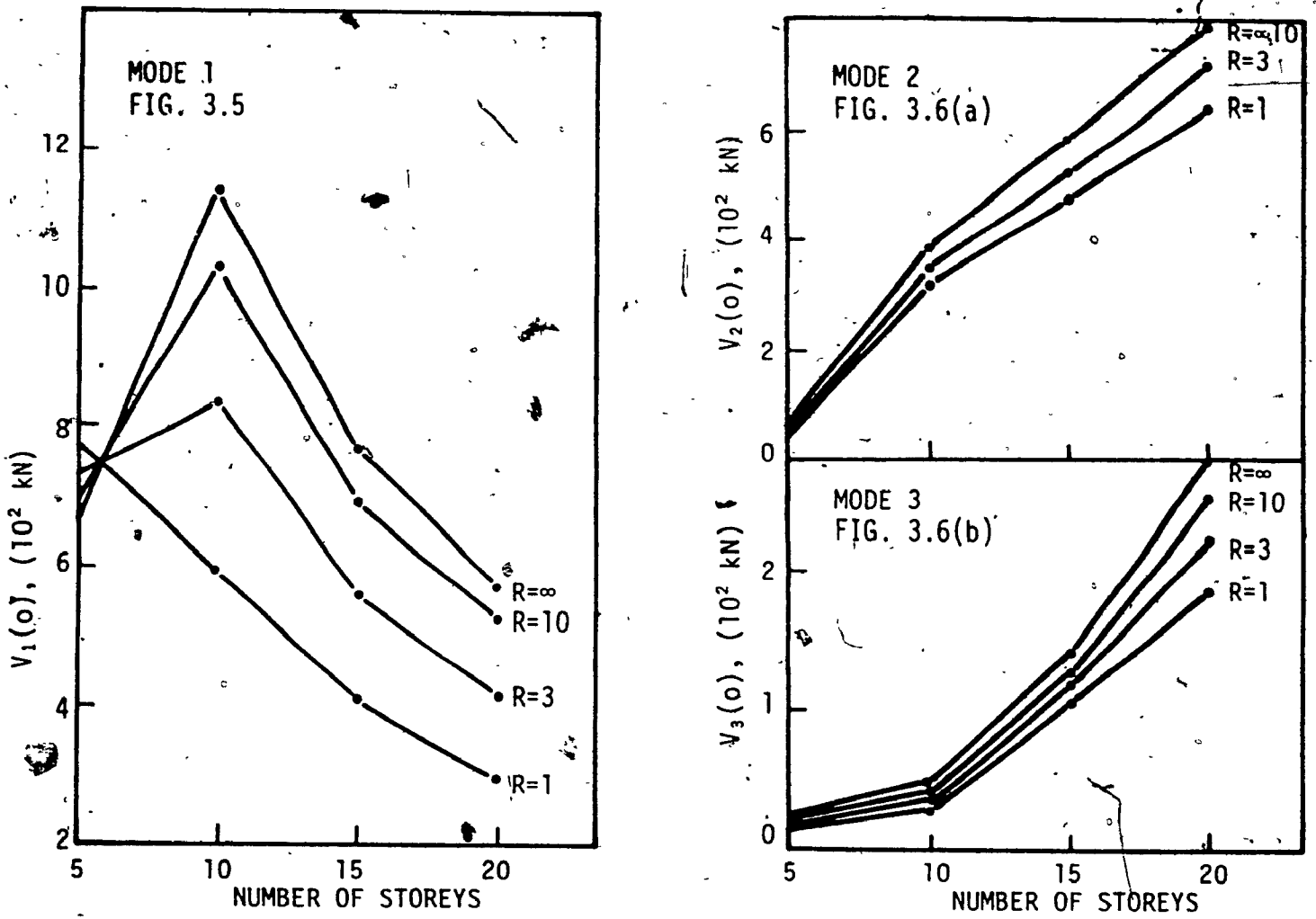

FIGS. 3.5 and 3.6 Variation of Base Shear with Number of Storeys for Different R - Modes 1, 2 and 3.

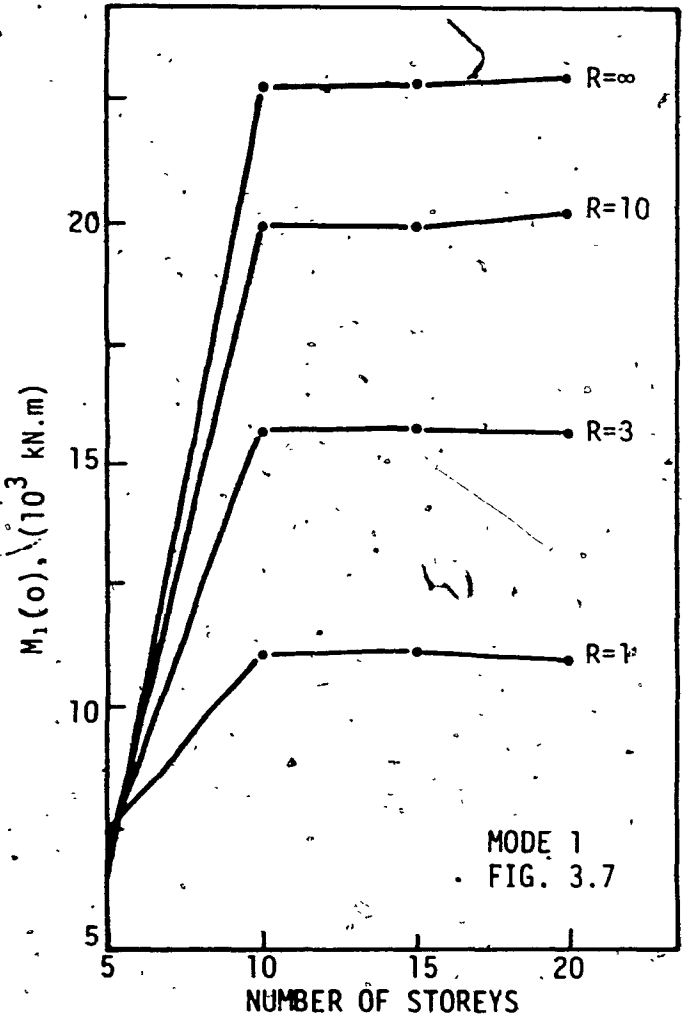

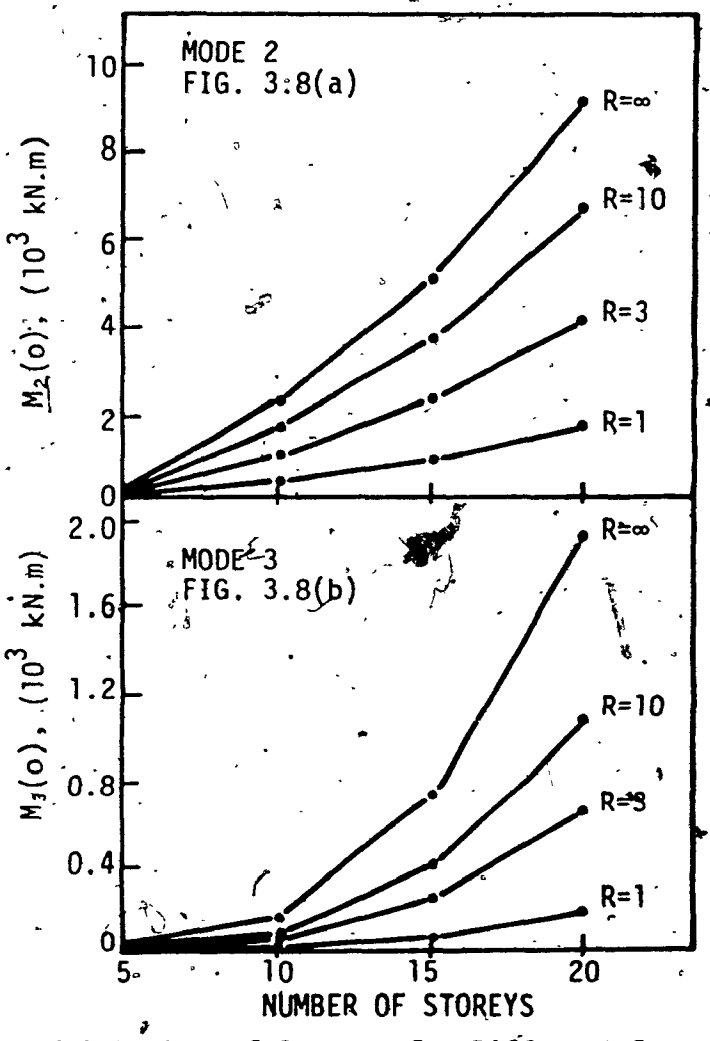

FIGS. 3.7 and 3.8 Variation of Base Moment with Number of Storeys for Different R - Modes 1, 2 and 3.

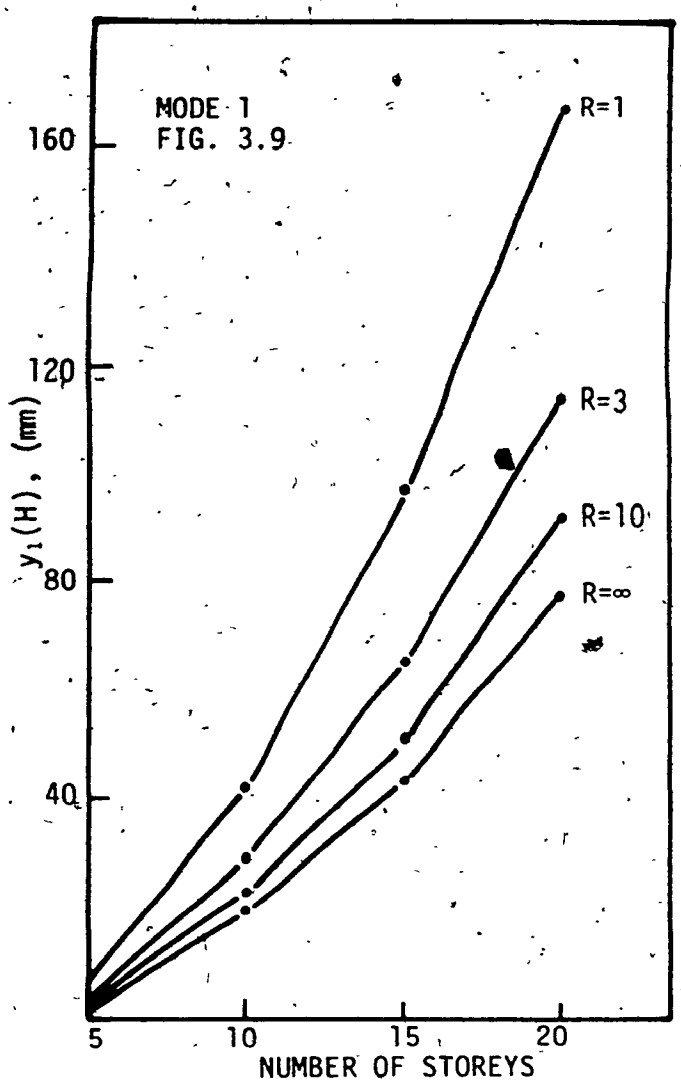

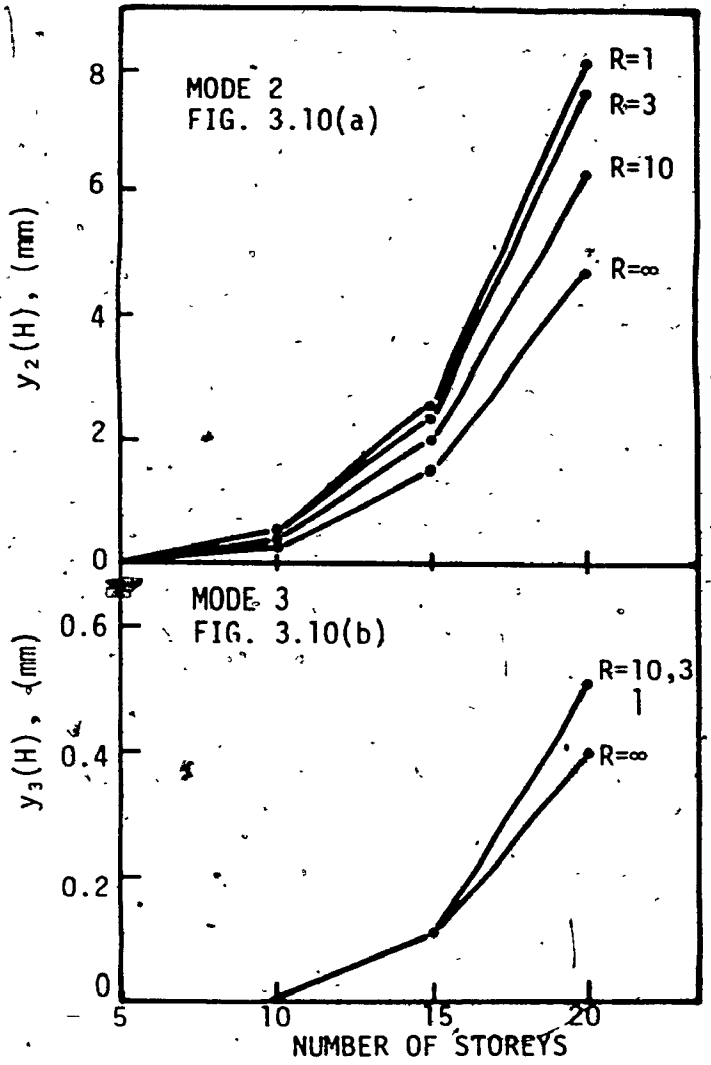

FIGS. 3.9 and 3.10 Variation of Top Defleetion with Number of Storeys for Different R - Modes 1, 2 and 3.

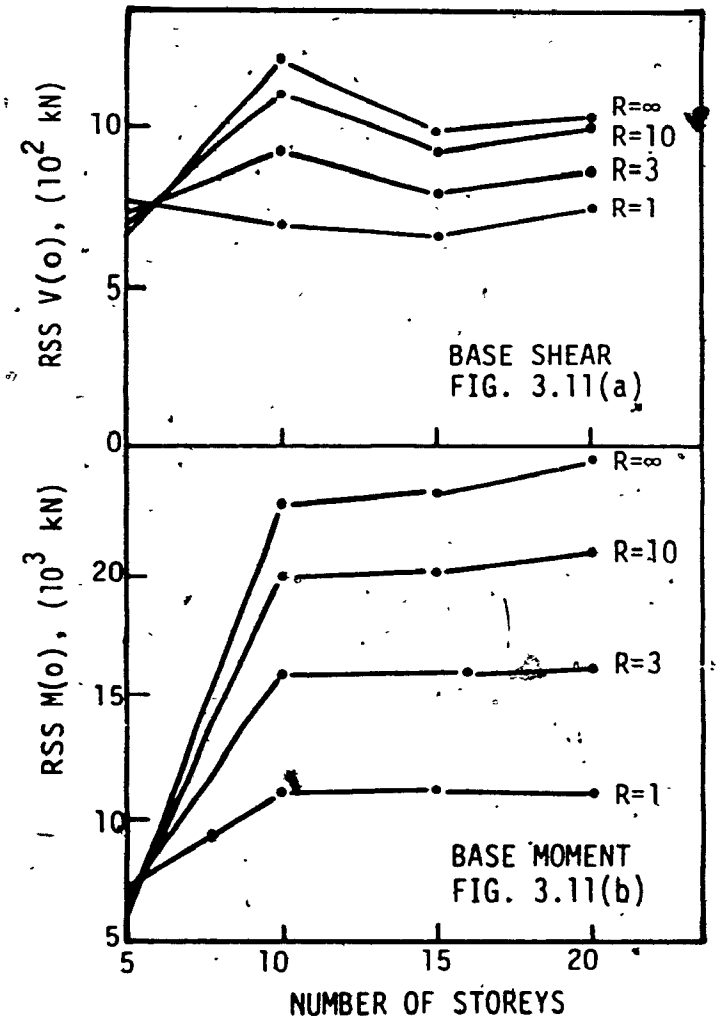

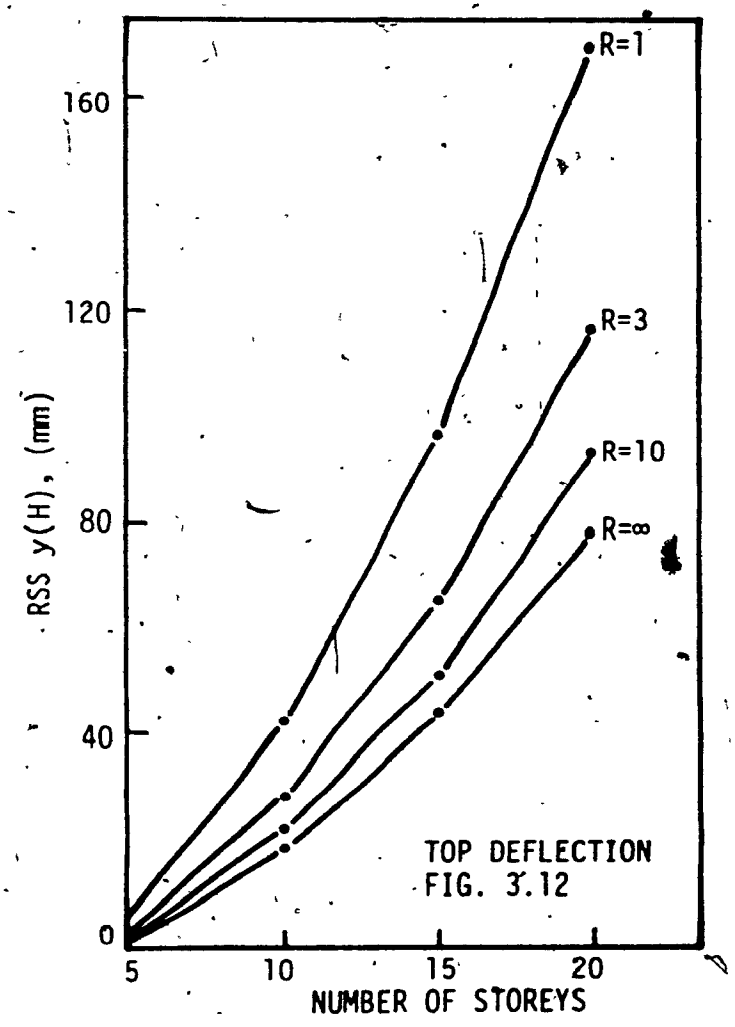

FIGS. 3.11 and 3.12 Base Shear, Base Moment and Top Deflection for Different R - RSS Values.

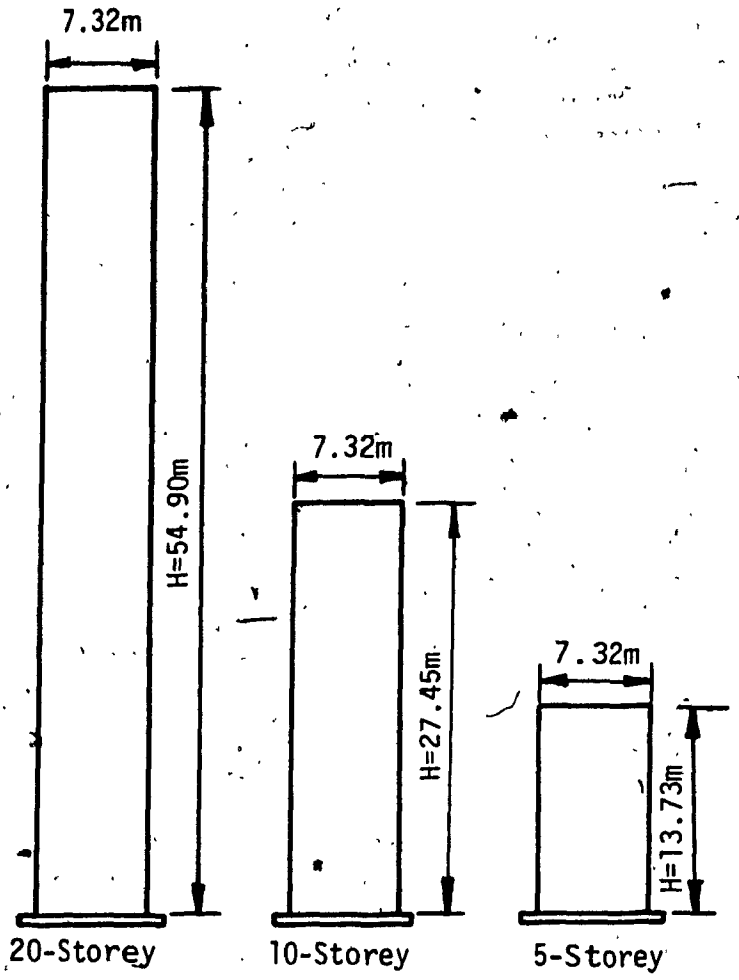

FIG. 3.13 Example Shear Walls with Prototype Foundations.

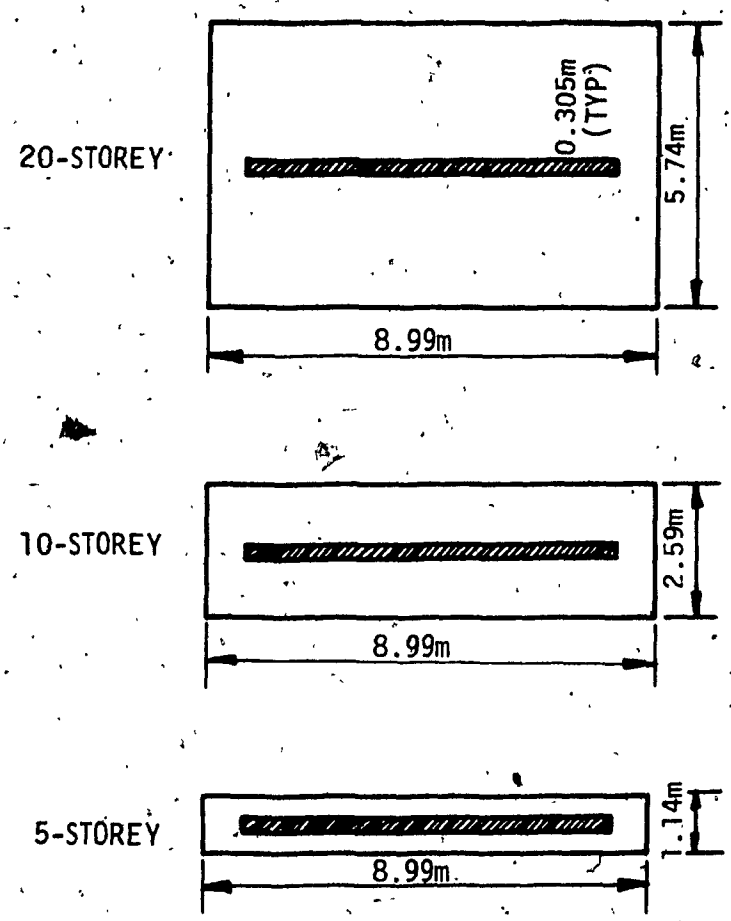

FIG. 3.14 Plan of Foundations for Example Shear Walls.

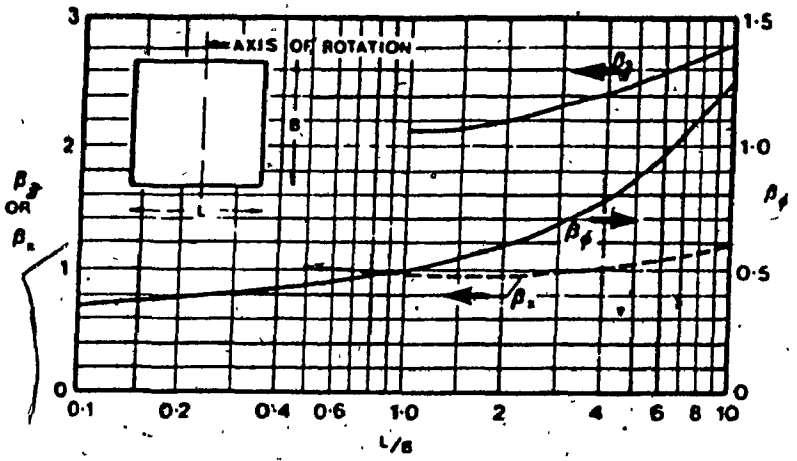

FIG. 3.15 Coefficients β_x, β_z and β_ϕ for Rectangular Footings (taken from Reference 22).

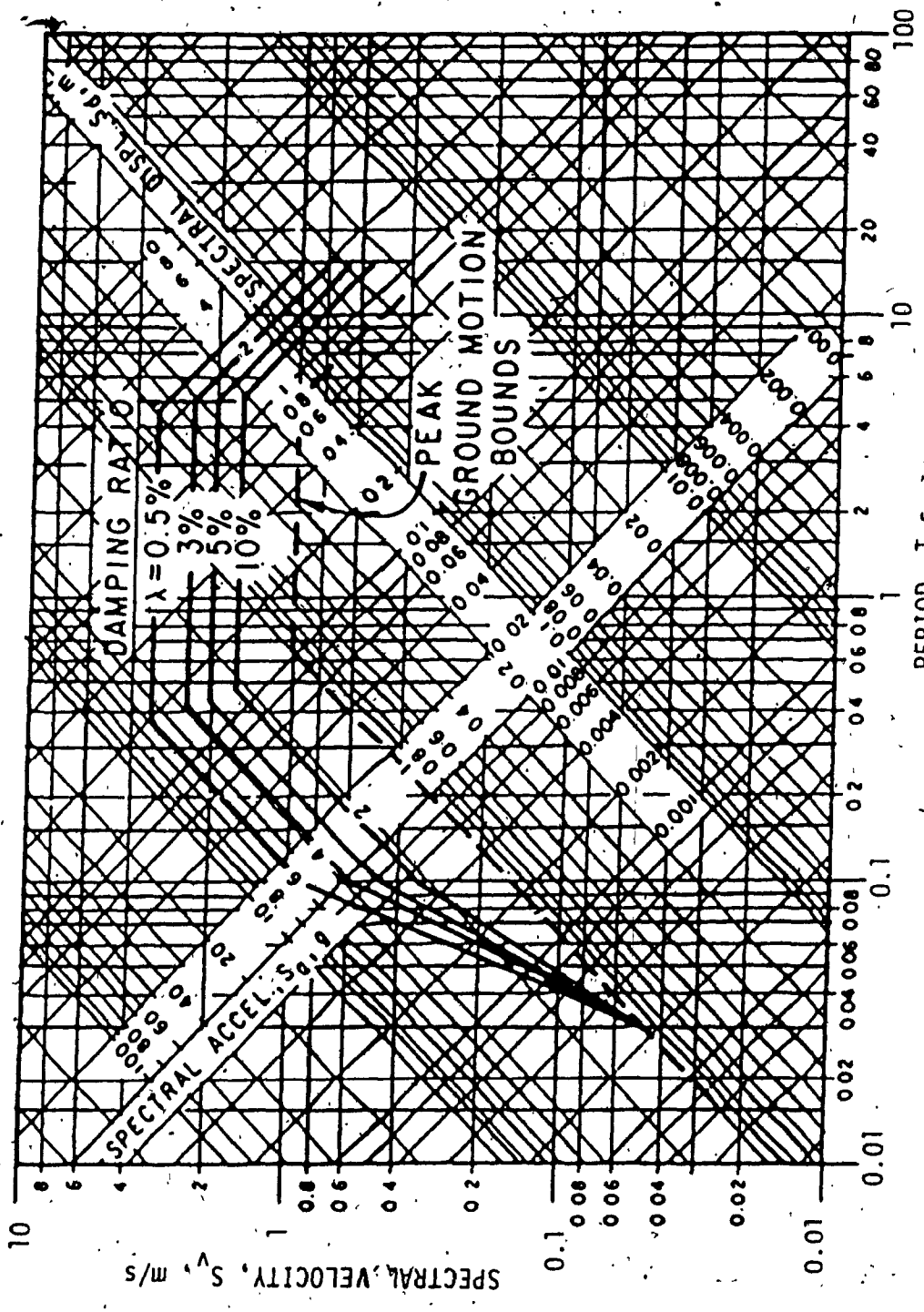

FIG. 3.16 Peak Ground Motion Bounds and Elastic Average Response Spectrum for 1.0g Max. Ground Acceleration (taken from Reference 23).

CHAPTER IV

SEISMIC RESPONSE OF COUPLED SHEAR WALLS WITH FLEXIBLE SUPPORT

4.1 INTRODUCTION

Employing the mode shapes of cantilever beams with rotationally flexible support derived in Chapter II, this chapter examines the importance of base flexibility on the seismic response of coupled shear walls. Response coefficients for wall base moment and top deflection are presented as functions of base flexibility parameter R, as well as functions of structural parameters representing axial deformation of the walls and relative stiffness of the coupling beams.

Assuming a flat acceleration response spectrum, the seismic response of two prototype coupled shear wall buildings is next examined. Here, 10 and 26-storey buildings are employed with rotational base flexibility represented by R = 5 and 10, respectively, and the importance of base flexibility is determined by comparison with results for rigid foundations.

4.2 GOVERNING DIFFERENTIAL EQUATION AND BOUNDARY CONDITIONS

Fig. 4.1 represents a coupled whar wall on a flexible foundation. The foundation flexibility is represented by two springs attached at the bases of the two shear walls. If it is assumed that the structural properties of the coupled shear wall are constant throughout the total height H, the governing differential equation for the structural

behaviour can be found [15]; after replacing the connecting beams by a continuous medium, shown in Fig. 4.2, one obtains

$$\frac{d^4y}{dx^4} - \alpha^2 \frac{d^2y}{dx^2} = \frac{1}{EI}\left[w - \frac{\alpha^2(\mu-1)}{\mu} M\right] \qquad (4.1a)$$

where y, w, M and EI denote horizontal displacement, distributed load, overturning moment, and flexural rigidity, respectively. The other parameters involved in Eq. (4.1a) are defined by

$$\mu = \left(1 + \frac{I}{Aa^2}\right) \qquad (4.1b)$$

$$I = I_1 + I_2 \qquad (4.1c)$$

$$\frac{1}{A} = \left(\frac{1}{A_1} + \frac{1}{A_2}\right) \qquad (4.1d)$$

$$\alpha^2 = \frac{ka^2}{EI}\mu \qquad (4.1e)$$

$$k = \frac{12EI_b}{hc^3}\left(1 + \frac{12EI_b}{GA_b^* c^2}\right)^{-1} \qquad (4.1f)$$

where,

I_1, I_2 = moments of inertia of walls 1 and 2

I_b = moment of inertia of lintel beam

A_1, A_2 = the cross-sectional areas of walls 1 and 2

a = distance between centroidal axes of walls

c = net span of lintel beam

h = height of storey

G = shear modulus

A_b^* = effective shear area of lintel beam

The complete derivation of Eq. (4.1a) is given in Appendix A [4].

In coupled shear walls, αH and μ are the two principal (non-dimensional) structural parameters. In a physical sense parameter μ, which is a function of the section properties, measures the axial deformation of the walls and falls within the range 1.0 to 1.4. Parameter αH denotes the ratio of the stiffness of the connecting beams to the stiffness of the walls. For buildings of common proportions, parameter αH usually ranges from 0 to 20. When $\alpha H < 0.8$, the two walls may be treated as two isolated single shear walls [24].

The boundary conditions for the walls on flexible foundation are:

i) at the base of the walls where $x = 0$,

$$y(o) = 0 \tag{4.2}$$

$$K_\theta \frac{dy}{dx}(o) = EI \frac{d^2y}{dx^2}(o) \tag{4.3}$$

ii) and at the top of the walls where $x = H$,

$$\frac{d^2y}{dx^2}(H) = 0 \tag{4.4}$$

$$\frac{d^3y}{dx^3}(H) - \alpha^2 \frac{dy}{dx}(H) + \frac{\alpha^2(\mu-1)}{EI\mu} \int_0^H M(x)\,dx = 0 \tag{4.5}$$

In the above boundary conditions, K_θ denotes the equivalent rotational stiffness of the foundation represented by springs. It is given by

$$K_\theta = K_{\theta 1} + K_{\theta 2} \tag{4.6}$$

where $K_{\theta 1}$ and $K_{\theta 2}$ are the rotational spring stiffness at the bases of walls 1 and 2.

4.3 APPROXIMATE METHOD OF ANALYSIS

It is difficult to obtain the actual mode shapes of a coupled shear wall on a flexible foundation. These mode shapes are a complicated function of parameter K_θ, as well as of structural parameters αH and μ. Thus, an approximate method identical to that suggested by Tso and Rutenberg [15] is used in the present investigation.

In this study the mode shapes of the coupled shear wall resting on a flexible foundation are approximated by the mode shapes of the cantilever beam with rotationally flexible base already used in Chapter III for the seismic analysis of single shear walls. The mode shapes of the rotational spring-supported cantilever are represented by the expression given in Chapter II as Eq. (2.33) and repeated here for convenience:

$$\phi_r(x) = \sin \beta_r x - \sinh \beta_r x - \gamma_r \left(\cos \beta_r x - \cosh \beta_r x - \frac{2\beta_r H}{R} \sinh \beta_r x\right) \tag{4.7}$$

The constants γ_r and β_r have the same meaning as in Chapter II.

The expression for modal participation factor, modal loading, as well as modal base moment derived in Chapter III (Eqs. (3.3) - (3.15)) remain valid for this investigation.

Differential Eq. (4.1a) can be solved once modal loading $w_r(x)$ is known. The resulting solution is given by

$$y_r(x) = C_{1r} + C_{2r}x + C_{3r} \sinh \alpha x + C_{4r} \cosh \alpha x$$
$$+ C_{5r} \left[\cosh \beta_r x + \left(\frac{2\beta_r H}{R} - \frac{1}{\gamma_r}\right) \sinh \beta_r x\right]$$
$$+ C_{6r} \left[\cos \beta_r x - \frac{1}{\gamma_r} \sin \beta_r x\right] \qquad (4.8)$$

The constants C_{1r}, C_{2r}, C_{3r} and C_{4r} are determined from the boundary conditions of Eqs. (4.2) to (4.5), whereas C_{5r} and C_{6r} represent the coefficients of the particular solution. The expressions for all six coefficients are given in Appendix B.

The expressions for the bending moment at the base of the walls, and the top deflection may be expressed as follows:

$$M_{w,r}(o) = V_r(o) \left(\frac{2\gamma_r}{N_r \beta_r} + \frac{\alpha^2}{\mu(\beta_r^4 - \alpha^4)} \left[\frac{2\gamma_r \alpha^2}{N_r \beta_r} - \frac{1}{N_r D_1} (D_2 - D_3 D_4 + D_5 D_6)\right]\right) \qquad (4.9)$$

$$y_r(H) = \frac{V_r(o)}{N_r \mu EI(\beta_r^4 - \alpha^4)} \left(- \left[\frac{1}{D_1} (D_2 - D_3 D_4 - D_5 D_6)\right] \times \right.$$
$$\left[\frac{\alpha^2 H^2}{R} + \frac{\alpha H}{\tanh \alpha H} + \frac{\alpha H}{R} \sinh \alpha H \right.$$
$$\left. - \left(\frac{\alpha H}{R} + \frac{1}{\tanh \alpha H}\right) \sinh \alpha H + \cosh \alpha H - 1\right] +$$
$$- \frac{2\gamma_r \alpha^2}{\beta_r} \left[\left(\frac{\beta_r^2 H}{R\alpha} - \frac{\beta_r}{\gamma_r \alpha}\right) \sinh \alpha H + 1\right]$$
$$+ \frac{\mu(\beta_r^4 - \alpha^4)}{\beta_r^3} [\phi_r(H)] + \frac{\alpha^4 \phi_r(H)}{\beta_r^3}$$
$$\left. + H \left[\frac{\alpha \beta_r \phi_r(H)}{\sinh \alpha H} - 2\gamma_r \alpha^2 \left(\frac{\beta_r H}{R} - \frac{1}{\gamma_r}\right)\right] \times \left[1 - \frac{\sinh \alpha H}{\alpha H}\right]\right) \qquad (4.10)$$

In Eqs. (4.9) and (4.10) D_1, D_2, D_3, D_4, D_5 and D_6 are expressions

given in Appendix B. It should be noted that modal responses $M_{w,r}(o)$ and $y_r(H)$ are expressed in terms of base shear $V_r(o)$.

4.4 PARAMETRIC EVALUATION OF DYNAMIC RESPONSE COEFFICIENTS

4.4.1 Results and Discussion

The dynamic response coefficients, namely $C_{m,r}$ for base wall moment and $C_{d,r}$ for top deflection are examined in the form of curves obtained by employing the approximate analysis discussed in Section 4.3.

Since the natural frequencies for the coupled shear wall on flexible foundation are not known and frequency parameter curves are not available, the calculation of base shear, base moment and top deflection is based on the flat response spectrum of Fig. 4.18.

4.4.1a Wall Base Moment Coefficient Curves

The effect of rotational flexibility parameter R on the modal base wall moment coefficients are shown in Figs. 4.3, 4.4 and 4.5 for the first three modes of vibration. In these figures, the base wall moment coefficients are plotted against the structural parameter αH ranging from 0 to 20, for flexibility parameter $R = \infty$, 50, 25, 10, 5 and 1. The base wall moment coefficients in coupled shear walls are also functions of structural parameter μ which ranges from 1.0 to 1.4; however, in the figures only the average case $\mu = 1.2$ is considered.

Fig. 4.3 shows that, when flexibility of the base increases from rigid to very flexible (i.e., when R varies from ∞ to 50, 25, 10, 5 and 1) the magnitude of $C_{m,1}$ decreases continuously for the first

mode for all values of αH. However, it is noticed that the moment coefficient curve for $R = 1$ intersects the curve for $R = 5$ when αH lies between 14 and 15; for $\alpha H = 15$ to 20 the magnitude of $C_{m,1}$ for $R = 1$ is slightly greater than for $R = 5$. These two curves are shown in the figure as dotted lines.

For the higher modes of Figs. 4.4 and 4.5, it is observed that the effect of rotational flexibility parameter R on moment coefficient $C_{m,r}$ gradually becomes less significant if the value of R decreases below 10. Figs. 4.4 and 4.5 also show that the moment coefficient curves for lower values of R (R = 10, 5, 1) intersect the curves for higher R values (R = 25, 50, ∞) in different regions of αH. This indicates that, for relatively flexible foundations, the moment coefficient curves have a tendency of folding in an upward direction as αH increases.

Since there are no data available for moment coefficient curves of coupled shear walls on flexible foundations in the existing literature, to check the results expressed by the curves of Figs. 4.3 to 4.5 additional data are presented in Figs. 4.6 and 4.7. The latter represent the sections of the moment coefficient curves taken at $\alpha H = 5$ and 10 for the three modes of vibration, with $\mu = 1.2$ and R varied from 1 to 50. This graphical check shows a smooth trend, with $C_{m,r}$ first decreasing and then increasing as the magnitude of R becomes small. This explains the upward folding nature of the moment coefficient curves obtained in Figs. 4.3 to 4.5.

Figs. 4.8 to 4.10 present the effect of parameter μ on moment coefficient $C_{m,r}$ for a particular foundation flexibility parameter (R = 5). In these figures the moment coefficient is plotted against

parameter αH ranging from 0 to 20 for variation of μ from 1.0 to 1.4.

For the first mode (Fig. 4.8), the variation of $C_{m,1}$ with μ is not significant when αH varies from 0 to 8. Within this range of αH the magnitude of the moment coefficient for all μ values are very close. The effect of μ on moment coefficient becomes more significant when αH varies from 10 to 20. In this range, it is noticed that the magnitude of the moment coefficient is greater as the magnitude of μ increases. The opposite is true for rigid foundations as noted by Tso and Rutenberg [15] (see Figs. C1 - C4, Appendix C).

In the second and third modes of vibration shown in Figs. 4.9 and 4.10, the effect of μ on moment coefficient is pronounced for all values of αH. The magnitude of the moment coefficient associated with lower values of μ is still greater than for higher values of μ, which has already been noted for the first mode of Fig. 4.8.

4.4.1b Top Deflection Coefficient Curves

The top deflection coefficient curves presented in Figs. 4.11 to 4.16 are generated on the basis of Eq. (4.8) for different magnitude of base flexibility parameter R. Figs. 4.11 to 4.13 show how the base flexibility parameter affects the modal top deflection coefficients $C_{d,r}$ for $\mu = 1.2$ with variation of αH from 0 to 20.

Fig. 4.11 shows that the top deflection coefficient for the first mode increases with decreasing R when αH is small, but when $\alpha H > 2.0$ the deflection coefficient decreases with decreasing value of R (i.e. displacement decreases for flexible foundations). It is also noticed that; within this range of αH (i.e. $2 < \alpha H \leq 20$), the difference in the

magnitude of the top deflection coefficient for rigid ($R = \infty$) and flexible ($R = 10, 5, 1$) base conditions is approximately constant for varying αH.

In the higher modes, the effect of base flexibility on top deflection coefficient, shown in Figs. 4.12 and 4.13, is large over the entire range of αH. Thus, for higher modes the top deflection coefficient is sensitive to the flexibility of the foundation and increases with increasing foundation flexibility.

Top deflection curves for the first three modes of vibration of a particular shear wall structure on a flexible foundation ($R = 5$) are presented in Figs. 4.14 to 4.16. It is noticed that coefficient $C_{d,r}$ is influenced by the magnitude of structural patameter μ in all modes. Although the first mode $C_{d,1}$ is affected significantly by μ (Fig. 4.14), the second and third modes are seen to be particularly sensitive to this parameter (Figs. 4.15 and 4.16).

The above observations are important to seismic response since they indicate that the contributions to total deflection by the higher modes can be expected to become substantial when the foundation flexibility is considered, whereas for the rigid base modes 2 and 3 contribute little to top deflection of a coupled shear wall regardless of the structural parameter αH and μ.

4.4.2 Effect of Base Flexibility on Two Example Structures

To illustrate the approximate method and to study the effect of base flexibility on various dynamic responses, two shear wall buildings are considered for example purposes. These two buildings have different

numbers of storeys. One is 26 and the other is 10 storeys high. The 26-storey building is identical to the building used by Tso and Rutenberg [15] in their example problem for a rigid foundation condition. The 10-storey building is identical to the 26-storey structure in all respects except overall height. In the present example structures the principal different from that of Reference [15] is the introduction of flexible foundation bases.

Fig. 4.17 shows the floor plan of the example buildings. Both buildings are 45.8 m long and 16.3 m wide in plan. Each building has six pairs of coupled shear walls, equally spaced along the length of the building. The dimensions of the example buildings are shown in Table 4.1.

In order to evaluate the seismic responses of the example buildings, it is assumed that the seismic loading is applied in the narrow direction and that the six pairs of coupled shear walls in each building form the main lateral load resisting elements. Thus, the elevator shaft and the stairwells do not contribute to the stiffness in the narrow direction.

To analyse the example structure, an equivalent single pair of coupled walls is assumed in each building after lumping the properties of the six pairs of walls. Table 4.2 presents the section properties of the equivalent single pair of coupled walls.

To determine the flexibility parameter R for the 26 and the 10-storey example structures, the procedures described in Chapter III (subsections 3.3.1 to 3.4.2) for a single isolated wall are employed. The equivalent spring stiffness for the coupled shear walls is calculated according to Eq. (4.6) with the equivalent K_θ for a single pair of

coupled shear walls. The magnitude of R is found to be 5.0 and 1.0 for the 26-storey and 10-storey buildings, respectively. The flat response spectrum presented in Fig. 4.18 gives the spectral accelerations $S_{a_1} = S_{a_2} = S_{a_3} = 1.0g$. The structural parameters μ and αH for the two buildings are obtained using Eqs. (4.1b) and (4.1e). The values are: (1) 26-storey building, $\mu = 1.2$ and $\alpha H = 5.0$: (2) 10-storey building, $\mu = 1.2$ and $\alpha H = 2.0$.

The modulus of elasticity of concrete and the weight per unit height of the buildings are 25×10^6 kN/m^2 and 3,210 kN/m, respectively.

Tables 4.3 and 4.4 present the results obtained for the seismic response of the example structures. These tables are made on the assumption that both example structures are situated on rigid as well as on flexible foundations. Table 4.3 provides the various seismic responses of the 26-storey structure and also shows the comparison of the two assumed foundation conditions. Similarly, Table 4.4 gives the corresponding results and comparison for the 10-storey coupled shear wall.

The tables show that, for the 26-storey structure, the RSS of three modes for base shear, base moment and total wall moment are approximately of the same magnitude for rigid and flexible foundations. However, top deflection for the flexible foundation (R = 5) is greater than for the rigid foundation. On the other hand, for the 10-storey structure the total wall moment for the flexible (R = 1) foundation is 62 percent less than obtained for the rigid foundation, while the top deflection increases by 96 percent. Base shear and base moment are only marginally affected by the foundation flexibility of the structure.

4.5 CONCLUSIONS

This chapter concerns the effect of rotational foundation flexibility on the dybamic response of coupled shear wall structure subjected to seismic loading.

Various curves for the dynamic response coefficient for base wall moment and top deflection are presented for selective magnitude of foundation flexibility and varying values of the structural parameters αH and μ. In addition, a numerical example is presented considering two example structures resting on flexible foundations. The most important conclusions noted are itemized below.

1. The moment coefficients are influenced significantly by the value of foundation flexibility parameter R in all 3 lower modes of vibration.

2. For a particular magnitude of flexibility parameter ($R = 5$), the effect of structunal parameter μ is significant for larger values of αH, particularly in the higher modes.

3. In the first mode, the top deflection coefficient increases with foundation flexibility when αH is small but is found to decrease for large αH. For higher modes the deflection coefficient increases with foundation flexibility for all αH.

4. For a flexible foundation, the contribution of the higher modes to the top deflection may become very important, and may exceed the contribution of the fundamental mode.

TABLE 4.1

Dimensions for Example Structures

DIMENSION	VALUE
Overall Height, H, in m	71.32
Width of Walls, $d_1=d_2$, in m	7.32
Storey Height, h, in m	2.74
Corridor Width, c, in m	1.68
Effective Width of Coupling Slab, C_b, in m	1.52
Thickness of Walls, t, in m	0.30
Thickness of Slab, t_b, in m	0.20
Length of Building, L, in m	45.80
Width of Building, B, in m	16.32

TABLE 4.2

Section Properties for Equivalent Single Pair of Coupled Shear Walls for 26-Storey and 10-Storey Example Structures

WALLS						BEAMS
A_1 (m^2)	A_2 (m^2)	$A = \frac{A_1 A_2}{(A_1+A_2)}$ (m^2)	I_1 (m^4)	I_2 (m^4)	$I=(I_1+I_2)$ (m^4)	I_b (m^4)
13.4	13.4	6.7	60	60	119.3	.0064

$$A_b^* = \left(\frac{G_b t_b}{1.2}\right) = .253 \text{ m}^2$$

TABLE 4.3

Seismic Responses of Example 26-Storey with Rigid (R=∞) and Flexible (R=5) Foundations (H=71.3m, μ=1.2, αH=5)

	RIGID FOUNDATION (R=∞)				FLEXIBLE FOUNDATION (R=5)			
	MODE 1	MODE 2	MODE 3	RSS	MODE 1	MODE 2	MODE 3	RSS
Parameter (1)	(2)	(3)	(4)	(5)	(6)	(7)	(8)	(9)
Spectral Acceleration, S_a	1g	1g	1g	-	1g	1g	1g	-
$V_r(o)/m\ S_a H$	0.613	0.188	0.065	-	0.679	0.180	0.054	-
Base Shear, $V_r(o)$ (kn)	140.4×10^3	43×10^3	14.8×10^3	14.8×10^3	155.6×10^3	41.2×10^3	12.4×10^3	161.4×10^3
$M_r(o)/V_r(o)$ H	0.727	0.209	0.127	-	0.699	0.123	0.056	-
Base Moment, $M_r(o)$ (kn.m)	7247.4×10^3	639×10^3	134.3×10^3	7292×10^3	7718.6×10^3	360×10^3	49.2×10^3	7727.1×10^3
$Mw/(v_rH)$ *	0.280	0.165	0.115	-	0.101	-0.202	-2.973	-
Total Wall Moment, Mw (kN.m)	2791.3×10^3	504.5×10^3	121.6×10^3	2839.1×10^3	1115.3×10^3	-591.3×10^3	2611×10^3	2900×10^3
$y_r(H)\ EI/(V_rH^3)$ *	0.052	0.000	0.000	-	0.042	-0.102	-1.086	-
Top Deflection, y (mm)	888	0.000	0.000	888	794.51	-512.07	-1633.73	1887.50

* Values taken from the curves

TABLE 4.4

Seismic Responses of Example 10-Storey Structure
Structure with Rigid (R=∞) and Flexible (R=1) Foundations
(H=27.45m, μ=1,2, αH=2)

	RIGID FOUNDATION (R=∞)				FLEXIBLE FOUNDATION (R=1)			
	MODE 1	MODE 2	MODE 3	RSS	MODE 1	MODE 2	MODE 3	RSS
Parameter (1)	(2)	(3)	(4)	(5)	(6)	(7)	(8)	(9)
Spectral Acceleration, S_a	1g	1g	1g		1g	1g	1g	
$V_r(o)/m\ S_a H$	.613	.188	.065	-	.727	.153	.044	-
Base Shear, $V_r(o)$ (kN)	$54x10^3$	$16.6x10^3$	$5.7x10^3$	$56.8x10^3$	$64.1x10^3$	$13.5x10^3$	$3.9x10^3$	$65.6x10^3$
$M_r(o)/V_r(o)H$	.727	.209	.127	-	.676	.048	.018	-
Base Moment, $M_r(o)$ kN/m	$1072.1x10^3$	$94.5x10^3$	$19.9x10^3$	$1076.5x10^3$	$1182.3x10^3$	$17.7x10^3$	$1.9x10^3$	$1182.4x10^3$
$M_w/(V_r H)$*	.453	.210	.124	-	.133	-.064	-1.020	-
Total Wall Moment, Mw (kN.m)	$668x10^3$	$95x10^3$	$19.4x10^3$	$675x10^3$	$232.6x10^3$	$-236x10^3$	$-108x10^3$	$257.5x10^3$
$Y_r EI/(V_r H^3)$*	.103	-.002	.001	-	.147	-.145	-1.313	-
Top Deflection, y(mm)	38.40	-.31	0	38.4	65.23	-13.41	35.36	75.40

* Values taken from the curves

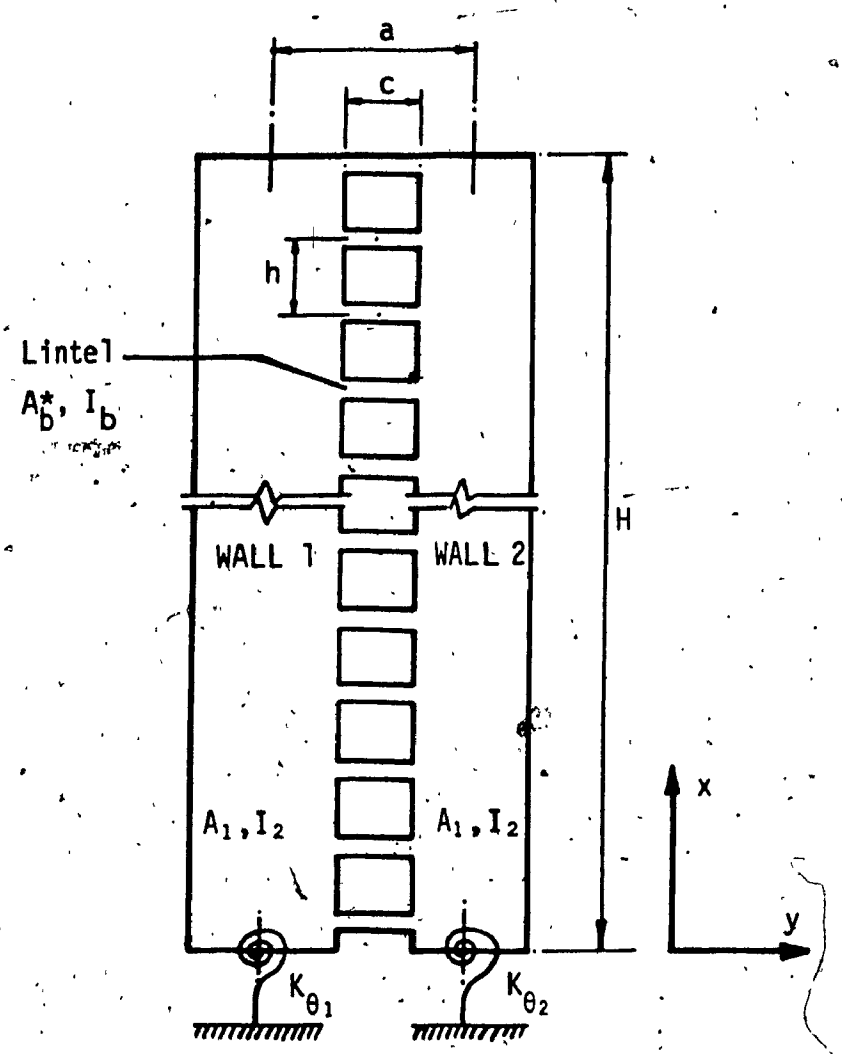

FIG. 4-1 Coupled Shear Wall on Flexible Foundation.

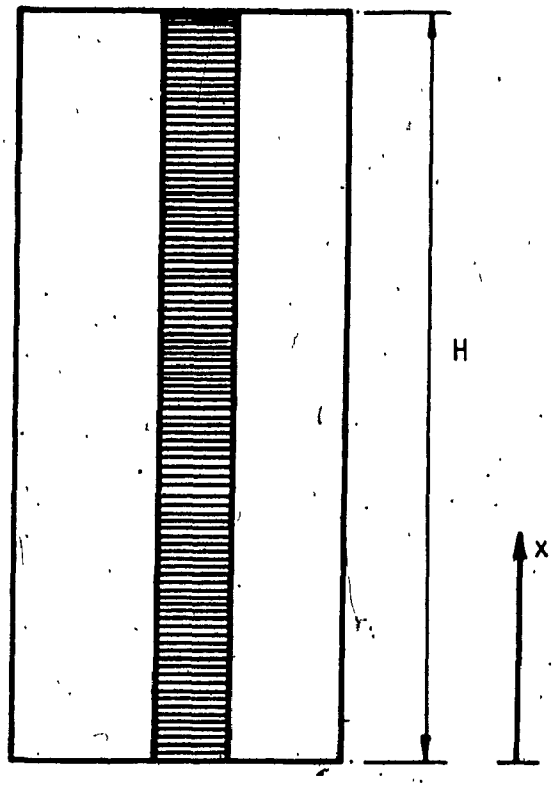

FIG. 4.2 Connecting Beams are Replaced by Infinite Number of Laminae.

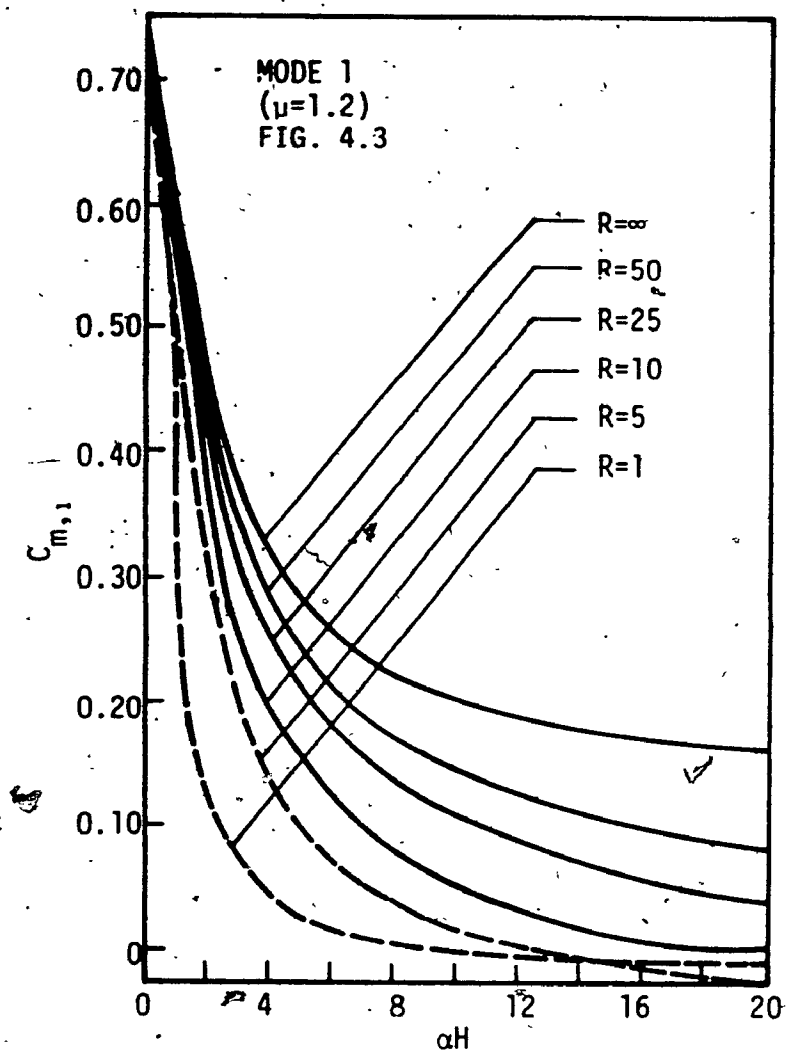

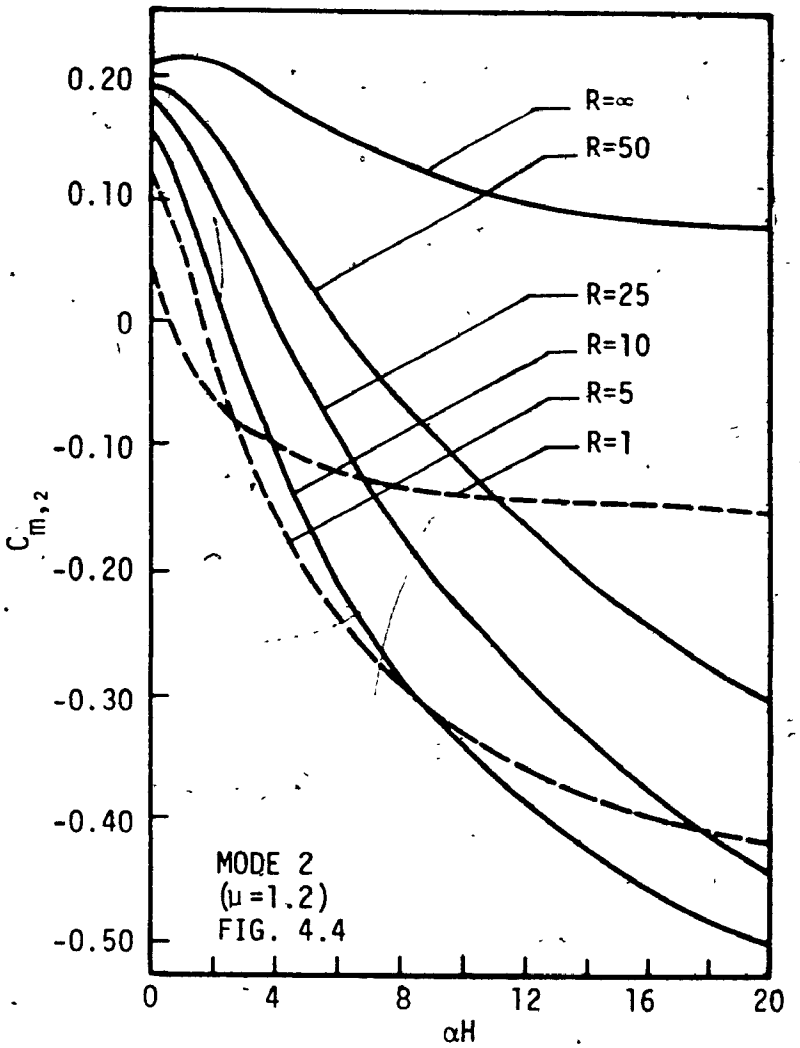

FIGS. 4.3 and 4.4 Moment Coefficient Curves for Different R - Modes 1 and 2 (μ=1.2).

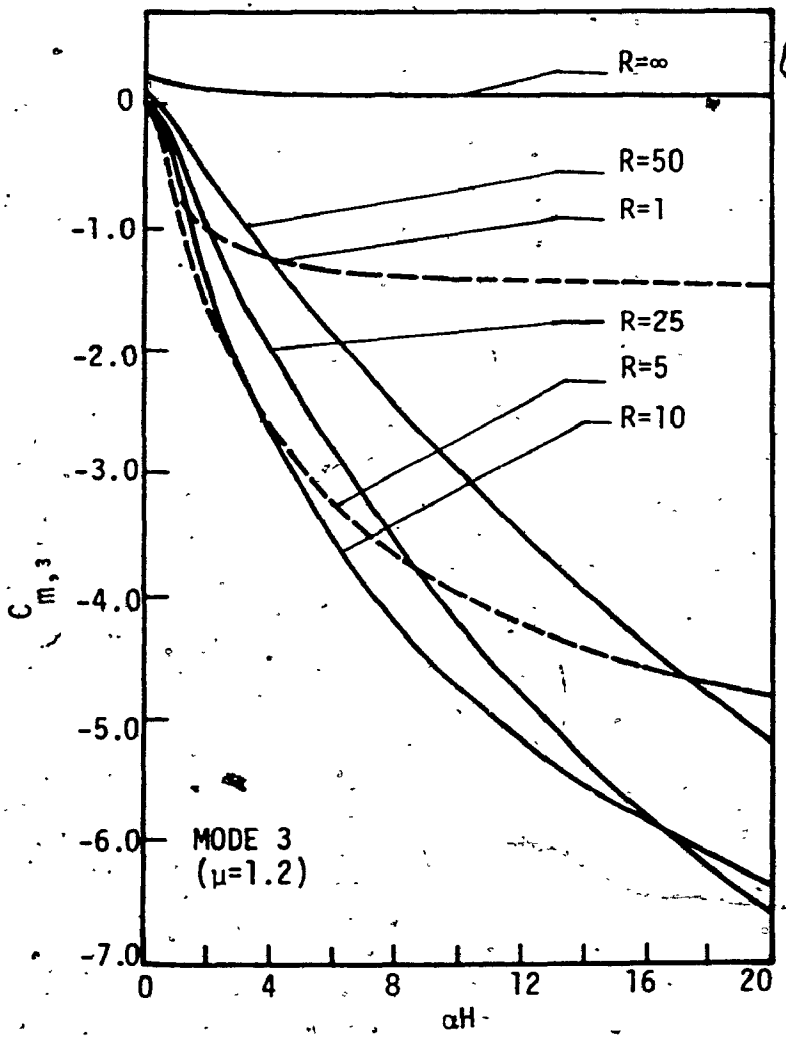

FIG. 4.5 Moment Coefficient Curves for Different R - Mode 3 (μ=1.2).

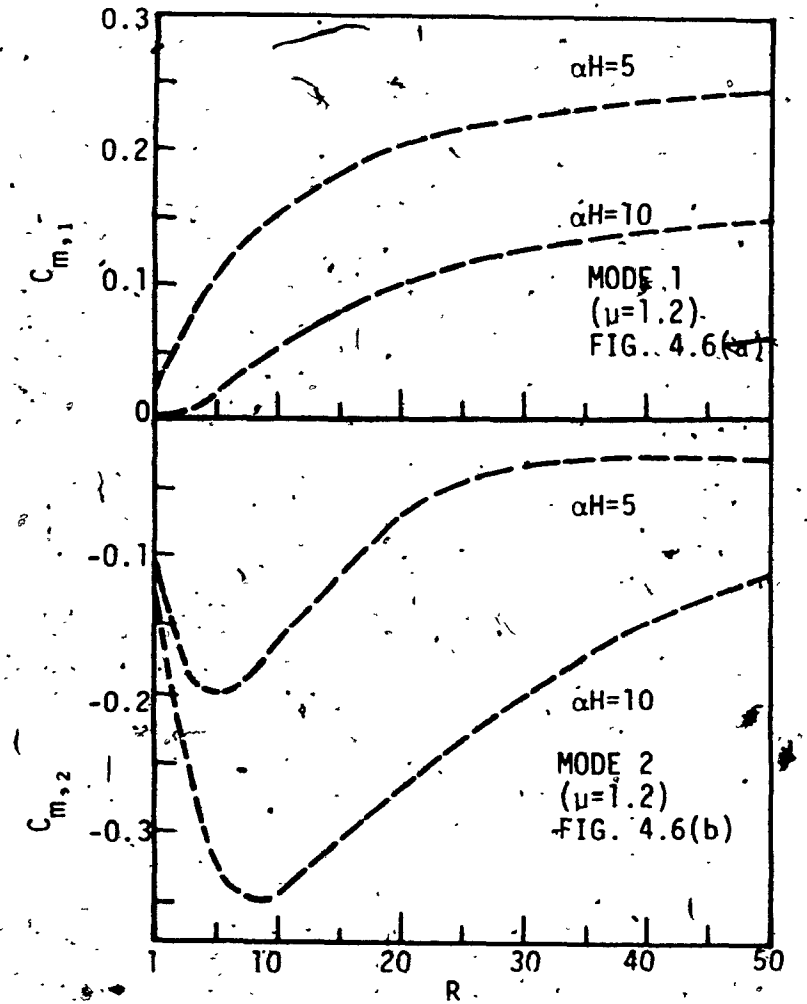

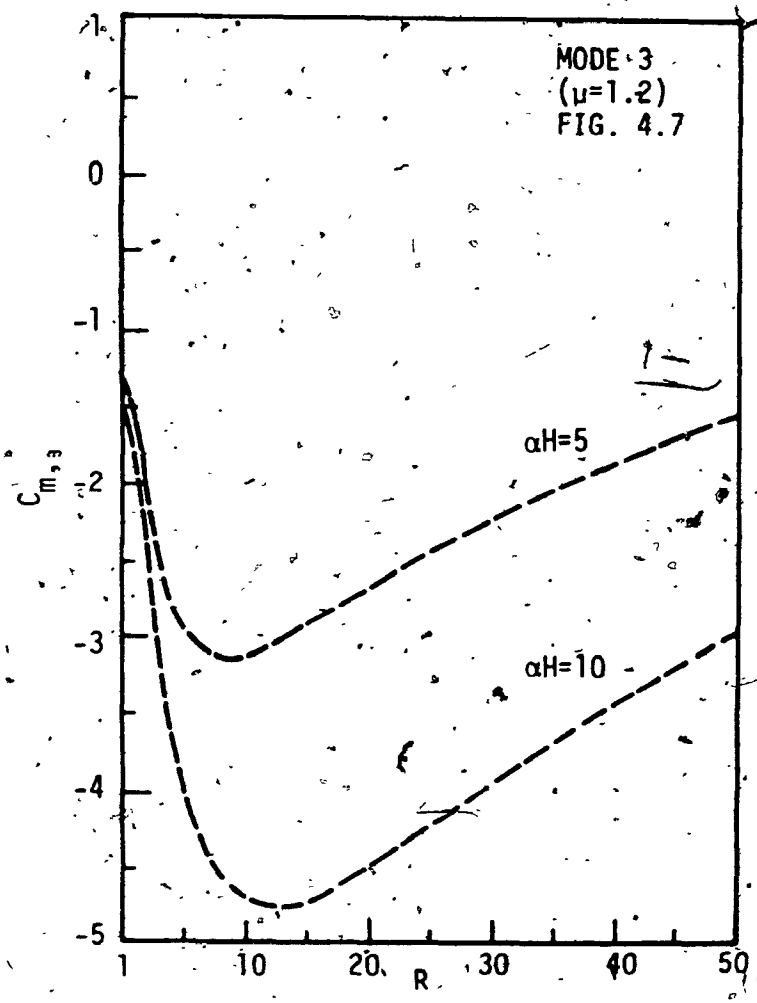

FIGS. 4.6 and 4.7 Section of Moment Coefficient Curves for Different R at αH=5 and 10 - Modes 1, 2 and 3 (μ=1.2).

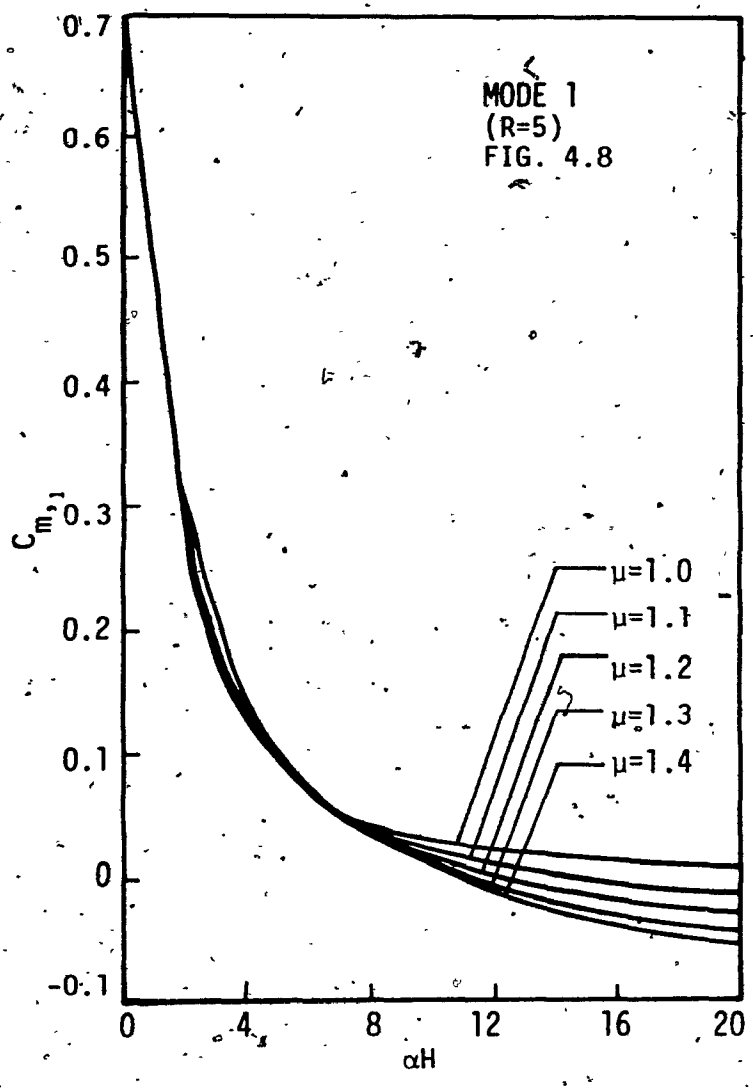

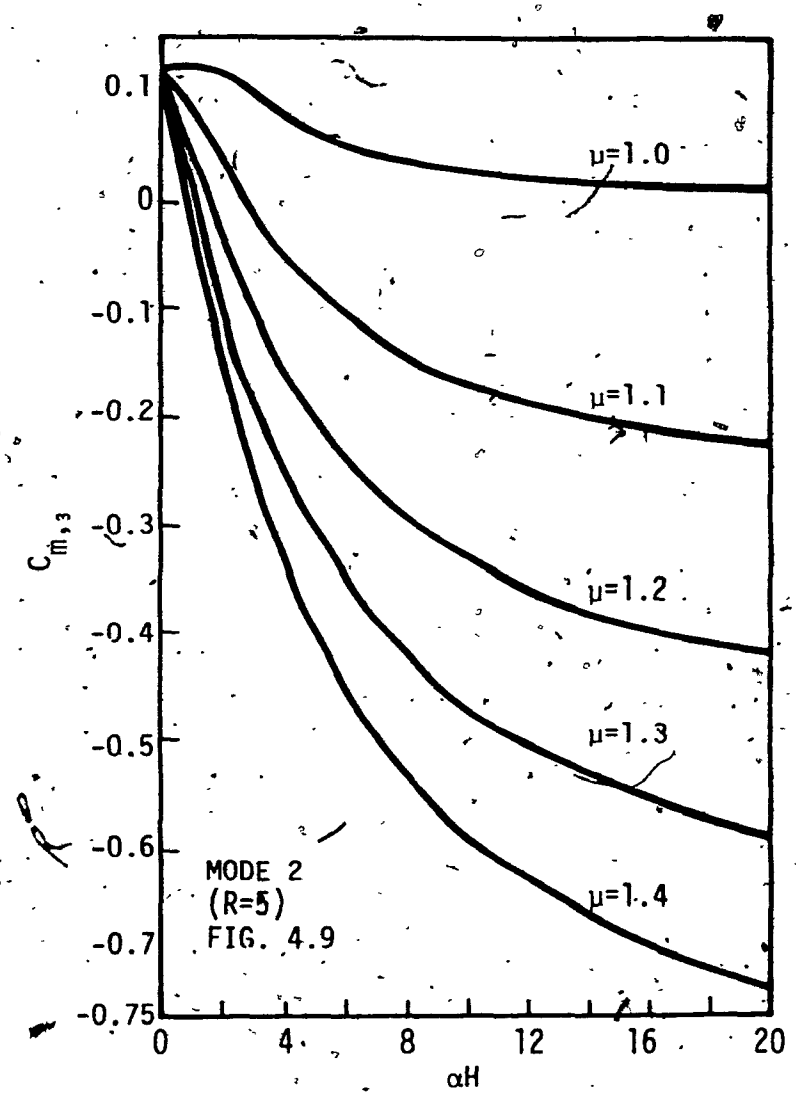

FIGS. 4.8 and 4.9 Moment Coefficient Curves for R=5 - Modes 1 and 2.

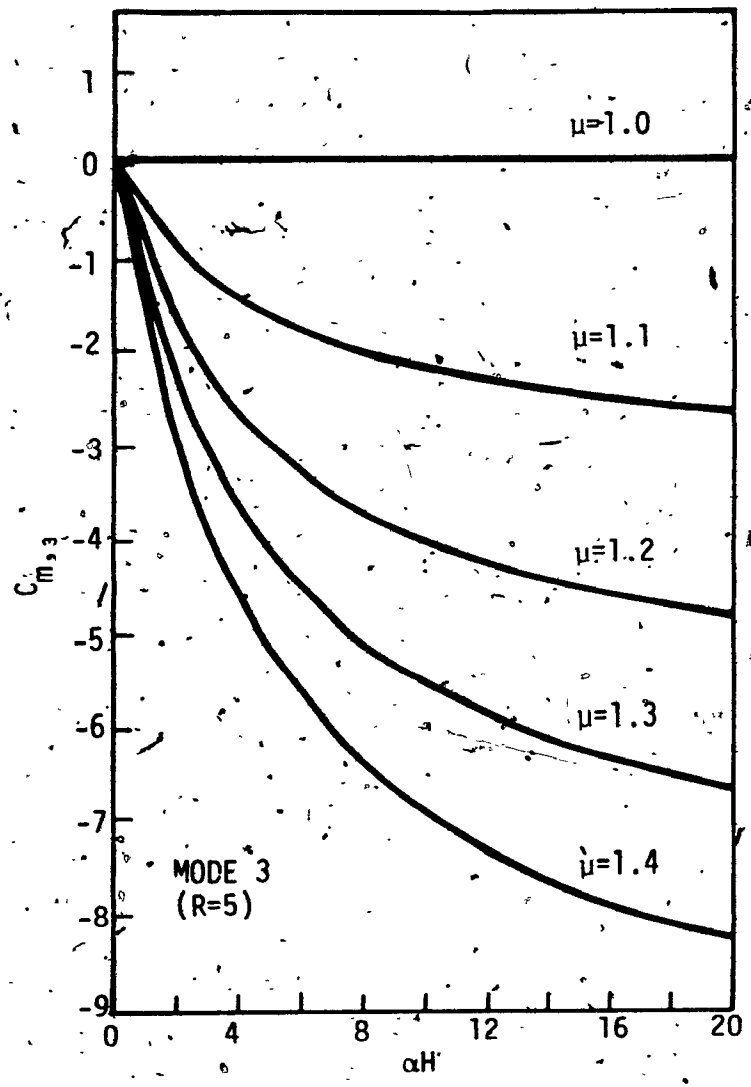

FIG. 4.10 Moment Coefficient Curves for R=5 - Mode 3.

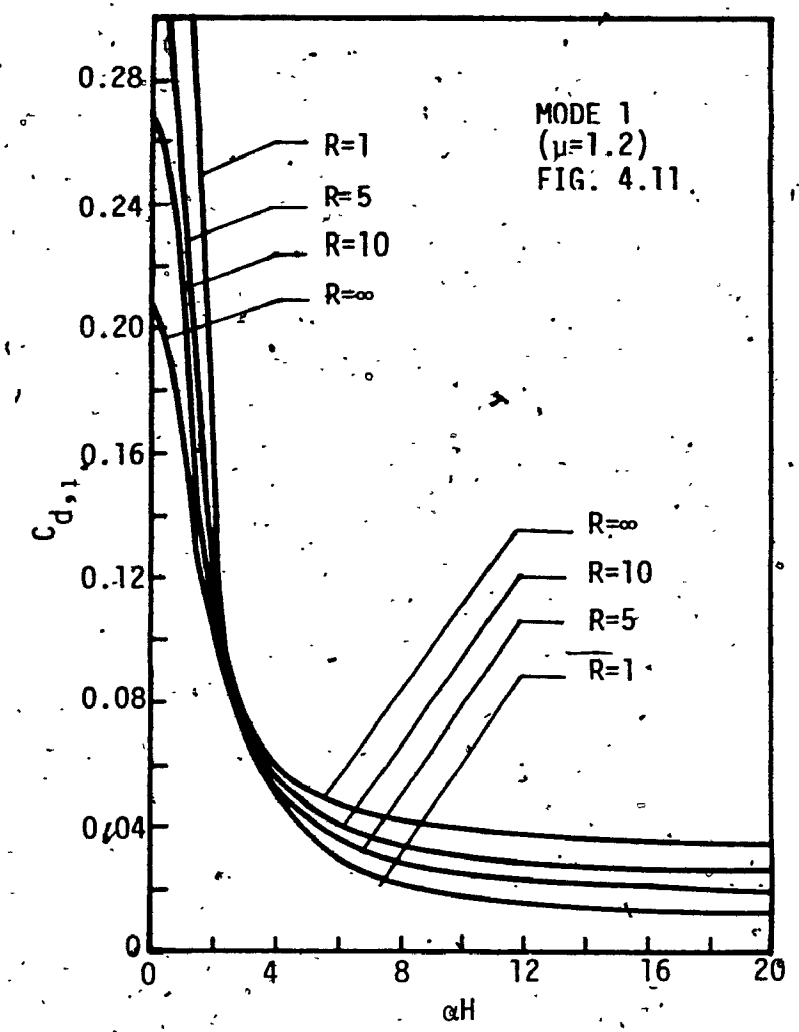

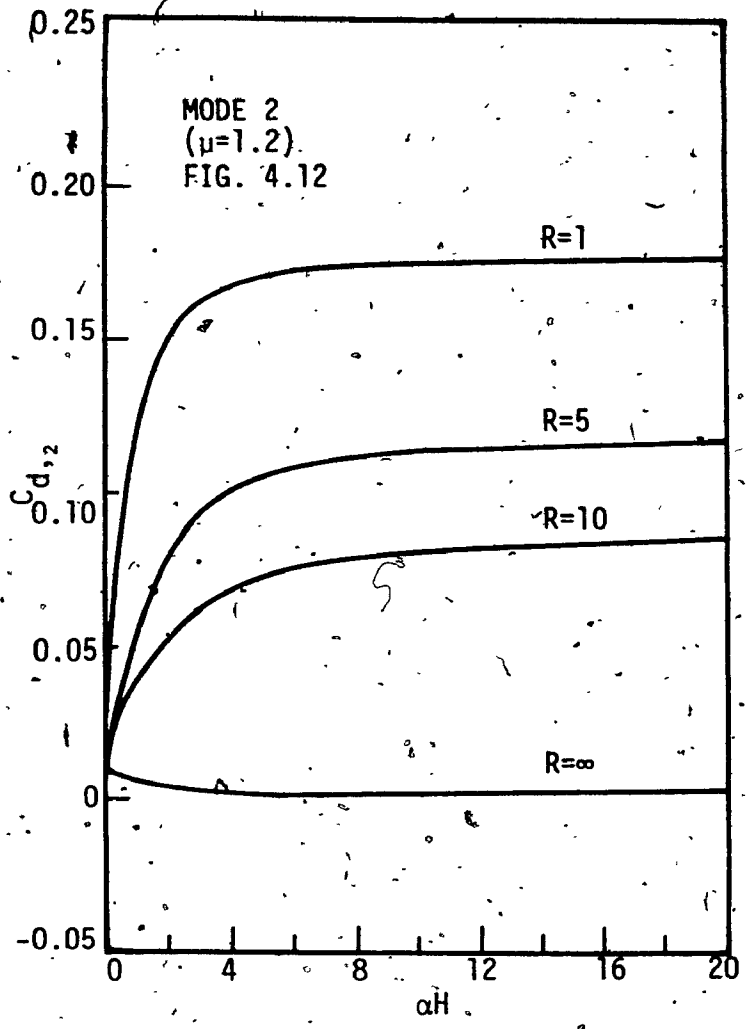

FIGS. 4.11 and 4.12 Top Deflection Coefficient Curves for Different R - Modes 1 and 2 (μ=1.2).

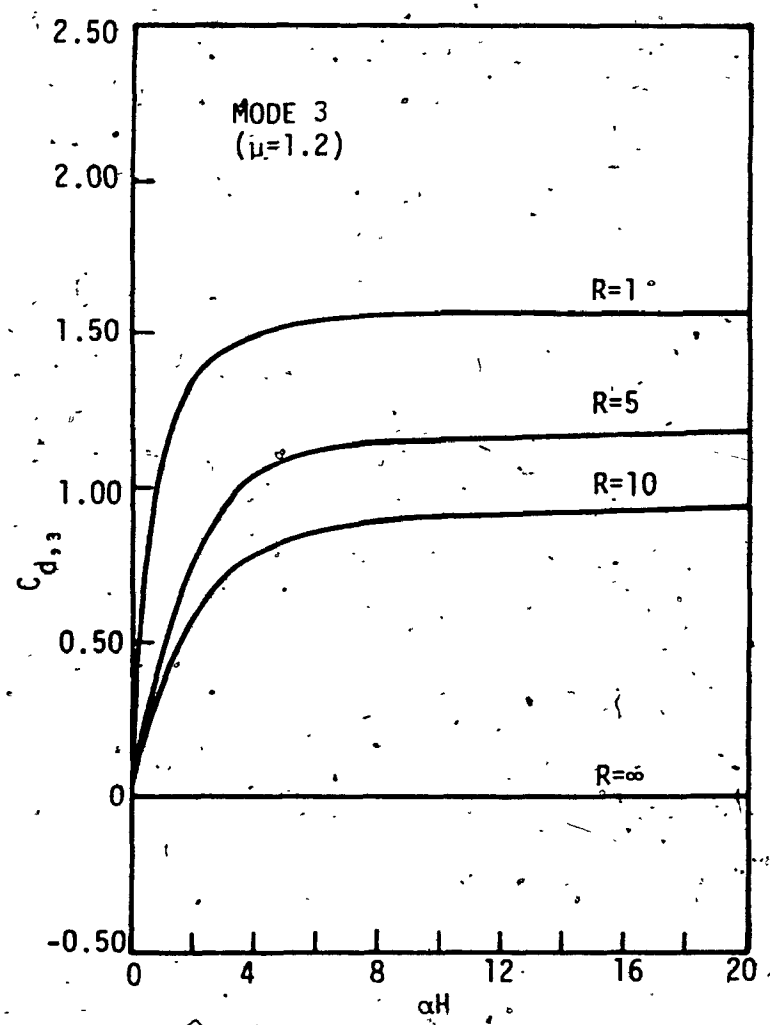

FIG. 4.13 Top Deflection Coefficient Curves for Different R - Mode 3 (μ=1.2).

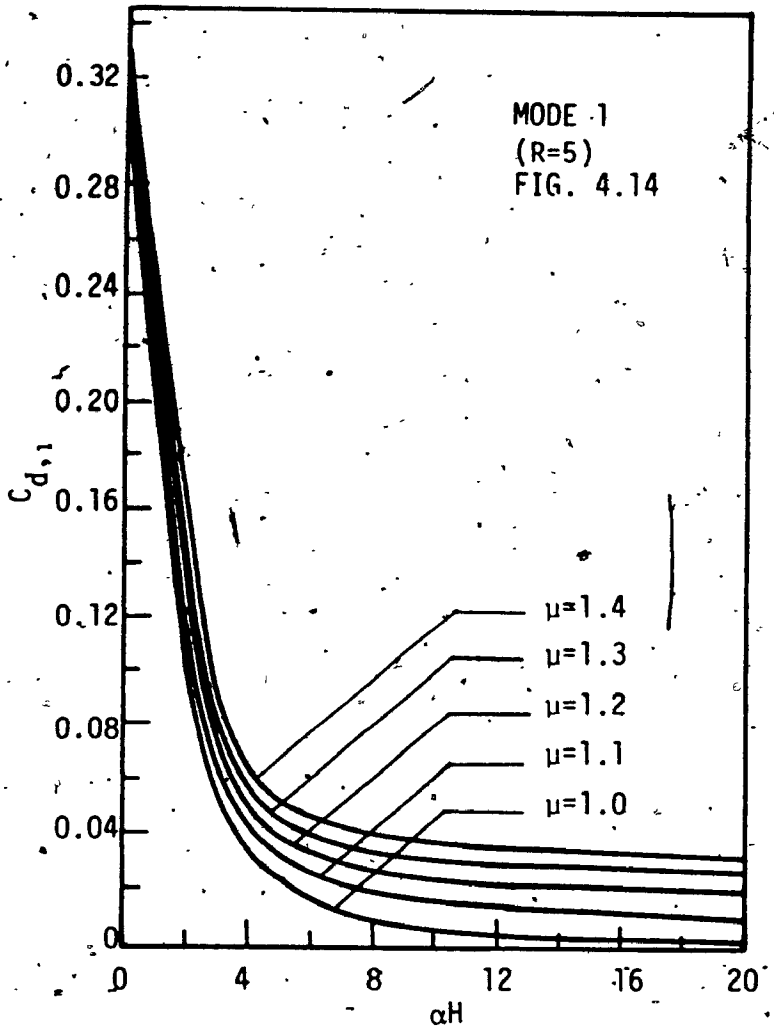

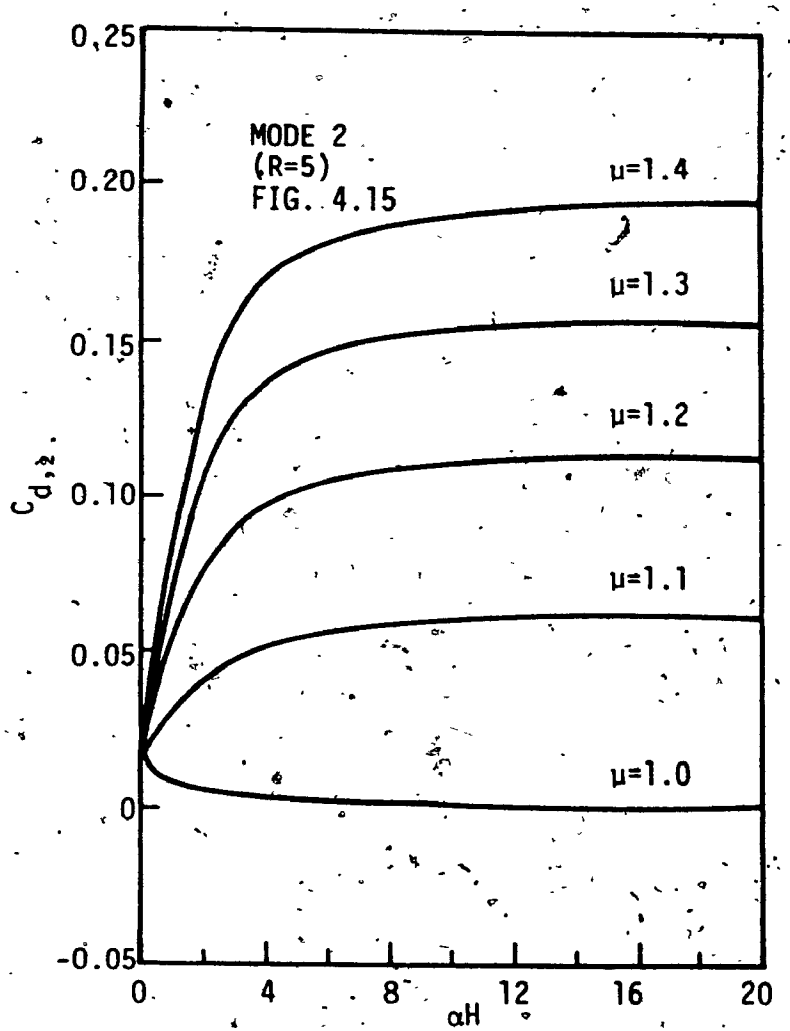

FIGS. 4.14 and 4.15 Top Deflection Coefficient Curves for Different μ - Modes 1 and 2 (R=5).

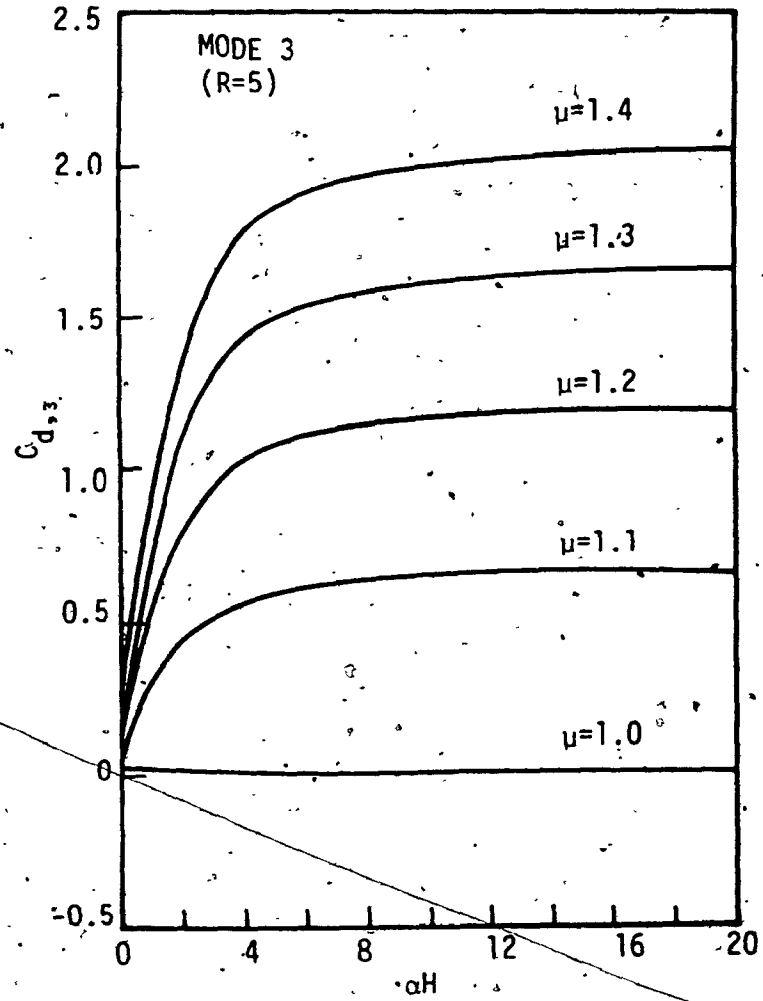

FIG. 4.16 Top Deflection Coefficient Curves for Different μ - Mode 3 (R=5).

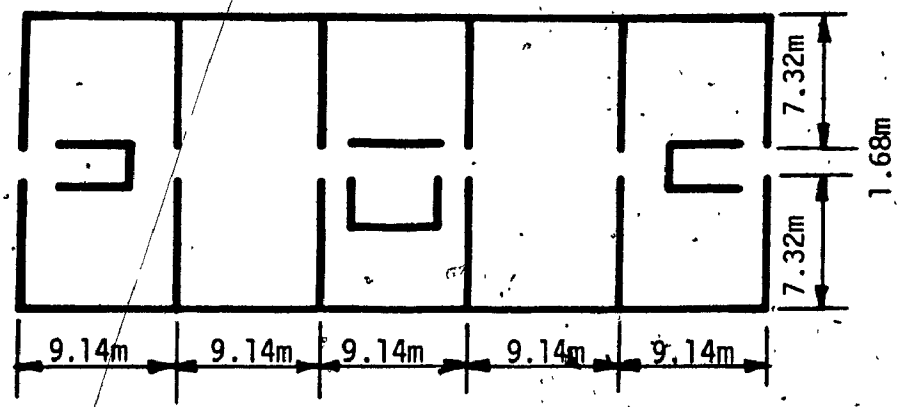

FIG. 4.17 Floor Plan of Example Buildings.

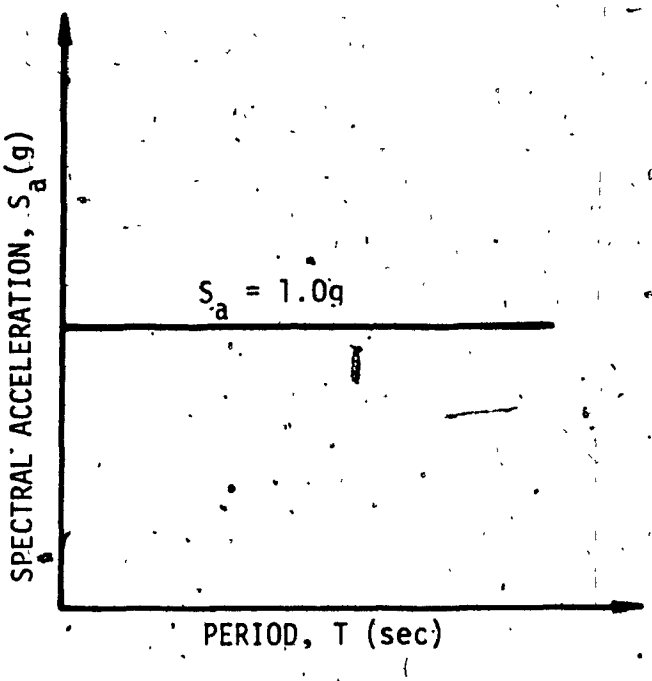

FIG. 4.18 Flat Reponse Spectrum.

CHAPTER V

CONCLUSION

5.1 SUMMARY

A study has been made on the seismic response of single and coupled shear walls resting on rotationally flexible foundations, employing the dynamic properties of flexibly mounted cantilever beams as reviewed in Chapter II.

In Chapter III the effect of rotational base flexibility on single shear walls was examined. In this investigation 5-, 10, 15 and 20-storey walls were chosen, various dynamic response coefficients and corresponding responses were obtained. These were presented as curves and tables for a selective set of foundation flexibility parameter values, ($R = \infty$, 10, 3 and 1). In addition, a comparison between the seismic response of single walls on rigid ($R = \infty$) and flexible prototype foundations (R = 0.5, 1.36 and 4.5) was made.

In Chapter IV work was confined to coupled shear walls on flexible foundations as an extention to the earlier study made by Tso and Rutenberg [15] for rigid foundations. This study examined the importance of rotational flexibility on seismic responses as function of structural parameters μ and αH, as well as foundation flexibility parameter R. In addition, two example problems showed the importance of foundation flexibility for 26 and 10-storey coupled shear wall buildings considering foundation flexibility given by $R = 5$ and 1, respectively.

The inclusion of rotational flexibility was found to be significant

for the response spectrum analysis of both the single and coupled shear walls. The various response parameters, namely, base shear, base moment and top deflection were found to be influenced by the foundation flexibility in different modes of vibration. For single walls the RSS of the three modes for top deflection is the parameter which is most affected by the rotational flexibility of the foundation. Similarly, for coupled shear walls the effect of base flexibility is most significant for top deflection also.

5.2 Future Research

Study of the effect of base flexibility in soil-structure interaction is becoming an important research area, but only little research is available in this area; thus, future research is warranted. The following topics for further investigation of soil-structure interaction are suggested.

1. In the present investigation only the rotational flexibility of the foundation was considered. In real problems the foundation may experience rotational as well as both lateral and vertical settlements. Therefore, research should be conducted to include both these degrees of freedom.
2. In the present research only elastic behaviour of both the soil and the structure was considered. Thus, study should be made on the importance of inelastic behaviour in the soil-structure system.
3. The moment coefficient curves for coupled shear walls (presented in Figs. 4.6 and 4.7) show behaviour which suggests an optimum foundation flexibility to minimize wall moments in the higher modes. Additional study of this phenomenon would be useful.

4. For comparison purposes time-history analysis of coupled shear walls on flexible foundation should be made in addition to the existing response spectrum analysis.

5. Thus far only theoretical results are available for the seismic response of single and coupled shear walls. Experimental results, although a difficult task, are desirable to verify these theoretical results.

REFERENCES

1. Gorman, D.J., "Free Vibration Analysis of Beams and Shafts", John Willey & Sons, August 1974.

2. Macbain, J.C., and Genin, J., "Effect of Support Flexibility on the Fundamental Frequency of Vibrating Beams", Journal of the Franklin Institute, Vol. 206, No. 4, October 1973, pp. 259-273.

3. Cardan, B., "Concrete Shear Walls Combined with Rigid Frames in Multistory Buildings Subjected to Lateral Loads", Journal of the American Concrete Institute, Vol. 58, Title No. 58-14, September 1961, pp. 299-315.

4. Beck, H., "Contribution to the Analysis of Coupled Shear Walls", Journal of the American Concrete Institute, Vol. 69, No. 8, August 1962, pp. 1055-1070.

5. Rosman, R., "Approximate Analysis of Shear Walls Subjected to Lateral Loadings", Journal of the American Concrete Institute, Vol. 61, No. 6, 1964, pp. 717-733.

6. Coull, A., and Choudhury, J.R., "Stresses and Deflections in Coupled Shear Walls", Journal of the American Concrete Institute, Vol. 64, No. 2, February 1967, pp. 65-72.

7. Coull, A., and Choudhury, J.R., "Analysis of Coupled Shear Walls", Journal of the American Concrete Institute, Vol. 64, No. 9, September 1967, pp. 587-593.

8. Heidebrecht, A.C., and Strafford Smith, B., "Approximate Analysis of Tall Wall-Frame Structures", Journal of the Structural Division, ASCE, Vol. 99, No. ST2, proc. paper 9550, February 1973, pp. 199-221.

9. Tso, W.K., and Chan, H.B., "Dynamic Analysis of Plane Coupled Shear Walls", Journal of the Engineering Mechanics Division, ASCE, Vol. 97, No. EM1, proc. paper 7899, February 1971, pp. 33-48.

10. Tso, W.K., and Biswas, J.K., "An Approximate Seismic Analysis of Coupled Shear Walls", Building Science, Vol. 7, 1972, pp. 249-256.

11. Mukherjee, P.R., and Coull, A., "Free Vibrations of Coupled Shear Walls", International Journal of Earthquake Engineering and Structural Dynamics, Vol. 1, 1973, pp. 377-386.

12. Coull, A., and Mukherjee, P.R., "Approximate Analysis of Natural Vibrations of Coupled Shear Walls", International Journal of Earthquake Engineering and Structural Dynamics, Vol. 2, 1973, pp. 171-183.

13. Rutenberg, A., "Approximate Natural Frequencies for Coupled Shear Walls", International Journal of Earthquake Engineering and Structural Dynamics, Vol. 4, 1975, pp. 95-100.

14. Basu, A.K., Nagpal, A.K. and Nagar, A.K., "Dynamic Characteristics of Frame-Wall Systems", Journal of the Structural Division, ASCE, Vol. 108, No. ST6, proc. paper 17171, June 1982, pp. 1201-1219.

15. Tso, W.K., and Rutenberg, A., "Seismic Spectral Response Analysis of Coupled Shear Walls", Journal of the Structural Division, ASCE, Vol. 103, No. ST1, proc. paper 12671, January 1977, pp. 181-196.

16. Coull, A., "Interaction of Coupled Shear Walls with Elastic Foundations", Journal of the American Concrete Institute, Vol. 68, No. 6, June 1971, pp. 456-461.

17. Tso, W.K., and Chan, P.C.K., "Flexible Foundation Effect on Coupled Shear Walls", Journal of the American Concrete Institute, Vol. 69, Title No. 69-65, November 1972, pp. 678-683.

18. Coull, A., and Chantaksinopas, B., "Design Curves for Coupled Shear Walls on Flexible Bases", Institution of Civil Engineers, Part 2, Vol. 57, December 1974, pp. 595-618.

19. Mukherjee, P.R., and Coull, A., "Free Vibrations of Coupled Shear Walls on Flexible Bases", Institution of Civil Engineers, Part 2, Vol. 57, September 1974, pp. 493-511.

20. Cheung, Y.K., and Swaddiwudhipong, S., "Free Vibration of Frame Shear Wall Structures on Flexible Foundations", International Journal of Earthquake Engineering and Structural Dynamics, Vol. 7, 1979, pp. 355-367.

21. Bowles, J.E., "Foundation Analysis and Design", 3rd Edition, McGraw-Hill, New York, 1982.

22. Dowrick, D.J., "Earthquake Resistance Design", John Willey & Sons, 1977.

23. National Building Code of Canada, National Research Council of Canada, Ottawa, Canada, 1980.

24. Response of Multistory Structures to Lateral Forces, Publication SP-36 American Concrete Institute, Detroit, 1973.

APPENDIX A

DERIVATION OF GOVERNING DIFFERENTIAL EQUATION FOR COUPLED SHEAR WALLS

For analysis the connecting beams (Fig. 4.1) are replaced by laminae (Fig. 4.2) where each has constant moment of inertia $= \frac{I_b dx}{h}$. In order to have a continuous set of laminae along the height of the shear wall, it is assumed that the end beam has cross-section and monent of inertia equal to one-half of the normal beams.

It is assumed that the connecting beams are rectangular in cross-section and do not undergo axial deformation. The point of contraflexure is assumed to occur at mid-span. If the laminae are assumed cut at the point of contraflexure, the delfection of the shear walls will introduce a gap $\delta_1(x)$ (Fig. A2(a)):

$$\delta_1(x) = \frac{ady}{dx} \tag{A1}$$

In addition, the distributed shear force $q(x)$ along the cut (Fig. A1) will produce deformation $\delta_2(x)$ due to bending moment and shear force (Figs. A2(b) and A2(c)):

$$\delta_2(x) = \left[\frac{hc^3}{12EI_b} + \frac{hc}{GA_b^*}\right] q(x) \tag{A2}$$

Finally, axial force introduces gap $\delta_2(x)$ caused by deformation of the shear walls (Fig. A2(d)):

$$\delta_3(x) = -\frac{1}{EI}\left(\frac{1}{A_1} + \frac{1}{A_2}\right) \int_0^x \left[\int_\eta^H q(\xi)\, d\xi\right] d\eta \tag{A3}$$

Compatibility requires that

$$\delta_1(x) + \delta_2(x) + \delta_3(x) = 0 \tag{A4}$$

Substituting Eqs. (A1), (A2), (A3) into Eq. (A4) gives

$$a\frac{dy}{dx} - \left[\frac{hc}{12EI_b} + \frac{hc}{GA_b^*}\right] q(x) - \frac{1}{E}\left(\frac{1}{A_1} + \frac{1}{A_2}\right) \int_0^x \left[\int_\eta^H q(\xi)\, d\xi\, d\eta = 0 \right. \tag{A5}$$

The moment-curvature relationship for the combined system is

$$E(I_1 + I_2)\frac{d^2y}{dx^2} = M - a\int_x^H q(\xi)\, d\xi \tag{A6}$$

Differentiating Eq. (A5) once and Eq. (A6) twice with respect to x gives

$$a\frac{d^2y}{dx^2} - \left[\frac{hc^3}{12EI_b} + \frac{hc}{GA_b^*}\right]\frac{dq}{dx} - \frac{1}{E}\left(\frac{1}{A_1} + \frac{1}{A_2}\right)\int_x^H q(\xi)\, d\xi = 0 \tag{A7}$$

and

$$E(I_1 + I_2)\frac{d^4y}{dx^4} = \frac{d^2M}{dx^2} + a\frac{dq}{dx} \tag{A8}$$

Eqs. (A8) and (A6) lead to

$$\frac{dq}{dx} = -\frac{1}{a}\cdot\frac{d^2M}{dx^2} + \frac{E(I_1 + I_2)}{a}\frac{d^4y}{dx^4} \tag{A9}$$

$$\int_x^H q(\xi)\, d\xi = \frac{M}{a} - \frac{E(I_1 + I_2)}{a}\frac{d^2y}{dx^2} \tag{A10}$$

Substituting Eqs. (A9) and (A10) into Eq. (A7) and re-arranging provides

$$\left[\frac{hc^3}{12EI_b} + \frac{hc}{GA_b^*}\right]\left[\frac{E(I_1 + I_2)}{a} \cdot \frac{d^4y}{dx^4}\right] - \left[a + \frac{1}{E}\left(\frac{1}{A_1} + \frac{1}{A_2}\right) \times \right.$$

$$\left. \frac{E(I_1 + I_2)}{a}\right] \frac{d^2y}{dx^2} - \left[\frac{hc^3}{12EI_b} + \frac{hc}{GA_b^*}\right]\left[\frac{1}{a} \cdot \frac{d^2M}{dx^2}\right]$$

$$+ \frac{1}{E}\left(\frac{1}{A_1} + \frac{1}{A_2}\right)\frac{M}{a} = 0 \qquad \text{(A11)}$$

After some mathematical steps and introducing the terms

$$\mu = 1 + \frac{I}{Aa^2} \qquad \text{(A12)}$$

$$I = I_1 + I_2 \qquad \text{(A13)}$$

$$\frac{1}{A} = \left(\frac{1}{A_1} + \frac{1}{A_2}\right) \qquad \text{(A14)}$$

$$\alpha^2 = \frac{ka^2}{EI}\mu \qquad \text{(A15)}$$

$$k = \frac{12EI_b}{hc^3}\left(1 + \frac{12EI_b}{GA_b^*c^2}\right)^{-1} \qquad \text{(A16)}$$

$$\frac{d^2M}{dx^2} = w = \text{distributed load} \qquad \text{(A17)}$$

leads to the required fourth-order differential equation

$$\frac{d^4y}{dx^4} - \alpha^2\frac{d^2y}{dx^2} = \frac{1}{EI}\left[w - \frac{\alpha^2(\mu-1)}{\mu}M\right] \qquad \text{(A18)}$$

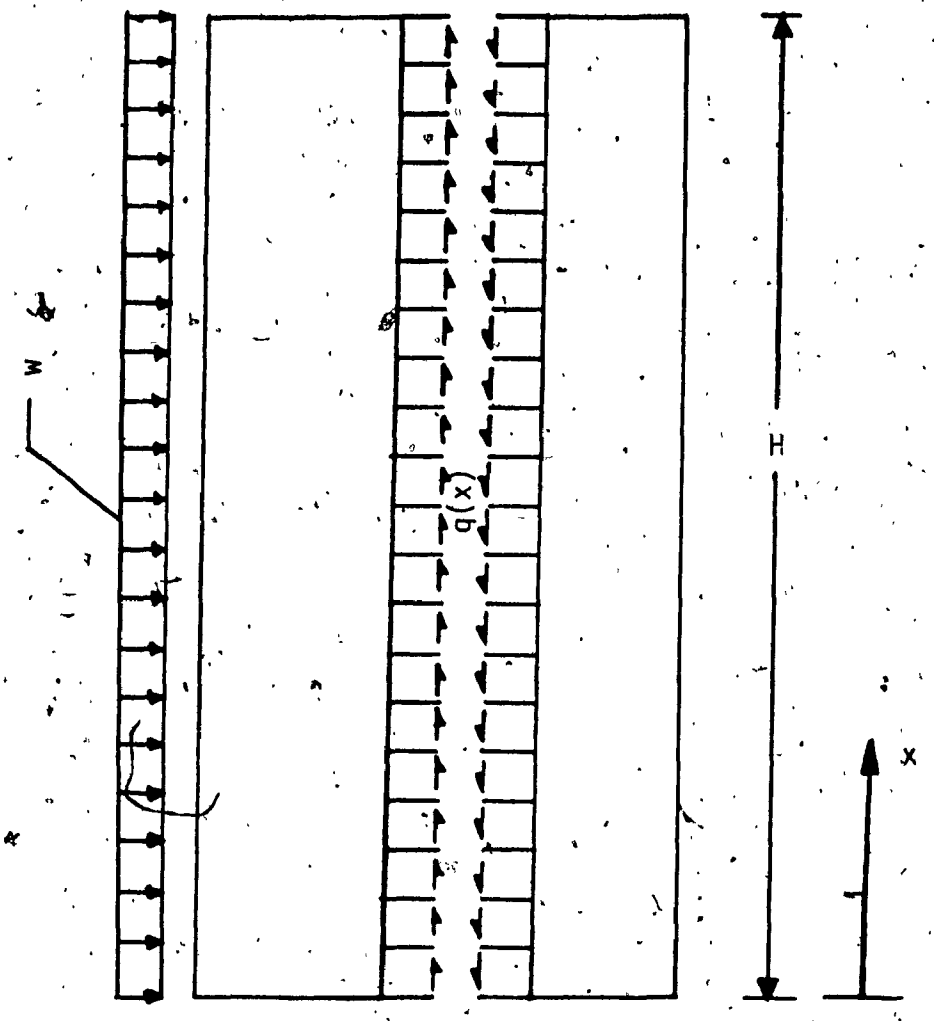

FIG. A1 Distributed Shear Force Along Cut.

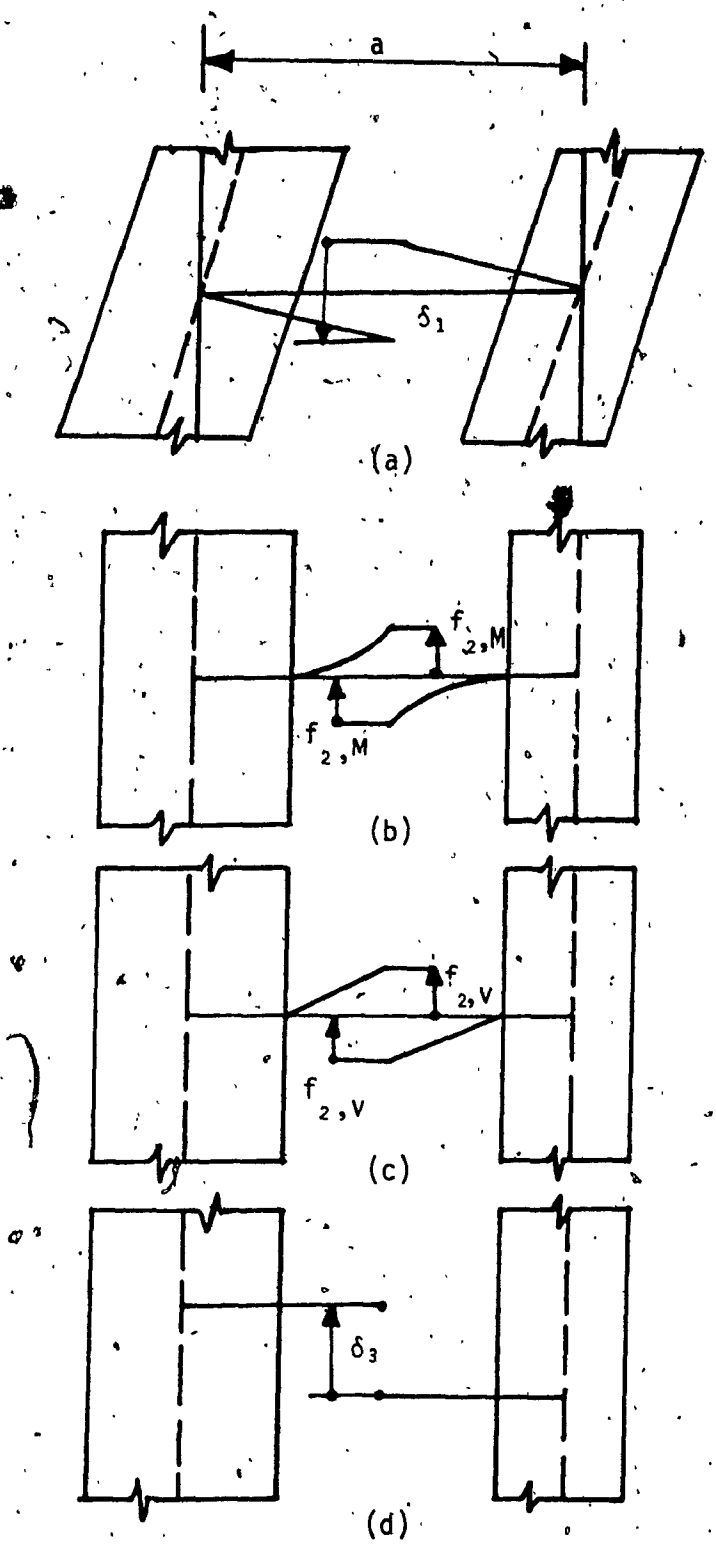

FIG. A2 Deformations of the Lamina [4].

APPENDIX B

B1 DERIVATION OF COEFFICIENTS $C_{1r}, C_{2r}, C_{3r}, C_{4r}, C_{5r}, C_{6r}$

In Chapter IV the general solution for differential Eq. (4.1a)

$$\frac{d^4y}{dx^4} - \alpha^2 \frac{d^2y}{dx^2} = \frac{1}{EI}\left[w - \frac{\alpha^2(\mu-1)}{\mu} M\right] \tag{4.1a}$$

which can further be written, in terms of differential oparator D, as

$$D^2(D^2-\alpha^2)y = \frac{1}{EI}\left[w - \frac{\alpha^2(\mu-1)}{\mu} M\right] \tag{B1}$$

is given by Eq. (4.8).

$$\begin{aligned} y(x) = {} & C_{1r} + C_{2r}x + C_{3r} \sinh \alpha x \\ & + C_{4r} \cosh \alpha x + C_{5r}\left[\cosh \beta_r x + \left(\frac{2\beta_r H}{R} - \frac{1}{\gamma_r}\right) \sinh \beta x\right. \\ & \left. + C_{6r}\left[\cos \beta_r x - \frac{1}{\gamma_r} \sin \beta_r x\right]\right. \end{aligned} \tag{4.8}$$

In Eq. (4.8) the complementary and particular solutions are represented, respectively, as

$$y_c = C_{1r} + C_{2r}x + C_{3r} \sinh \alpha x + C_{4r} \cosh \alpha x \tag{B2}$$

and

$$\begin{aligned} y_p = {} & C_{5r}\left[\cosh \beta_r x + \left(\frac{2\beta_r H}{R} - \frac{1}{\gamma_r}\right) \sinh \beta_r x\right] \\ & + C_{6r}\left[\cos \beta_r x - \frac{1}{\gamma_r} \sin \beta_r x\right] \end{aligned} \tag{B3}$$

In the following sections the derivation of the coefficeints of the general solution are presented. To simplify presentation, coefficents C_{5_r} and C_{6_r} are derived first.

B1.1 Derivation of Coefficients C_{5_r} and C_{6_r}

To determine coefficients C_{5_r} and C_{6_r} direct use of Eq. (B1) is made. From Eq. (B3) it follows that

$$Dy_p = C_{5_r}\beta_r \sinh \beta_r x + C_{5_r}\left(\beta_r\left(\frac{2\beta_r H}{H} - \frac{1}{\gamma_r}\right)\cosh \beta_r x\right.$$
$$+ C_{6_r}\beta_r \sin \beta_r x + C_{6_r}\frac{\beta_r}{\gamma_r}\cos \beta_r x \qquad \text{(B4)}$$

$$D^2y_p = C_{5_r}\beta_r^2 \cosh \beta_r x + C_{5_r}\beta_r^2\left(\frac{2\beta_r H}{R} - \frac{1}{\gamma_r}\right)\sinh \beta_r x$$
$$- C_{6_r}\beta_r^2 \cos \beta_r x + C_{6_r}\frac{\beta_r^2}{\gamma_r}\sin \beta_r x \qquad \text{(B5)}$$

$$D^3y_p = C_{5_r}\beta_r^3 \sinh \beta_r x + C_{5_r}\beta_r^3\left(\frac{2\beta_r H}{R} - \frac{1}{\gamma_r}\right)\cosh \beta_r x$$
$$+ C_{6_r}\beta_r^3 \sin \beta_r x + C_{6_r}\frac{\beta_r^3}{\gamma_r}\cos \beta_r x \qquad \text{(B6)}$$

$$D^4y_p = C_{5_r}\beta_r^4 \cosh \beta_r x + C_{5_r}\beta_r^4\left(\frac{2\beta_r H}{R} - \frac{1}{\gamma_r}\right)\sinh \beta_r x$$
$$+ C_{6_r}\beta_r^4 \cos \beta_r x - C_{6_r}\frac{\beta_r^4}{\gamma_r}\sin \beta_r x \qquad \text{(B7)}$$

Eq. (B1) can be written as

$$(D^4 - D^2\alpha^2)y_p = \frac{1}{EI}\left[mP_r s_{ar}\phi_r(x) - \frac{\alpha^2(\mu-1)}{\mu}M\right] \qquad \text{(B8)}$$

Substituting D^4y_p and D^2y_p in Eq. (B8) gives

$$C_{5r}\,\beta_r^4 \cosh \beta_r x + C_{5r}\,\beta_r^4 \left(\frac{2\beta_r H}{R} - \frac{1}{\gamma_r}\right) \sinh \beta_r x$$

$$+ C_{6r}\,\beta_r^4 \cos \beta_r x - C_{6r}\,\frac{\beta_r^4}{\gamma_r} \sin \beta_r x$$

$$- \alpha^2 \left[C_{5r}\,\beta_r^2 \cosh \beta_r x + C_{5r}\,\beta_r^2 \left(\frac{2\beta_r H}{R} - \frac{1}{\gamma_r}\right) \sinh \beta_r x\right.$$

$$\left. - C_{6r}\,\beta_r^2 \cos \beta_r x + C_{6r}\,\frac{\beta_r^2}{\gamma_r} \sin \beta_r x\right]$$

$$= \frac{V_r(o)\beta_r\gamma_r}{NEI} \left[\cosh \beta_r x + \left(\frac{2\beta_r H}{R} - \frac{1}{\gamma_r}\right) \sinh \beta_r x\right]$$

$$- \frac{V_r(o)\beta_r\gamma_r}{NEI} \left[\cos \beta_r x - \frac{1}{\gamma_r} \sin \beta_r x\right]$$

$$- \frac{2V_r(o)\gamma_r}{N\beta_r EI} \left[\frac{\alpha^2(\mu-1)}{\mu}\right] \qquad \text{(B9)}$$

Eq. (B9) can further be expressed as .

$$C_{5r}\,\beta_r^2 (\beta_r^2 - \alpha^2)\left[\cosh \beta_r x + \left(\frac{2\beta_r H}{R} - \frac{1}{\gamma_r}\right) \sinh \beta_r x\right]$$

$$+ C_{6r}\,\beta_r^2 (\beta_r^2 + \alpha^2)\left[\cos \beta_r x - \frac{1}{\gamma_r} \sin \beta_r x\right]$$

$$= \frac{V_r(o)\gamma_r}{NEI\beta_r^3} \left(\beta_r^4 \left[\cosh \beta_r x + \left(\frac{2\beta_r H}{R} - \frac{1}{\gamma_r}\right) \sinh \beta_r x\right]\right)$$

$$- \frac{V_r(o)\gamma_r}{NEI\beta_r^3} \left[\beta_r^4 \left(\cos \beta_r x - \frac{1}{\gamma_r} \sin \beta_r x\right)\right]$$

$$- \frac{V_r(o)\gamma_r}{NEI\beta_r^3} \left(\beta_r^2 \left[\frac{\alpha^2(\mu-1)}{\mu}\right]\right)$$

$$- \frac{V_r(o)\gamma_r}{NEI\beta_r^3} \left(\beta_r^2 \left[\frac{\alpha^2(\mu-1)}{\mu}\right]\right) \qquad \text{(B10)}$$

Since Eq. (B10) is to be an identity, the corresponding coefficients in the two members of Eq. (B10) must be equal. That is

$$C_{5_r}\,\beta_r^2(\beta_r^2-\alpha^2)\left[\cosh\beta_r x+\left(\frac{2\beta_r H}{R}-\frac{1}{\gamma_r}\right)\sinh\beta_r x\right]$$

$$=\frac{V_r(o)\gamma_r}{NEI\beta_r^3}\left(\beta_r^4\left[\cosh\beta_r x+\left(\frac{2\beta_r H}{R}-\frac{1}{\gamma_r}\right)\sinh\beta_r x\right]\right)$$

$$-\frac{V_r(o)\gamma_r}{NEI\beta_r^3}\left(\beta_r^2\left[\frac{\alpha^2(\mu-1)}{\mu}\right]\right) \qquad \text{(B11)}$$

and

$$C_{6_r}\,\beta_r^2\,(\beta_r^2+\alpha^2)\left(\cos\beta_r x-\frac{1}{\gamma_r}\sin\beta_r x\right)$$

$$=-\frac{V_r(o)\gamma_r}{NEI\beta_r^3}\left[\beta_r^4\left(\cos\beta_r x-\frac{1}{\gamma_r}\sin\beta_r x\right)\right]$$

$$-\frac{V_r(o)\gamma_r}{NEI\beta_r^3}\left(\beta_r^2\left[\frac{\alpha^2(\mu-1)}{\mu}\right]\right) \qquad \text{(B12)}$$

Finally Eqs. (B11) and (B12) provide the coefficients C_{5_r} and C_{6_r} as

$$C_{5_r}=\frac{V_r(o)\gamma_r}{NEI\beta_r^3}\left[1+\frac{\alpha^2}{\mu(\beta_r^2-\alpha^2)}\right] \qquad \text{(B13)}$$

and

$$C_{6_r}=-\frac{V_r(o)\gamma_r}{NEI\beta_r^3}\left[1-\frac{\alpha^2}{\mu(\beta_r^2+\alpha^2)}\right] \qquad \text{(B14)}$$

B1.2 Derivation of Coefficients C_{1_r}, C_{2_r}, C_{3_r} and C_{4_r}

Coefficients C_{1_r}, C_{2_r}, C_{3_r} and C_{4_r} are derived here using general solution Eq. (4.8) and the boundary conditions given by Eqs. (4.2)-(4.5);

i) at the base of the walls where $x = 0$,

$$y(o) = 0 \tag{4.2}$$

$$K_\theta \frac{dy}{dx}(o) = EI\, y''(o) \tag{4.3}$$

ii) at the top of the wall where $x = H$,

$$\frac{d^2y}{dx^2}(H) = 0 \tag{4.4}$$

$$\frac{d^3y}{dx^3}(H) - \alpha^2 \frac{dy}{dx}(H) + \frac{\alpha^2(\mu-1)}{EI\mu} \int_0^H M(x)\, dx = 0 \tag{4.5}$$

Differentiating Eq. (4.8) with respect to x three times gives

$$y'(x) = C_{2_r} + C_{3_r}\alpha \cosh \alpha x + C_{4_r}\, \alpha \sinh \alpha x$$
$$+ C_{5r}\, \beta_r \left[\sinh \beta_r x + \left(\frac{2\beta_r H}{R} - \frac{1}{\gamma_r}\right) \cosh \beta_r x\right]$$
$$- C_{6_r}\, \beta_r \left(\sin \beta_r x + \frac{1}{\gamma_r} \cos \beta_r x\right) \tag{B15}$$

$$y''(x) = C_{3_r}\, \alpha^2 \sinh \alpha x + C_{4_r}\, \alpha^2 \cosh \alpha x$$
$$+ C_{5_r}\, \beta_r^2 \left[\cosh \beta_r x + \left(\frac{2\beta_r H}{R} - \frac{1}{\gamma_r}\right) \sinh \beta_r x\right]$$
$$- C_6 \beta_r^2 \left(\cos \beta_r x - \frac{1}{\gamma_r} \sin \beta_r x\right) \tag{B16}$$

$$y'''(x) = C_{3_r}\, \alpha^3 \cosh \alpha x + C_{4_r}\, \alpha^3 \sinh \alpha x$$
$$+ C_{5_r}\, \beta_r^3 \left[\sinh \beta_r x + \left(\frac{2\beta_r H}{R} - \frac{1}{\gamma_r}\right) \cosh \beta_r x\right]$$

$$+ C_{6_r} \beta_r^3 \left[\sin \beta_r x + \frac{1}{\gamma_r} \cos \beta_r x\right] \tag{B17}$$

From Eqs. (4.8) and (4.2)

$$y(o) = C_{1_r} + C_{4_r} + C_{5_r} + C_{6_r} = 0 \tag{B18}$$

Therefore

$$C_{1_r} = -C_{4_r} - (C_{5_r} + C_{6_r}) \tag{B19}$$

Substituting $x = 0$ in Eqs. (B15) and (B16) and $x = H$ in Eqs. (B15), (B16) and (B17) gives

$$y'(o) = C_{2_r} + C_{3_r}\alpha + C_{5_r}\beta_r \left(\frac{2\beta_r H}{R} - \frac{1}{\gamma_r}\right) - C_{6_r}\frac{\beta_r}{\gamma_r} \tag{B20}$$

$$y''(o) = C_{4_r}\alpha^2 + C_{5_r}\beta_r^2 - C_{6_r}\beta_r^2 \tag{B21}$$

$$y'(H) = C_{2_r} + C_{3_r}\alpha \cosh \alpha H + C_{4_r}\alpha \sinh \alpha H$$
$$+ C_{5_r}\beta_r \left[\sinh \beta_r H + \left(\frac{2\beta_r H}{R} - \frac{1}{\gamma_r}\right) \cosh \beta_r H\right]$$
$$- C_{6_r}\beta_r \left(\sin \beta_r H + \frac{1}{\gamma_r} \cos \beta_r H\right) \tag{B22}$$

$$y''(H) = C_{3_r}\alpha^2 \sinh \alpha H + C_{4_r}\alpha^2 \cosh \alpha H$$
$$+ C_{5_r}\beta_r^2 \left[\cosh \beta_r H + \left(\frac{2\beta_r H}{R} - \frac{1}{\gamma_r}\right) \sinh \beta_r H\right]$$
$$- C_{6_r}\beta_r^2 \left[\cos \beta_r H - \frac{1}{\gamma_r} \sin \beta_r H\right] \tag{B23}$$

$$y'''(H) = C_{3_r}\,\alpha^3 \cosh \alpha H + C_{4_r}\,\alpha^3 \sinh \alpha H$$
$$+ C_{5_r}\,\beta_r^3 \left[\sinh \beta_r H + \left(\frac{2\beta_r H}{R} - \frac{1}{\gamma_r}\right) \cosh \beta_r H\right]$$
$$+ C_{6_r}\,\beta_r^3 \left(\sin \beta_r H + \frac{1}{\gamma_r} \cos \beta_r H\right) \qquad \text{(B24)}$$

Eq. (4.3) can be written, after the substitution of Eqs. (B20) and (B21), as

$$K_\theta \left[C_{2_r} + C_{3_r}\alpha + C_{5_r}\,\beta_r \left(\frac{2\beta_r H}{R} - \frac{1}{\gamma_r}\right) - C_{6_r}\,\frac{\beta}{\gamma_r}\right]$$
$$= EI \left[C_{4_r}\,\alpha^2 + C_{5_r}\,\beta_r^2 - C_{6_r}\,\beta_r^2\right] \qquad \text{(B25)}$$

Multiplying both sides of Eq. (B25) by H and dividing both sides of the same equation by EI, leads to

$$\frac{K_\theta H}{EI} \left[C_{2_r} + C_{3_r}\,\alpha^2 + C_{5_r}\,\beta_r \left(\frac{2\beta_r H}{R} - \frac{1}{\gamma_r}\right) - C_{6_r}\,\frac{\beta}{\gamma_r}\right]$$
$$= H \left[C_{4_r}\,\alpha^2 + C_{5_r}\,\beta_r^2 - C_{6_r}\,\beta_r^2\right] \qquad \text{(B26)}$$

The above expression becomes

$$R\left[C_{2r} + C_{3r}\alpha + C_{5r}\,\beta_r \left(\frac{2\beta_r H}{R} - \frac{1}{\gamma_r}\right) - C_{6r}\,\frac{\beta_r}{\gamma_r}\right]$$
$$= H\left[C_{4r}\alpha^2 + C_{5r}\,\beta_r^2 - C_{6r}\,\beta_r^2\right] \qquad \text{(B27)}$$

Thus, Eq. (B27) gives the expression for coefficeint C_{3_r} as

$$C_{3_r} = \left[C_{4_r}\left(\frac{\alpha H}{R}\right) - \left(\frac{\beta_r^2 H}{R\alpha} - \frac{\beta_r}{\gamma_r \alpha}\right)(C_{5_r} + C_{6_r}) - \frac{C_{2_r}}{\alpha}\right] \qquad \text{(B28)}$$

Substituting Eq. (B28) in Eq. (B23), which can be written according to Eq. (4.4) as

$$y''(H) = C_{3_r}\,\alpha^2 \sinh \alpha H + C_{4_r}\,\alpha^2 \cosh \alpha H + C_{5_r}\,\beta_r^2 \left[\cosh \beta_r H + \left(\frac{2\beta_r H}{R} - \frac{1}{\gamma_r}\right) \sinh \beta_r H\right] - C_{6_r}\,\beta_r^2 \left[\cos \beta_r H - \frac{1}{\gamma_r} \sin \beta_r H\right] = 0 \qquad \text{(B29)}$$

gives, after some further steps

$$C_{4_r}\left[\frac{\alpha H}{R} \tanh \alpha H + 1\right] = C_{6_r}\,\beta_r^2 \left[\frac{\gamma_r \cos \beta_r H - \sin \beta_r H}{\alpha^2 \gamma_r \cosh \alpha H}\right] - C_{5_r}\,\beta_r^2 \left[\frac{R\gamma_r \cosh \beta_r H + (2\beta_r \gamma_r H - R) \sinh \beta_r H}{R\alpha^2 \gamma_r \cosh \alpha H}\right] + \frac{C_{2_r} \tanh \alpha H}{\alpha} + (C_{5_r} + C_{6_r}) \left(\frac{\beta_r^2 H}{R\alpha} - \frac{\beta_r}{\gamma_r \alpha}\right) \tanh \alpha H \qquad \text{(B30)}$$

or

$$C_{2_r} = C_{4_r}\left[\frac{\alpha^2 H}{R} + \frac{\alpha}{\tanh \alpha H}\right] + C_{5_r}\,\beta_r^2 \left[\frac{R\gamma_r \cosh \beta_r H + (2\beta_r H\gamma_r - R) \sinh \beta_r H}{R\alpha\gamma_r \sinh \alpha H}\right] - C_{6_r}\,\beta_r^2 \left[\frac{\gamma_r \cos \beta_r H - \sin \beta_r H}{\alpha\gamma_r \sinh \alpha H}\right] - (C_{5_r} + C_{6_r}) \left(\frac{\beta_r^2 H}{R} - \frac{\beta_r}{\gamma_r}\right) \qquad \text{(B31)}$$

After substitution of the expressions for C_{5_r} and C_{6_r} from Eqs. (B13) and (B14), the expression for C_{2_r} becomes

$$C_{2_r} = C_{4_r}\left[\frac{\alpha^2 H}{R} + \frac{\alpha}{\tanh \alpha H}\right] + \left[\frac{V_r(\bar{o})}{NEI\ \mu(\beta^4-\alpha^4)}\right]\left[\frac{\alpha\beta_r\phi_r(x)}{\sinh \alpha H}\right.$$

$$\left. - 2\gamma_r \alpha^2 \left(\frac{\beta_r H}{R} - \frac{1}{\gamma_r}\right)\right] \qquad (B32)$$

Coefficient C_{4_r} is determined from the Eq. (4.5) as follows

$$\frac{d^3y}{dx^3}(H) - \alpha^2 \frac{dy}{dx}(H) + \frac{\alpha^2(\mu-1)}{EI\mu} \int_0^H M(x)\, dx = 0 \qquad (4.5)$$

where

$$\int_0^H M(x)\, dx = \frac{mP_r S_{ar} H}{\beta_r^2}\left(\frac{1}{\beta_r H}\left[\cos \beta_r H - \cosh \beta_r H\right.\right.$$

$$\left. + \gamma_r (\sin \beta_r H + \sinh \beta_r H)\right]$$

$$\left. + \frac{2\gamma_r}{R}\left[\cosh \beta_r H - 1\right]\right) \qquad (B33)$$

Employing Eqs. (B22), (B24) and (B33), Eq. (4.5) can be written as

$$C_{3_r} \alpha^3 \cosh \alpha H + C_{4_r} \alpha^3 \sinh \alpha H + C_{5_r} \beta_r^3 \left[\sinh \beta_r H\right.$$

$$\left. + \left(\frac{2\beta_r H}{R} - \frac{1}{\gamma_r}\right) \cosh \beta_r H\right] + C_{6_r} \beta_r^3 \left[\sin \beta_r H + \frac{1}{\gamma_r} \cos \beta_r H\right]$$

$$- \alpha^2 \left[C_{2_r} + C_{3_r} \cosh \alpha H + C_{4_r} \alpha \sinh \alpha H\right.$$

$$\left. + C_{5_r} \beta_r \left[\sinh \beta_r H + \left(\frac{2\beta_r H}{R} - \frac{1}{\gamma_r}\right) \cosh \beta_r H\right]\right.$$

$$\left. - C_{6_r} \beta_r \left(\sin \beta_r H + \frac{1}{\gamma_r} \cos \beta_r H\right)\right]$$

$$+ \left[\frac{\alpha^2(\mu-1)}{EI\mu}\right] \left(\frac{2mP_r S_{ar} H}{\beta_r^2}\right)\left(\frac{1}{2\beta_r H}\left[\cos \beta_r H - \cosh \beta_r H\right.\right.$$

$$\left.\left. - \gamma_r (\sin \beta_r H + \sinh \beta_r H)\right] + \frac{\gamma_r}{R} (\cosh \beta_r H - 1)\right) = 0 \qquad \text{(B34)}$$

The above equation, after substitution of the expressions for coefficients C_{2_r} and C_{3_r}, becomes

$$C_{4_r} \left[\frac{\alpha^4 H}{R} + \frac{\alpha^3}{\tanh \alpha H}\right] = C_{5_r} \left(\alpha^2 \beta_r [\sinh \beta_r H + \left(\frac{2\beta_r H}{R} - \frac{1}{\gamma_r}\right) \cosh \beta_r H]\right.$$

$$\left. \times \left(\frac{\beta_r^2}{\alpha^2} - 1\right)\right) - C_{5_r} \left(\alpha\beta^2 \left[\frac{R\gamma_r \cosh \beta_r H + (2\beta_r H\gamma_r - R) \sinh \beta_r H}{R\gamma_r \sinh \alpha H}\right]\right)$$

$$+ C_{5_r} \alpha^2 \left(\frac{\beta_r^2 H}{R} - \frac{\beta_r}{\gamma_r}\right) + C_{6_r} \left[\alpha^2 \beta_r \left(\sin \beta_r H + \frac{1}{\gamma_r} \cos \beta_r H\right)\left(\frac{\beta_r^2}{\alpha^2} + 1\right)\right]$$

$$+ C_{6_r} \left[\alpha\beta^2 \left(\frac{\gamma \cos \beta_r H - \sin \beta_r H}{\gamma_r \sinh \alpha H}\right)\right] + C_{6_r} \alpha^2 \left(\frac{\beta_r^2 H}{R} - \frac{\beta_r}{\gamma_r}\right)$$

$$+ \left[\frac{\alpha^2(\mu-1)}{EI\mu}\right]\left(\frac{mP_r S_{ar} H}{\beta_r^2}\right)\left(\frac{1}{\beta_r H}\left[\cos \beta_r H - \cosh \beta_r H + \gamma_r(\sin \beta_r H\right.\right.$$

$$\left.\left. + \sinh \beta_r H)\right] + \frac{2\gamma_r}{R} (\cosh \beta_r H - 1)\right) \qquad \text{(B35)}$$

Eq. (B35), after using the expression for coefficients C_{5_r} and C_{6_r} and performing numerous mathematical steps and substitutions, gives the final expression for C_{4_r} in terms of base shear as

$$C_{4_r} = -\frac{1}{D_1} \left[\frac{V_r(o)}{NEI\,\mu(\beta_r^4 - \alpha^4)} (D_2 - D_3 D_4 - D_5 D_6)\right] \qquad \text{(B36)}$$

where

$$D_1 = \left[\frac{\alpha^4 H}{R} + \frac{\alpha^3}{\tanh \alpha H}\right] \qquad \text{(B37)}$$

$$D_2 = \left[\frac{\alpha^3 \beta_r \phi_r(H)}{\sinh \alpha H} - 2\gamma_r \alpha^4 \left(\frac{\beta_r H}{R} - \frac{1}{\gamma_r}\right)\right] \tag{B38}$$

$$D_3 = \left[\cos \beta_r H - \cosh \beta_r H + \gamma_r (\sin \beta_r H + \sinh \beta_r H) + \frac{2\beta_r H}{R} \cosh \beta_r H\right] \tag{B39}$$

$$D_4 = \left[\alpha^2 \beta_r^2 - \frac{\alpha^2 \mu (\beta_r^4 - \alpha^4)}{\beta_r^2} - \frac{\alpha^6}{\beta_r^2}\right] \tag{B40}$$

$$D_5 = \left[\frac{\alpha^2 H(\mu-1)(\beta_r^4 - \alpha^4)}{\beta}\right] \tag{B41}$$

$$D_6 = \frac{1}{\beta_r H}\left[\cos \beta_r H - \cosh \beta_r H + \gamma_r (\sin \beta_r H + \sinh \beta_r H)\right]$$

$$+ \frac{2\gamma_r}{R} (\cosh \beta_r H - 1)$$

APPENDIX C

ADDITIONAL DATA FOR COUPLED SHEAR WALLS ON RIGID FOUNDATION

Moment and top deflection coefficient curves are presented in this Appendix for rigid foundation condition ($R = \infty$). Although these curves are available in the work by Tso and Rutenberg [15], they are included here for the sake of completeness of the present investigation.

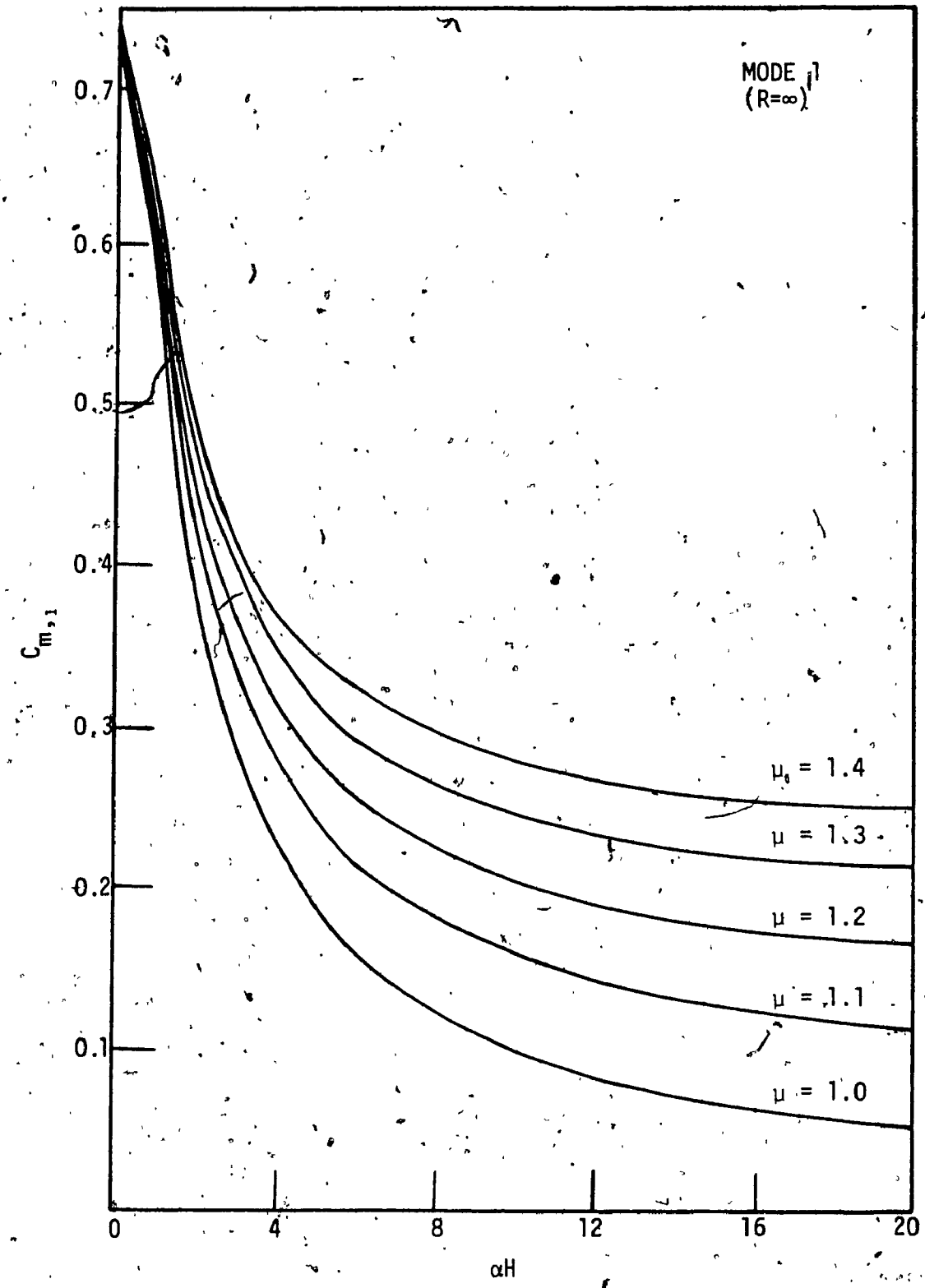

FIG. C1 Moment Coefficient Curves for R=∞ - Mode 1.

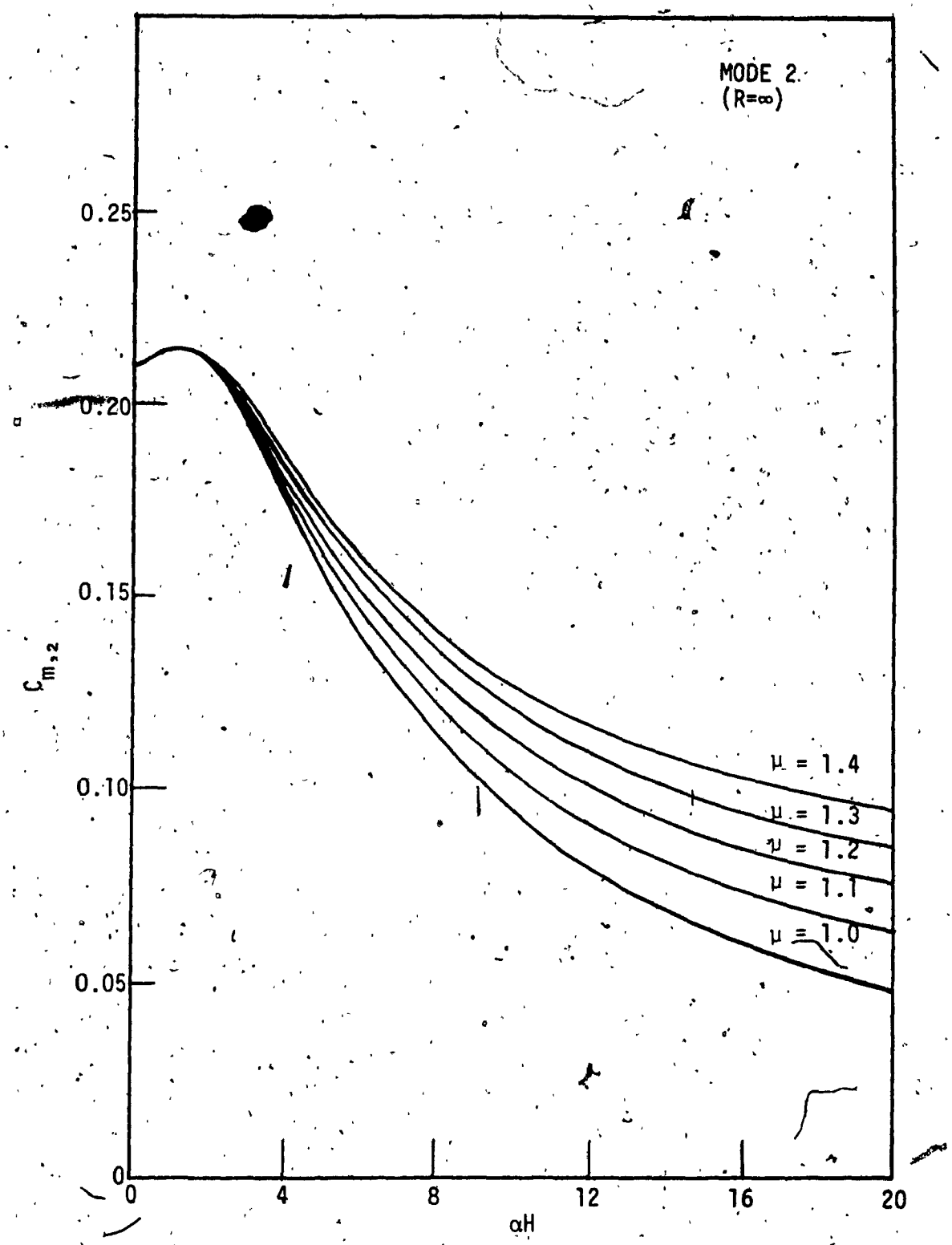

FIG. C2 - Moment Coefficient Curves for R=∞ - Mode 2.

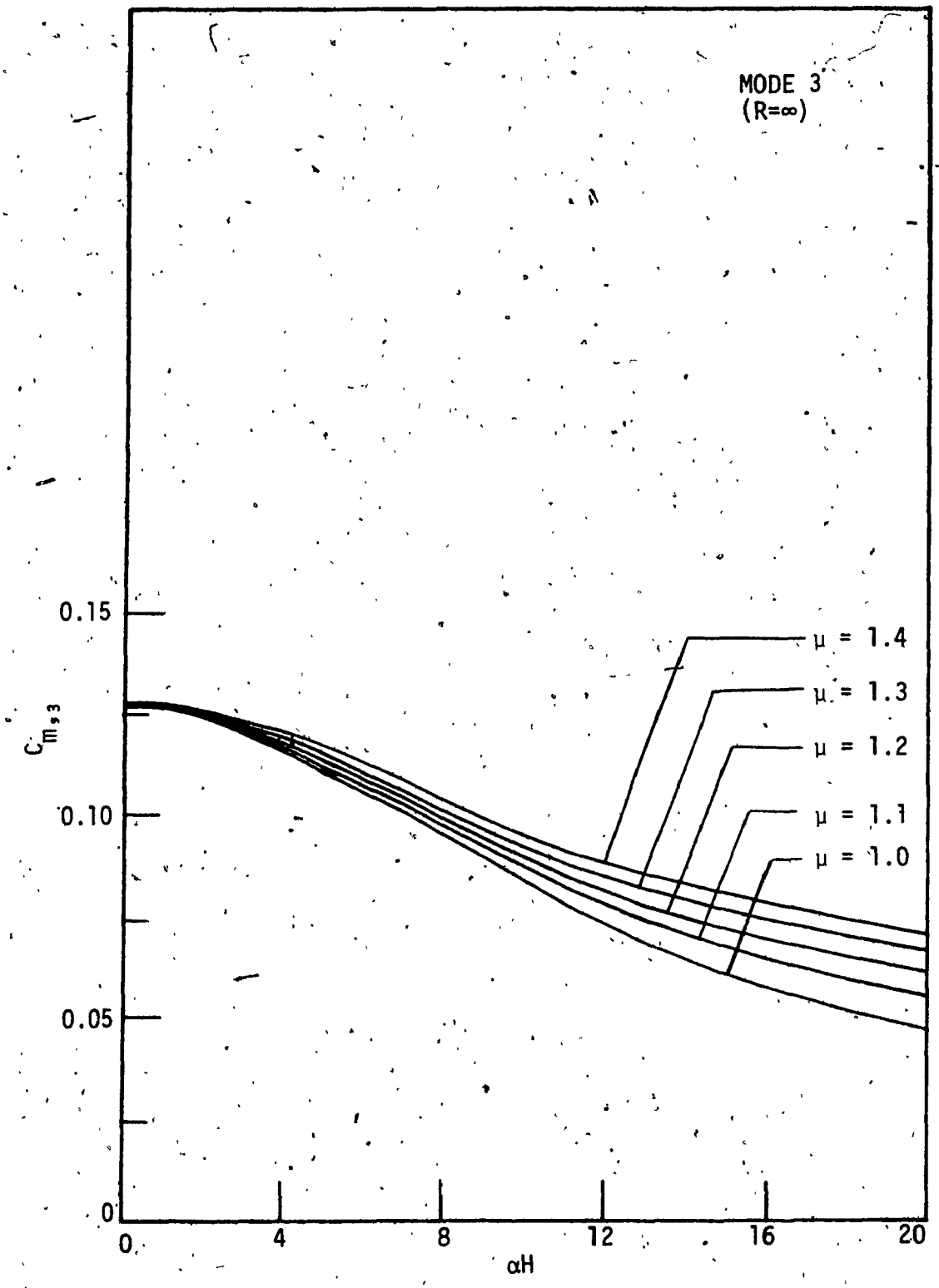

FIG. C3 Moment Coefficient Curves for R=∞ - Mode 3.

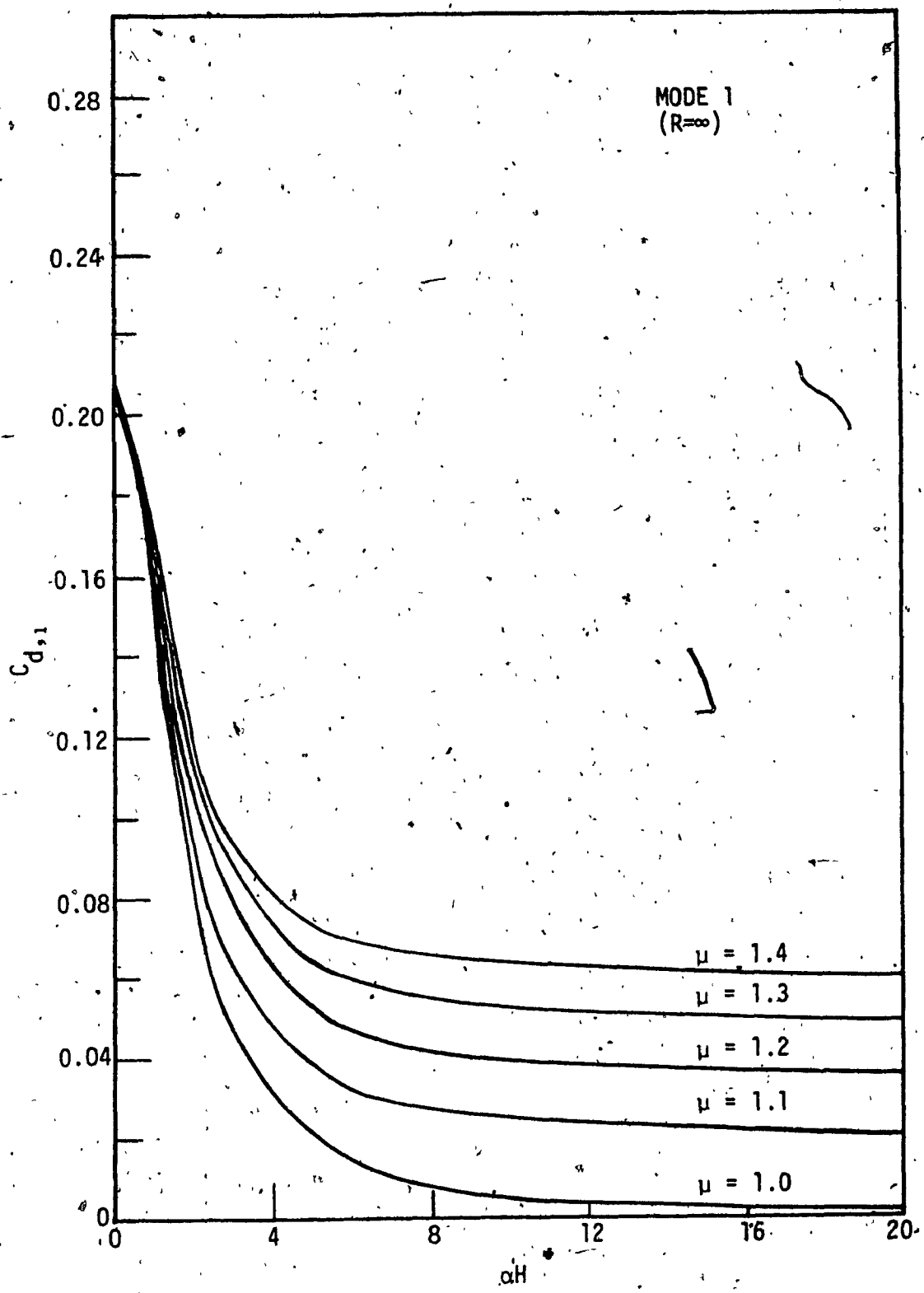

FIG. C4 Top Deflection Coefficient Curves for R=∞ - Mode 1.

APPENDIX D

MISCELLANEOUS DATA FOR COUPLED SHEAR WALLS ON FLEXIBLE FOUNDATIONS

Additional data for moment coefficient $C_{m,r}$ and top deflection coefficient $C_{d,r}$ for $\mu = 1.0$ and 1.4, not presented in Chapter IV, is included in this Appendix.

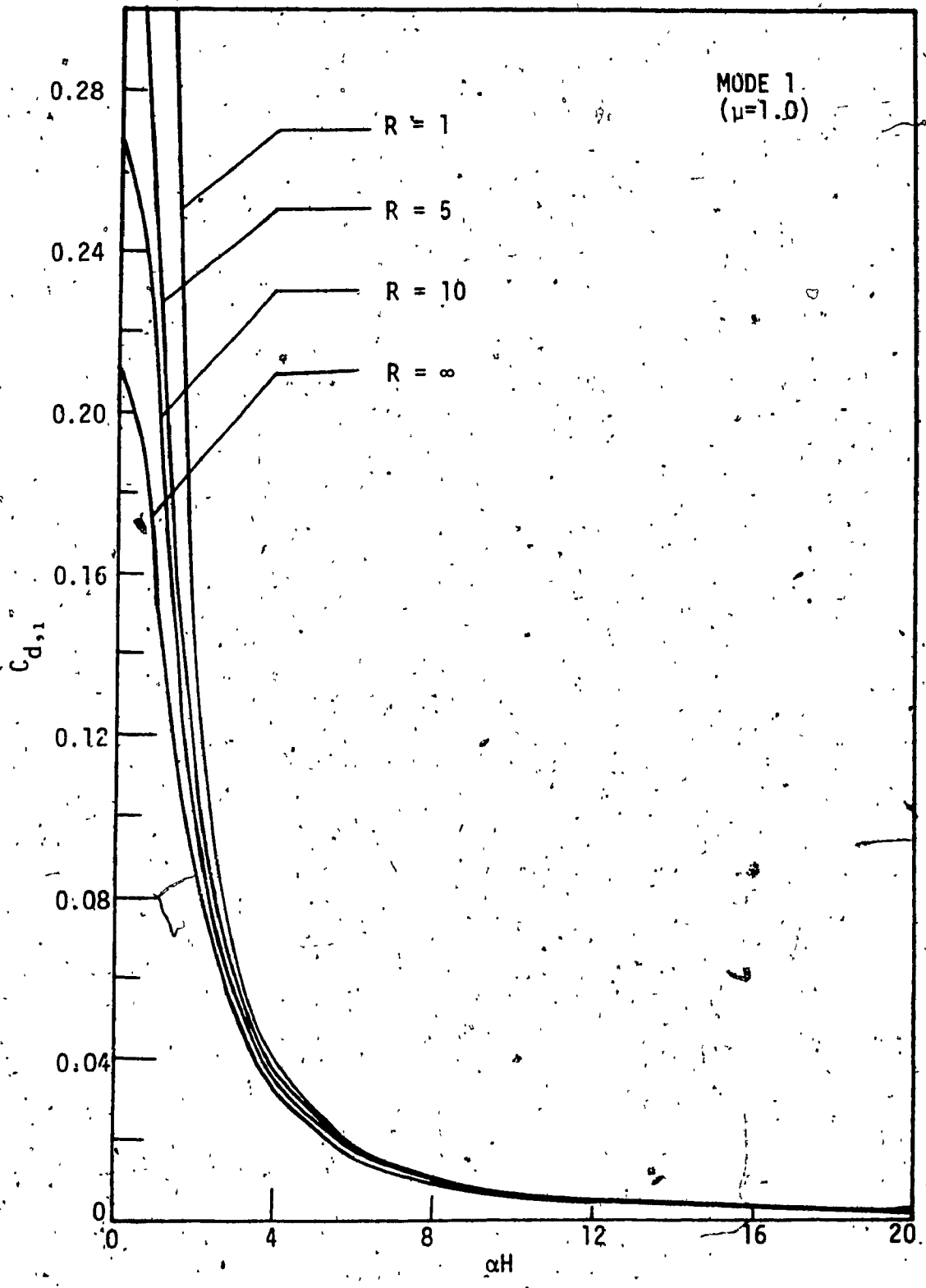

FIG. D1 Top-Deflection Coefficient Curves for Different R - Mode 1 (μ=1.0).

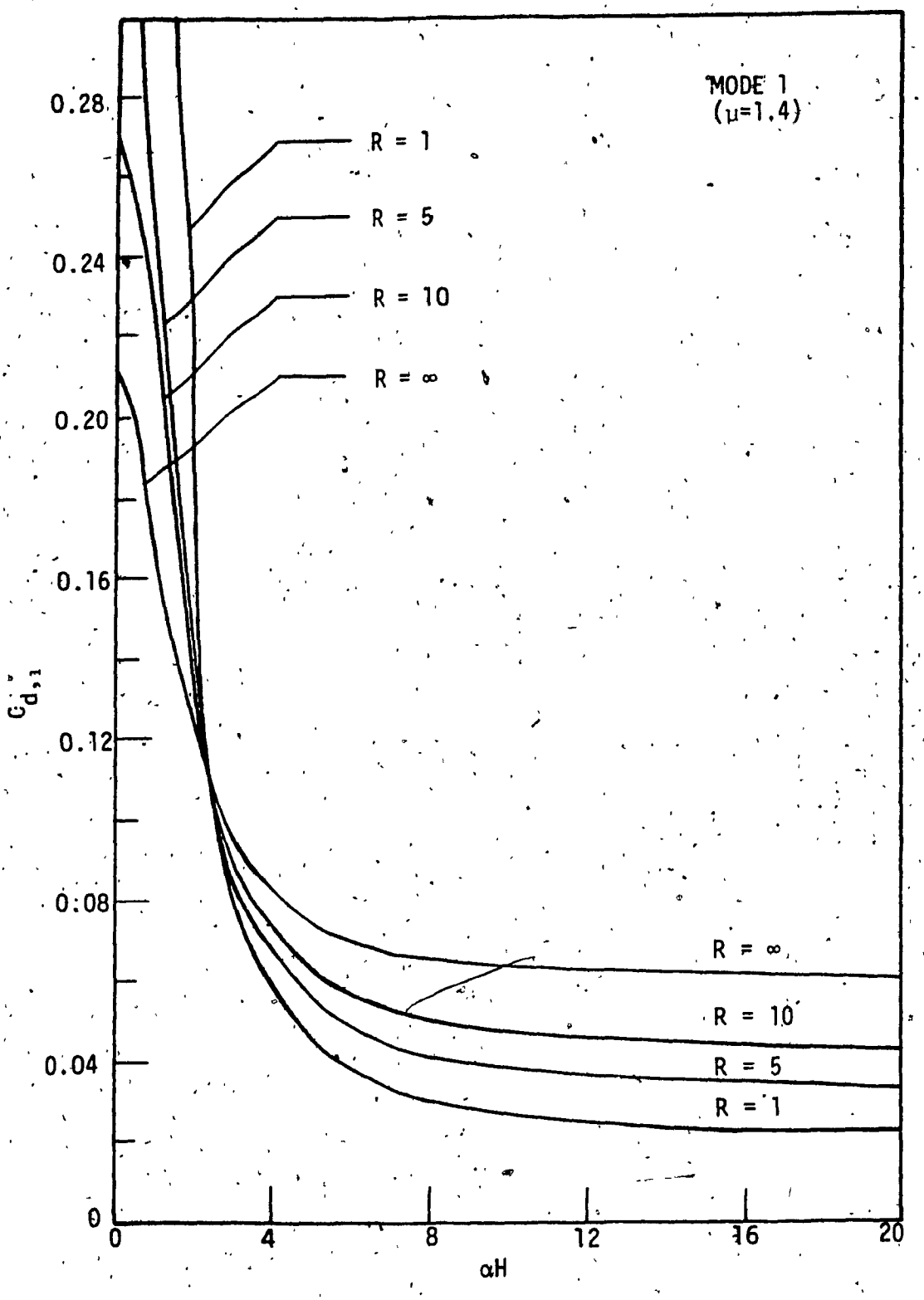

FIG. D2 Top Deflection Coefficient Curves for Different R - Mode 1 (μ=1.4).

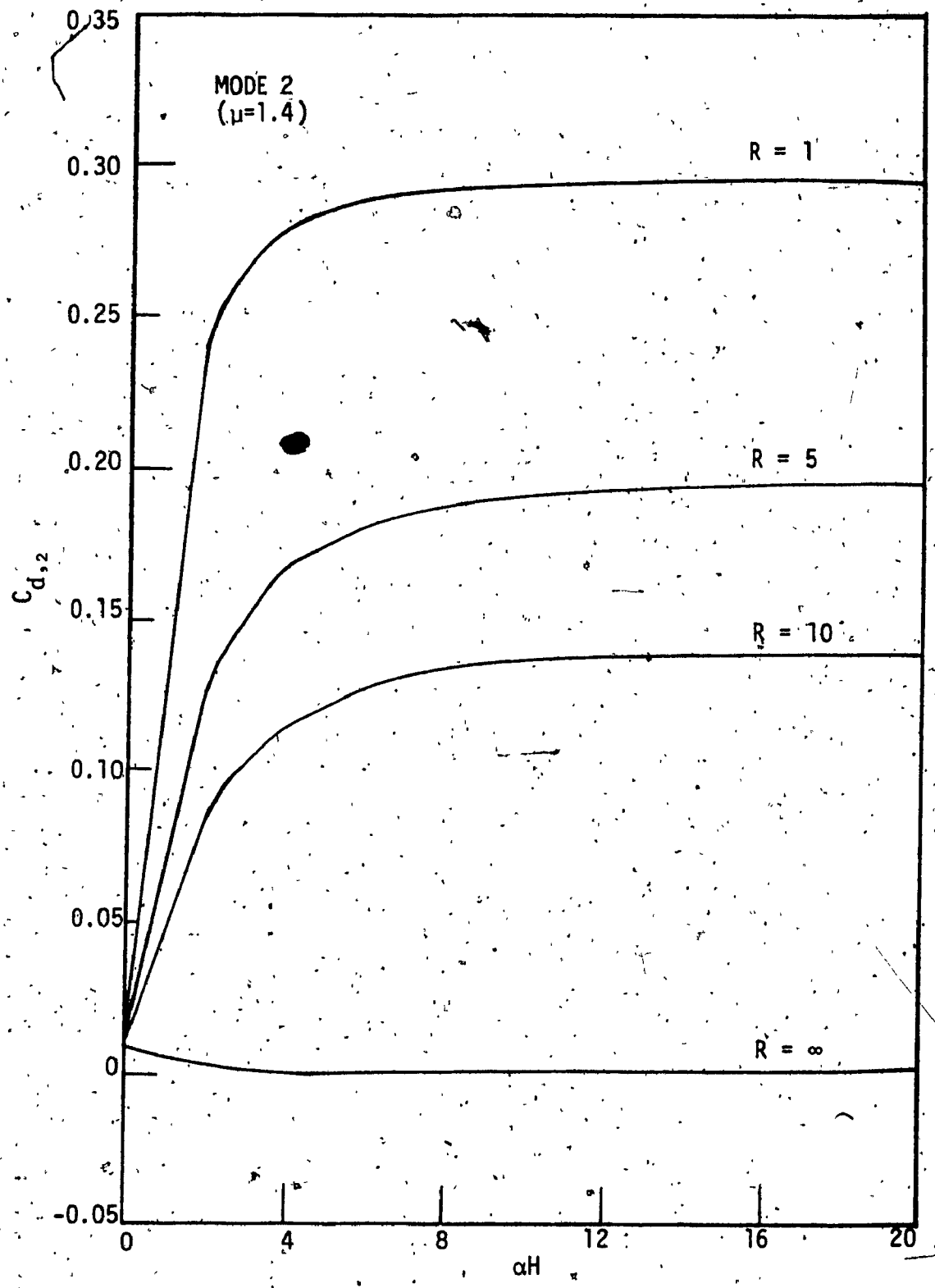

FIG. D3 Top Deflection Coefficient Curves for Different R - Mode 2 (μ=1.4).

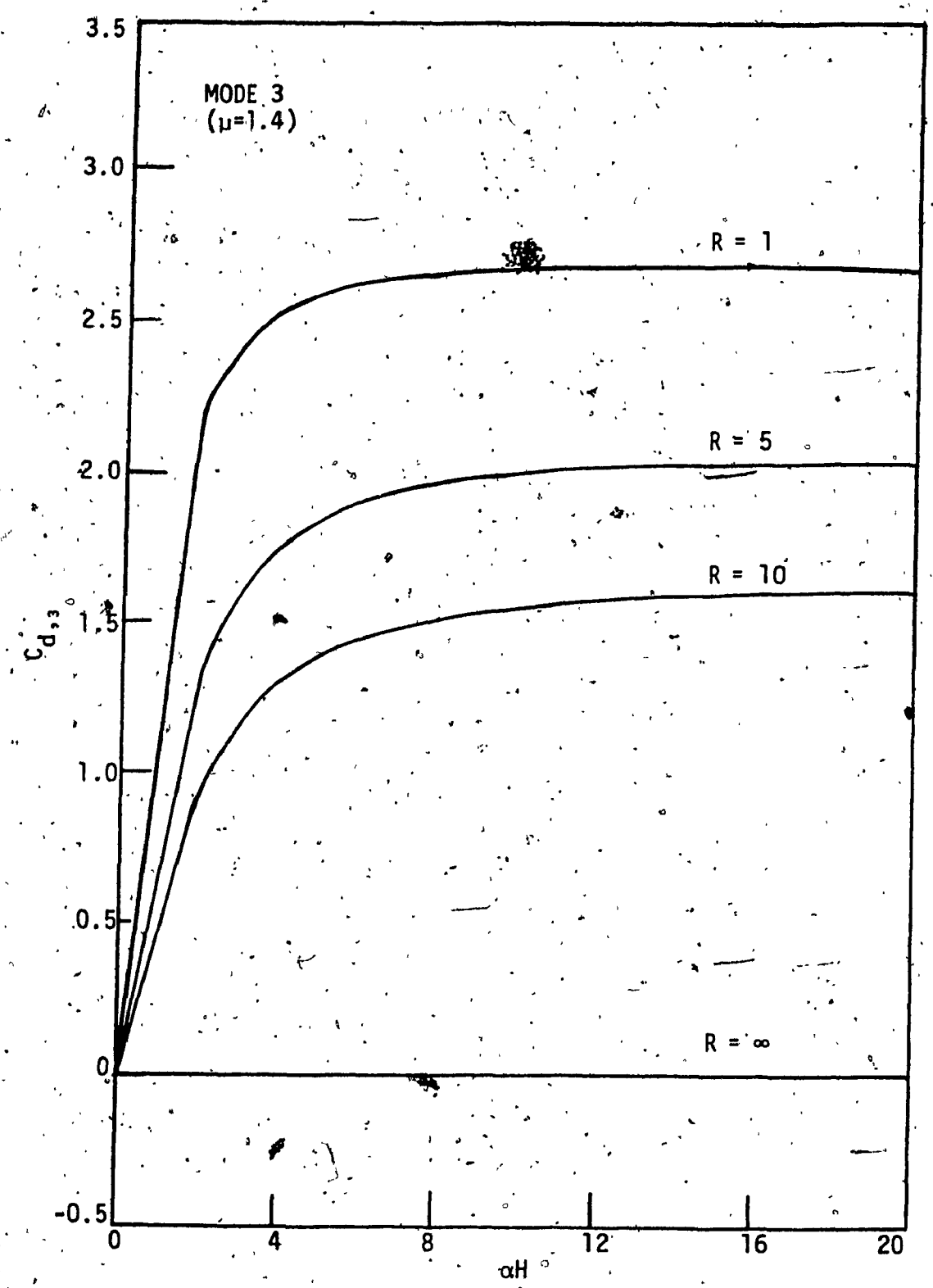

FIG. D4 Top Deflection Coefficient Curves for Different R - Mode 3 (μ=1.4).

APPENDIX E

ADDITIONAL DATA FOR PARTICIPATION FACTOR

The variation of modeal participation factor P_r ((Eq. 3.4)) with the variation of nondimensional rotational flexibility parameter β for the first three modes of vibration are presented in Fig. E1. These curves are plotted using the values given in Table E1.

TABLE E1

βH and Participation Factor of Three Modes of Vibration for Different Values of R

R	βH			PARTICIPATION FACTOR, P_r		
	MODE 1	MODE 2	MODE 3	MODE 1	MODE 2	MODE 3
10^4	1.875	4.694	7.855	0.575	0.442	0.254
10^3	1.873	4.689	7.847	0.576	0.444	0.256
10^2	1.857	4.650	7.783	0.589	0.461	0.271
50	1.839	4.610	7.722	0.602	0.476	0.284
10	1.723	4.400	7.451	0.684	0.537	0.315
5	0.616	4.267	7.319	0.749	0.555	0.314
1.0	1.248	4.031	7.135	0.931	0.546	0.295
0.5	1.076	3.983	7.103	1.014	0.537	0.289
0.1	0.736	3.939	7.076	1.269	0.527	0.284

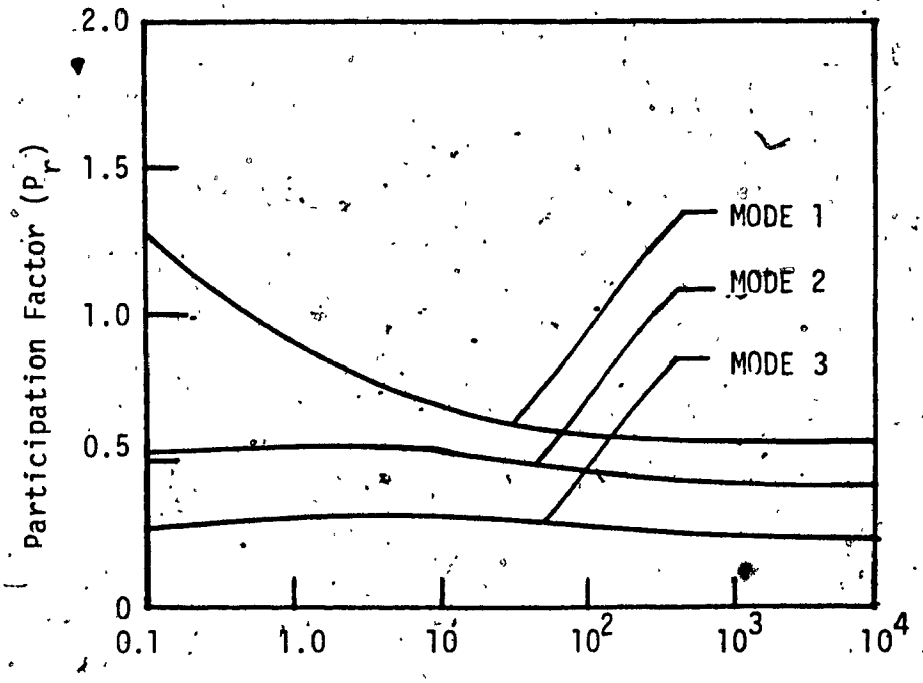

FIG. E1 Variation of Modal Participation Factor with Foundation Flexibility Parameter R - Modes 1, 2, and 3.